Non-Hermitian Integrable Quantum Chains and their Applications To Equilibrium Crystal Shapes and Reaction-Diffusion Problems

Dissertation von

Silvio Renato Dahmen

BONN-IR-97-03

01/1997

Contents

Chapter 1

Introduction

1.1 Overview

This thesis is concerned with applications of integrable systems, more specifically of one– and two–dimensional exactly solvable models of statistical mechanics, to the problem of Nonequibrium Reaction–Diffusion Processes and Equilibrium Crystal Shapes respectively. It is divided into two main parts, each containing the work conducted under the guidance of V. Rittenberg at the Physikalisches Institut der Universität Bonn on these topics. The results here presented were published in Dahmen (1994) and Albertini, Dahmen and Wehefritz (1996a,b,c). Three appendices on the Bethe Ansatz technique are also included.

1.1.1 Part I

The first part deals with the work done on the *Asymmetric Six–Vertex Model* (Lieb, 1967b; Yang, 1967). The physical motivations for studying this model are numerous. In two dimensions, it is one of the earliest and most fundamental models of statistical mechanics, being the natural extension of the model introduced more than half a century ago in an attempt to explain the properties of planar ice (Slater, 1941). Its free energy was calculated in the late 1960's using the Bethe Ansatz and published practically without derivation (Sutherland, Yang and Yang, 1967). Only recently has this gap been filled, but even though some features of the phase diagram have been clarified, many questions regarding the nature of the phase transitions were left open (Nolden, 1992).

The richness of this model stems also from the many mappings onto seemingly unrelated problems. In this particular context, it has not long ago been realized that the six–vertex model is intimately related to the problem of Equilibrium Crystal Shapes (van Beijeren, 1977). In some industrial applications in particular, many situations arise where it is desirable to have a detailed understanding of the equilibrium surface structure of crystals which have been subject to some sort of heat treatment, and this is in most cases determined by various mechanisms of transport such as condensation, diffusion, chemical reaction rates and so on (Herring, 1951).

There are a few situations however where these rather complex phenomena may be cast aside and the surface tension alone plays the determining role[1]. One may then refer to the so–called equilibrium crystal shape (ECS) problem. Considering a simplified one–component thermodynamical system with two coexisting phases (solid–fluid) in equilibrium, the main questions could be thus formulated: what does the solid inclusion look like? Are the edges where crystal facets with different Miller indices meet sharp or are they rounded? Are there any flat portions at all or is the macroscopic sample completely rounded? What exponent characterizes such rounding? Is it universal? This is the main motivation behind the present study.

To tackle the ECS problem one may resort to the thermodynamical approach, which amounts to showing how the equilibrium shape of crystals can be determined for a given surface tension through the Gibbs–Curie minimization condition (Landau, 1965). However, in order to obtain the surface tension one has to write a concrete model for the interatomic interactions.

[1]This is particularly the case when crystals are not exceedingly large and surface irregularities are small enough with respect to the size of the sample. See Herring, *op. cit.* for further discussion.

In more recent years, great progress has been made in this arena mainly through the connection with the theory of 2–dimensional integrable models, the six–vertex model in particular (van Beijeren, 1977; Jayaprakash and Saam, 1984; Rottman and Wortis, 1984). Nonetheless the statistical mechanical theory of ECS has not yet been fully explored, and many questions remain open. For instance, the nature of the phase transitions that the asymmetric six–vertex model presents and their significance to the ECS problem are not undertood in their entirety. From the more technical point of view, the treatment of the Bethe Ansatz equations poses a real challenge if compared to the symmetric case, due to the complex character of its solutions. Finite–size studies and the computation of exponents require non trivial generalizations of the standard methods.

Within this spirit, the goal of the first part of this thesis is therefore to study the asymmetric six–vertex by means of a detailed treatment, both numerical and analytical, of the Bethe Ansatz Equations, extending previous works while giving them an interpretation in terms of shapes of equilibrium crystals.

From a remarkable result of surface shape theory (Andreev, 1981), namely that it is a general feature of the ECS problem that the surface free energy of the system is also the equation of the equilibrium surface[2], it follows that one may obtain surface curvature exponents directly from the exponents of the free energy. These exponents, being experimentally measurable, would give extra validation to the predicability power of the six–vertex, and at the same time reassure the correcteness of the theoretical methods employed in solving the problem. Therefore a great part of this work is devoted to finding relevant expansions of the free energy using the Bethe Ansatz technique and interpreting the exponents thus obtained in the ECS language.

The first part of this dissertation is divided as follows: in chapter 2 a statistical mechanical model for the shape of an *fcc* crystal is introduced, and its connection to the asymmetric six–vertex model is established. Chapter 3 contains a detailed treatment of the model using the Bethe Ansatz technique. By means of appropriate expansions of the quantities leading to the free energy, a new curvature exponent is found. A discussion on a possible experimental setup to confirm its value is presented. This part closes with an interpretation of the phase transition associated to the new exponent. Some open questions are discussed.

1.1.2 Part II

The second part of this dissertation deals with some N–state vertex models in the context of reaction-diffusion processes. Their associated one–dimensional quantum counterparts (the so–called Perk–Schultz Chains) can be regarded as evolution operators of a linear system of N-species of particles diffusing and reacting according to some established rules. Although already known for a couple of years (Perk and Schultz, 1983; Schultz 1983), these one–dimensional systems were, in their most general non hermitian form, of more interest as integrability paradigms. The scenario changed however substantially with the discovery of the mapping between the master equation of certain reaction–diffusion systems and the imaginary–time Schrödinger equation, whose dynamics was governed by these Hamiltonians (Alcaraz *et al* 1994a,b).

Reaction-diffusion-limited processes have had a forefront position in nonequilibrium statistical physics since the pioneering work of Smoluchowski in 1917. They can be portrayed as bimolecular processes of the type

$$A + B \underset{r}{\overset{k}{\rightleftharpoons}} C + D$$

where species A and B (C and D) react to form C and D (A and B) with a reaction rate k (r). The main interest here is on those irreversible ($r = 0$) and vacuum-driven chemical reactions, i.e. those for which at least one of the final products is an inert state, a precipitate or a non-reacting species

(i) Diffusion of species A_i: $A_i + \emptyset \rightleftharpoons \emptyset + A_i$

(ii) Interchange of species A_i, A_j ($i \neq j$): $A_i + A_j \rightleftharpoons A_j + A_i$

[2] Up to some irrelevant constant which sets the length scale of the solid inclusion. Crystals of different macroscopic sizes have the same equilibrium shape.

(iii) Annihilation: $A_i + A_j \to \emptyset + \emptyset$

(iv) Coagulation: $A_i + A_i \to A_i + \emptyset$

(v) Polymerization (Spouge, 1988): $A_i + A_i \to A_j + \emptyset$

(vi) Death: $A_i + \emptyset \to \emptyset + \emptyset$

(vii) Trapping (Chopard *et al*, 1993; Rodriguez *et al*, 1993): $A_i + A_j \to A_i + \emptyset$.

Two new vacuum–driven processes are also considered here

(viii) Mutation: A_j: $A_i + \emptyset \to A_j + \emptyset$

(ix) Transmutation: $A_i + \emptyset \to \emptyset + A_j$

In spite of their apparent simplicity, tackling nonequilibrium problems described by such reaction rates remains a most demanding task. The mapping of such systems onto integrable models is therefore welcome, once it might shed some new light into the physics they present. Among the gains, one is the equivalence of the spectra, which implies the equivalence of phase diagrams. The physical behavior of chemical systems is then in principle determined by that of the chains they are mapped onto. For instance, if one considers the long–time behavior of a system whose underlying dynamics is governed by processes of the type described above, the time decay of the mean concentration for species j is expected to be of the form

$$c_j \sim \left\{ \begin{array}{l} t^{-\alpha} \\ e^{-t/\tau} \end{array} \right.$$

where α and τ are characteristic of each problem[3]. These regimes correspond, respectively, to the massless and massive phases in the quantum chains mapping the chemical systems. Second, a major gain from the mapping is the existence of the Bethe Ansatz, which may yield valuable information information through its solution.

Therefore the first aim of the second part of the present thesis is to extend previous works (Alcaraz *et al, op. cit.*) by finding three-state integrable quantum chains whose Hamiltonians are time-evolution operators of diffusion-reaction processes and whose spectra are known or can be easily calculated.

The second problem of interest is intimately related to the role of boundary conditions in reactive–diffusive systems. In the case of quantum chains appearing in equilibrium problems, the boundaries are expected to play no significant role in the determination of the phase diagram. However, for chemical processes where the associated quantum Hamiltonian is nonhermitian, this picture is far from correct and the physics is boundary-dependent[4]. For periodic boundaries, the same is not true. This problem was well understood in connection to 2-state chains (Alcaraz and Wreszinski, 1990; Henkel and Schütz, 1994). The main question is whether something can be said about higher–state chains.

To this avail, the second part of this thesis is divided into two chapters. The discussion starts with the Master Equation formalism for reaction–diffusion models, in chapter 4. The rest of the chapter deals with the study of the quantum chains proper: first, the $U_q\widehat{SU}(2)$-invariant model (Alcaraz *et al, op. cit.*), which is introduced as a workbench for the application of the method and whose phase diagram is reinterpreted inthe language of chemical processes. These results are then

[3]As an example, in the 2-specie annihilation process ($A + B \to \emptyset + \emptyset$ where $\emptyset$ is a vacancy), it has been found that in one dimension and for an initial random distribution of particles one has an algebraic fall–off with exponent $\alpha = \frac{1}{4}$ (Toussaint and Wilczek, 1983). The other regime can be attained by the inclusion of certain processes (or reversible reactions) which lead to a local steady state and therefore a quicker (exponential) approach to equilibrium

[4]This is intuitively clear if one thinks of a biased ($k \neq r$) diffusion process $A + \emptyset \underset{r}{\overset{k}{\rightleftharpoons}} \emptyset + A$. For open bondaries (equivalent to an impenetrable wall) one gets an asymptotic limit with particles concentrated to one side of the lattice (Schütz, 1993)

extended to treat the Perk–Schultz models with external fields. A nonlocal similarity transformation is defined to study the role played by the boundaries. Chapter 5 is devoted to its detailed study. A proof on its validity for the general N–state diffusion process with all different reaction rates is given. The chapter closes with some conclusions and open questions.

1.1.3 The Appendices

The last part of this thesis comprises three appendices on the Bethe Ansatz The results here presented were mostly obtained from numerical and/or analytical studies of the Bethe Ansatz Equations. The first appendix deals with the method in its coordinate version, as applied to treat the asymmetric XXZ chain (*i.e.* the 2–state non hermitian Perk–Schultz Hamiltonian). In the second appendix the algebraic method is applied to the six–vertex model. The last appendix is devoted to a discussion of the numerical methods employed in solving Bethe's Equations.

1.2 Acknowledgments

It is a great pleasure for me to thank all those who, through their incentive and friendship, helped me pave my way towards this goal.

My most sincere and special gratitute belongs to Prof. V. Rittenberg, whose unconditional support and example will certainly not fade from my memory.

I would like also to thank the Physikalisches Institut der Universität Bonn for the financial support, which allowed me to carry on my studies in Bonn. Partial support from the Konrad Adenauer Stiftung (Germany) as well as from the Conselho Nacional de Desenvolvimento Científico e Tecnológico (Brazil) is also gratefully acknowledged.

To Birgit Wehefritz I owe the most sincere gratitute for the many hours of fruitful work and above all for her friendship. To Horatiu Simon I owe some of my happiest moments at the Institute. It is also a pleasure to thank Giuseppe Albertini for the great collaboration and for sharing his insights with me. I would also like to thank Prof. F.C. Alcaraz, who shared his expertise with me and gave me his ubiquitious support. I would like to thank A.L. Malvezzi for the friendship of all these years.

The encouradgement I received from Prof. R. Flume, Prof. G. von Gehlen, and Dr. W. Pfeil is gratefully acknowledged.

Our secreterial staff was of imensurable help and I would like to thank Mrs. D. Faßbender, Mrs. C. Marikar, Ms. P. Zündorf as well as our librarians Mrs. M. Muehl und Mrs. R. Wendorf for their professionality.

To my fellow colleages from the theoretical group, P. Arndt, U. Billstein, J. Gerbhardt, T. Heinzel, H. Hinrichsen, F. Kopitzki, K. Krebs, M. Pfannmüller, M. Pröbsting and T. Wittlich my thanks for the many pleasant hours in the Institute.

During these years in Bonn, Prof. and Mrs. Bodenstedt went beyond their friendship by giving me their support and affection. Their enlightening presence will never be forgottten and certainly terribly missed.

My dearest thanks belong to my wife, Ana L. Cetertich Bazzan, for her supporting and professional attitude, and to my family, whose understanding and encouradgement throughout these years I could'nt do without. To them, I dedicated this work.

Part I

Equilibrium Crystal Shapes

Chapter 2

The Statistical Mechanics of Equilibrium Crystal Shapes

"God made solids, but surfaces are the work of the Devil"

Wolfgang Pauli

2.1 Introduction

In this chapter a microscopic model for the surface of an *fcc* crystal is introduced and its relation to the asymmetric six–vertex model, upon which this work is based, is explained.

2.2 The Solid–on–Solid and the Six–Vertex Models

The first spin model used in the description of the surface of a crystal was the Body–Centered Solid–on–Solid Model (van Beijeren, 1977). Since all other SOS models are based on this one, it is interesting to discuss its main features first. To each site of a three–dimensional *bcc* lattice one associates a positive spin (atom) or a negative one (vacancy). The boundary conditions are such that the uppermost layer of spins is kept negative, while the first one is positive. The fundamental feature of the model follows from the energy assignments of interatomic bonds plus boundary conditions: denoting the next–nearest–neighbor energy bonds in the three main axis directions by $-J_1$, $-J_2$, $-J_3$ ($J_1, J_2, J_3 > 0$) and the nearest neighbor interaction by $-J_0$ ($J_0 > 0$), and considering the limit $-J_0 \to \infty$ (with all other J's constant), there can be no more than one $(+-)$ bond between any two columns. Overhangs (height differences between columns higher than $\frac{l}{2}$) as well as voids (i.e. vacancies below the uppermost atom in a column, corresponding to excitations in the bulk) are forbidden. This defines some dividing surface Ω between a fully occupied lattice (below the surface) and a fully vacant one.

Moreover, there can be at most 6 different height configurations for each 4–column group (see fig. below). The identification with the six–vertex model follows by drawing a dual lattice rotated by $\frac{\pi}{4}$ with respect to the height surface[1]. The convention on arrow assignment is explained in the caption. The analogy surface model – vertex model can be made more clear: for instance, the macroscopically smooth surface with Miller indices (001) is invariant under removal of the top layer of atoms. In the vertex language this surface corresponds to a ground state configuration of alternating vertices of type 5 and 6, the invariance finding its correspondence in the degeneracy of this state (changing $5 \leftrightarrow 6$).

[1]For geometries other than that of the bcc lattice, a more general transformation is required.

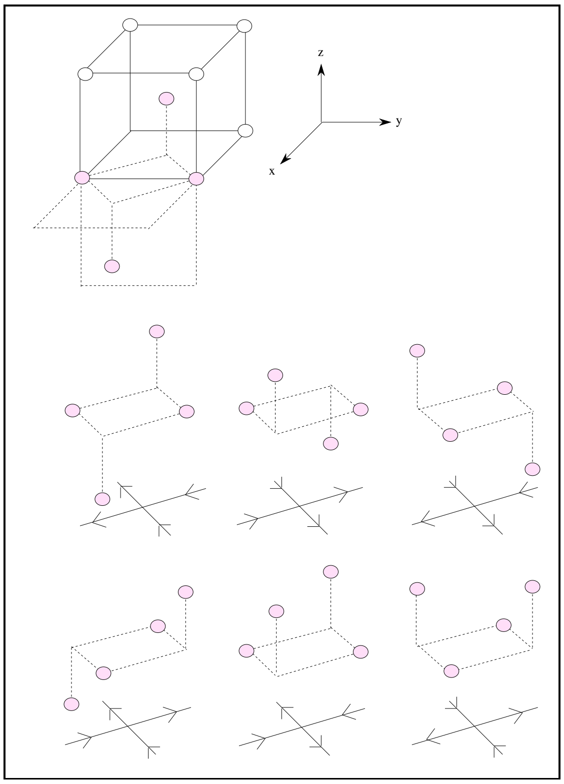

Figure 1. The BCC conventional cell and vertices (after van Beijeren, 1977). A vertex is defined for each combination of 4 atoms chosen as depicted above. The convention on the direction of arrows is such that the column to the right of each arrow is always higher than the one to its left.

Since this surface has no slope, one may further draw the analogy between the slope of a surface and the polarization of a vertex, since both vertices 5 and 6 have no net dipole moment. Moreover one may associate to the horizontal and vertical electric fields h, v of the six–vertex the so–called Andreev's fields η_x, η_y, which are the conjugated variables to the slopes (see (Andreev, 1981). See def. (2.2.14).

It is possible to extend this mapping to other lattice geometries (Jayaprakash and Saam, 1984). This is done next for the (110) facet of the *fcc* lattice, where the results of chapter 3 apply.

2.2.1 The Solid–on–Solid FCC and the Asymmetric Six–Vertex Models

Upon dividing an infinite ideal crystal into two parts through a cleavage plane (hkl) two new surfaces of Miller indices (hkl) and $(\overline{hkl})$ are created. One may regard these surfaces as the result of breaking interatomic bonds across the cleavage plane. These broken bonds can be described on a purely geometrical basis and one may associated an energy to a certain primitive cell of the lattice as a function only of the number and type of broken bonds, *i.e.* whether such bonds are nearest neighbors, next–nearest neighbors and so on (McKenzie, Moore and Nicholas, 1962).

Consider an *fcc* conventional cell (volume $V^{cc} = l^3$) which is to be broken by the cleavage planes (100), (110) and (111) (it suffices to consider planes with $h \geq k \geq l \geq 0$. All other planes follow by symmetry considerations). Let $\vec{n}_{hkl} = h\hat{x} + k\hat{y} + l\hat{z}$ be the normal of the cleavage plane and $\vec{b}$ the vector connecting any two atoms in the lattice. The corresponding $\vec{b}$–bond can only be broken if $\vec{b} \cdot \vec{n}_{hkl} > 0$ and the atom whose bond is being broken lies within a distance of $\frac{\vec{b} \cdot \vec{n}_{hkl}}{|\vec{n}_{hkl}|}$ from the cleavage plane. From a standard result of solid state theory, if V^{pc} is the volume of the primitive cell, than $V^{pc}|\vec{n}_{hkl}|$ is the projection of the primitive area onto the cleavage plane. Therefore the total number of $\vec{b}$–type bonds which are broken in each of these units of area is

$$N(\vec{b}) = \vec{b} \cdot \vec{n}_{hkl} \tag{2.2.1}$$

For each atom (one may consider for simplicity, as in the figure below, the one at the origin) there exists a total of 6 nearest–neighbors along the direction $< 110 >$ and 3 next–nearest neighbors along $< 001 >$, as given by

$$\begin{array}{lll} 2\vec{b}_1 = [110] & 2\vec{b}_4 = [1\bar{1}0] & \vec{b}_7 = [100] \\ 2\vec{b}_2 = [101] & 2\vec{b}_5 = [011] & \vec{b}_8 = [010] \\ 2\vec{b}_3 = [10\bar{1}] & 2\vec{b}_6 = [01\bar{1}] & \vec{b}_9 = [001] \end{array}$$

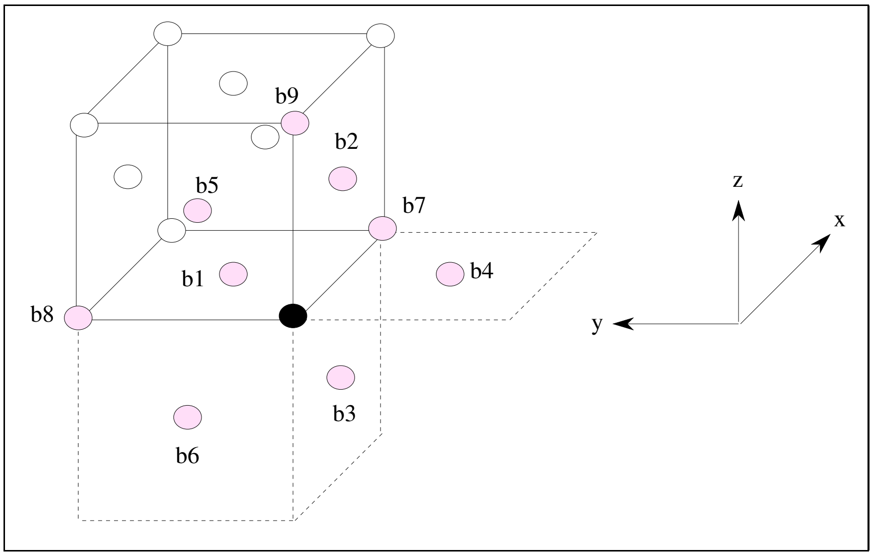

Figure 2. The fcc conventional cell and the bonds as defined with respect to the atom at the origin of coordinate system (filled circle).

The number of broken bonds per primitive projected area reads

Bonds	(100)	(110)	(111)
$N(\vec{b}_1)$	1	1	2
$N(\vec{b}_2)$	1	1	2
$N(\vec{b}_3)$	1	1	0
$N(\vec{b}_4)$	1	0	0
$N(\vec{b}_5)$	0	1	2
$N(\vec{b}_6)$	0	1	0
$N(\vec{b}_7)$	2	2	2
$N(\vec{b}_8)$	0	2	2
$N(\vec{b}_9)$	0	0	2
Proj. Area	$\frac{l^2}{2}$	$\frac{\sqrt{2}l^2}{4}$	$\frac{\sqrt{3}l^2}{4}$

Assigning the bond energy $-J_1$ to nearest–neighbors and $-J_2$ otherwise ($J_1, J_2 > 0$) one has (McKenzie, Moore and Nicholas, 1962)

$$\zeta(\vec{n}_{hkl}) = \frac{\vec{n}_{hkl}}{V^{pc}|\vec{n}_{hkl}|} \cdot \Big(J_1[210] + J_2[111] \Big) \tag{2.2.2}$$

where $\zeta(\vec{n}_{hkl})$ is the surface tension. Explicitly

$$\zeta(100) = \left(\frac{2}{l^2}\right)(4J_1 + 2J_2) \tag{2.2.3}$$

$$\zeta(110) = \left(\frac{2\sqrt{2}}{l^2}\right)(3J_1 + 2J_2) \tag{2.2.4}$$

$$\zeta(111) = \left(\frac{4}{\sqrt{3}l^2}\right)(3J_1 + 3J_2) \tag{2.2.5}$$

The free energies associated to each face follows directly

$$f(100) = 4J_1 + 2J_2 \tag{2.2.6}$$

$$f(110) = 3J_1 + 2J_2 \tag{2.2.7}$$

$$f(111) = 3J_1 + 3J_2 \tag{2.2.8}$$

2.2.2 The (110)–fcc Facet and Vertex Configurations

Viewed from the [110] direction, the geometry is that of the figure below. There are six different height configurations and to each one may associated a vertex. An alternating configuration of vertices 5 and 6 defines the ground state (no slope). Vertices 1 through 4 represent excitations (tilts away from the (110) face) and each is associated with a slope p, q in the x and y directions respectively. Considering the fields η_x and η_y conjugated to the slopes, the vertex energies read (Lieb and Wu, 1972; Jayaprakash and Saam, 1984)

$$\begin{aligned}
\widetilde{e}_1 &= 3J_1 + 3J_2 + \eta_y \frac{\widetilde{A}}{\sqrt{2}} \\
\widetilde{e}_2 &= 3J_1 + 3J_2 - \eta_y \frac{\widetilde{A}}{\sqrt{2}} \\
\widetilde{e}_3 &= 4J_1 + 2J_2 + \eta_x \widetilde{A} \\
\widetilde{e}_4 &= 4J_1 + 2J_2 - \eta_x \widetilde{A} \\
\widetilde{e}_5 &= 3J_1 + 2J_2 \\
\widetilde{e}_6 &= 3J_1 + 2J_2
\end{aligned} \tag{2.2.9}$$

where $\widetilde{A} = \frac{l^2}{2\sqrt{2}}$ is the area per vertex. The relation between the fields $\widetilde{A}\eta_x$, $\widetilde{A}\eta_y$ and the horizontal and vertical fields h, v of the six–vertex model reads

$$\begin{aligned}
h &= -\frac{\widetilde{A}}{2}\left(\eta_x + \frac{\eta_y}{\sqrt{2}}\right) \\
v &= -\frac{\widetilde{A}}{2}\left(\eta_x - \frac{\eta_y}{\sqrt{2}}\right)
\end{aligned} \tag{2.2.10}$$

It is convenient to measure the energies from those values corresponding to the ground state ($\widetilde{e}_5$ and $\widetilde{e}_6$ for $\vec{\eta} = 0$). Subtracting an overall factor of $3J_1 + 2J_2$ from all energies leads to

$$e_1 = J_2 - h - v = J_2 + \widetilde{A}\eta_x$$

$$
\begin{aligned}
e_2 &= J_2 + h + v &= J_2 - \widetilde{A}\eta_x \\
e_3 &= J_1 - h + v &= J_1 + \frac{\widetilde{A}}{\sqrt{2}}\eta_y \\
e_4 &= J_1 + h - v &= J_1 - \frac{\widetilde{A}}{\sqrt{2}}\eta_y \\
e_5 &= 0 \\
e_6 &= 0
\end{aligned} \tag{2.2.11}
$$

This energy parametrization defines (for $h = v = 0$) the so–called intrinsically antiferroelectric six–vertex model.

The shape of the crystal face follows from the Gibbs–Curie condition (Landau, 1965)

$$f(T,p,q) = \nu(z - px - qy)(T) \tag{2.2.12}$$

where $z(x,y)(T)$ is the equation of the surface in cartesian coordinates, $f(T,p,q)$ is the free energy as a function of the slopes and ν is a constant which sets the scale of the problem. Following Andreev (1981), one may define a Legendre transformed potential $\overline{f}(T,\eta_x,\eta_y)$ through

$$\overline{f}(T,\eta_x,\eta_y) = f(T,p,q) - p\eta_x - q\eta_y \tag{2.2.13}$$

where η_x, η_y are the conjugate variables to the slopes p and q

$$\eta_x = \frac{\partial f}{\partial p}, \qquad \eta_y = \frac{\partial f}{\partial q} \tag{2.2.14}$$

It follows from (2.2.12) and (2.2.14) that

$$\eta_x = -\nu x, \qquad \eta_y = -\nu y, \tag{2.2.15}$$

Substituted back into (2.2.13), these expressions yield

$$\overline{f}(T,\eta_x,\eta_y) = \overline{f}(T,-\nu x,-\nu y) = \nu z \tag{2.2.16}$$

From the mapping of the crystal surface onto the assymmetric six–vertex model one finally obtains

$$\nu z(T,J_1,J_2,\eta_1,\eta_2) = f(110) + f_{6-\mathrm{VERTEX}}(T,J_1,J_2,\eta_1,\eta_2) \tag{2.2.17}$$

where $f_{6-\mathrm{VERTEX}}(T,J_1,J_2,\eta_1,\eta_2)$ is the free energy of the asymmetric six–vertex.

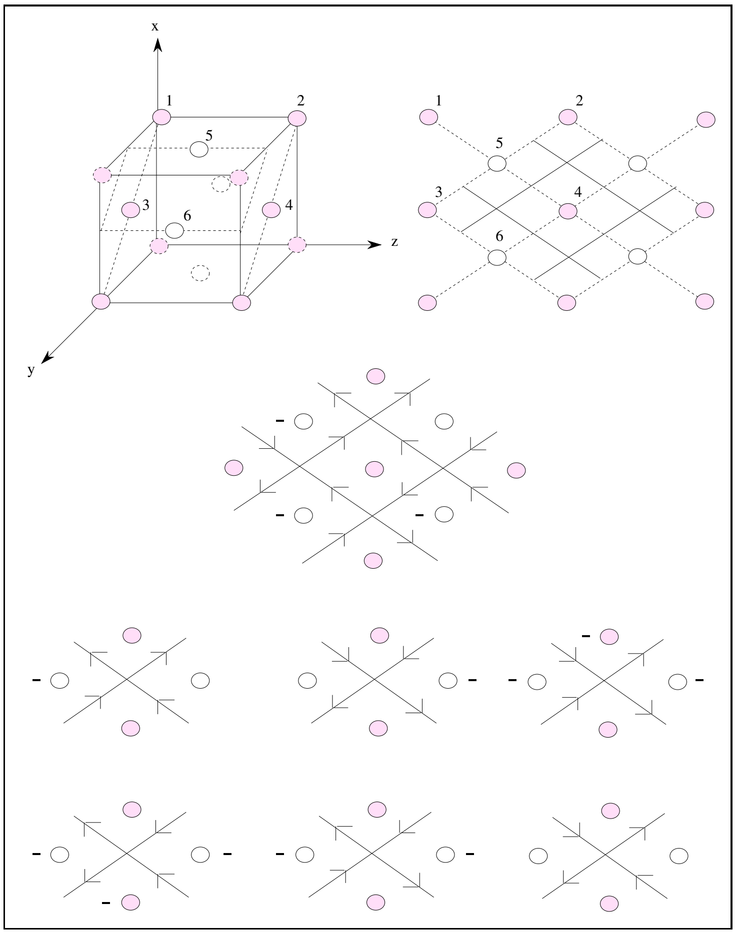

Figure 3. The fcc cell and vertices. On the top left the (110) plane is depicted (full circles). Atoms in the plane immediately above are represented by empty circles. Two such planes combined define the macroscopically smooth (110) crystal surface. Vertices (full lines, top right) are defined for each group of 4 atoms (two filled and two empty circles). In the middle, one particular configuration of 4 vertices is depicted (a $-$ sign indicates a missing atom). At the bottom vertices 1 through 6 with their corresponding vacancies are depicted. Vertices 1 through 4 represent tilts away from the $< 110 >$ direction, and correspond locally to planes $(11\bar{1})$, (111), (100) and (010) respectively. Vertices 5 and 6 correspond to the (110) surface (*cf.* with the definitions of figure 4). After Jayaprakash and Saam (1984).

Chapter 3

The Asymmetric Six–Vertex Model

3.1 Introduction

In this chapter a detailed study of the Bethe Ansatz Equations of the asymmetric six–vertex model is presented. Most of the results of section 3.3 have appeared in earlier publications (Nolden, 1992; Sutherland, Yang and Yang, 1967). New results are discussed in section 3.4. Using the mapping of chapter 2, these are interpreted under the light of crystal shape theory.

3.2 The Bethe Ansatz Equations

It is convenient to use a different parametrization of the vertex energies (fig. 4). The relation between the new variables and those of the preceeding chapter read

$$\sinh\theta = e^{\beta J_1}\sqrt{1+\cosh^2\gamma} \tag{3.2.1}$$

$$\cosh\gamma = \cosh\beta(J_1-J_2) - \frac{1}{2}e^{\beta(J_1+J_2)} \tag{3.2.2}$$

$\beta^{-1} = k_{\mathrm{B}}T$ is the usual Boltzmann factor.

In the asymmetric six–vertex model, fluctuating two–valued variables (dipoles, here represented by arrows) are attached to the links of an $N\times M$ square lattice and Boltzmann weights $S^{\beta\beta'}_{\alpha\alpha'}(\theta)$ are assigned to the vertices so that the row–to–row transfer matrices (see (B.1.21))

$$\tau^{[N]}(\theta)|^{\{\alpha'\}}_{\{\alpha\}} = \sum_{\{\beta\}}\prod_{k=1}^{N} S^{\beta_k\beta_{k+1}}_{\alpha_k\alpha'_k}(\theta) \tag{3.2.3}$$

form a commuting family

$$[\tau(\theta),\tau(\theta')] = 0$$

for any two values θ, θ' of the spectral parameter (Perk and Schultz, 1983; Schultz, 1983). The set of variables $\{\alpha\} = \alpha_1,\alpha_2,\cdots,\alpha_N$ is associated to a row of N vertical links and the model is defined on a torus.

The transfer matrix can be diagonalized exactly by the Bethe Ansatz in its coordinate or algebraic version (see Lieb and Wu, 1972; Jayaprakash and Sinha, 1982 and Appendices A and B). Denoting its eigenvalues by $\Lambda(\theta)$, it follows that they are given by the expression

$$\Lambda(\theta) = e^{v(N-2n)}e^{hN}\left[\frac{\sinh(\gamma-\theta)}{\sinh\gamma}\right]^N\prod_{j=1}^{n}\frac{\sinh(\frac{\gamma}{2}+\theta-\frac{i\alpha_j}{2})}{\sinh(\frac{\gamma}{2}-\theta+\frac{i\alpha_j}{2})}$$

$$
\begin{aligned}
&+e^{v(N-2n)}e^{-hN}\left[\frac{\sinh\theta}{\sinh\gamma}\right]^N\prod_{j=1}^{n}\frac{\sinh(\frac{-3\gamma}{2}+\theta-\frac{i\alpha_j}{2})}{\sinh(\frac{\gamma}{2}-\theta+\frac{i\alpha_j}{2})}\\
=\;&\Lambda_R(\theta)+\Lambda_L(\theta)
\end{aligned}
\tag{3.2.4}
$$

where the rapidities α_j are the roots of the so–called Bethe Ansatz equations

$$
\left[\frac{\sinh(\frac{\gamma}{2}+\frac{i\alpha_k}{2})}{\sinh(\frac{\gamma}{2}-\frac{i\alpha_k}{2})}\right]^N=(-1)^{n+1}e^{2hN}\prod_{l=1}^{n}\frac{\sinh(\gamma+\frac{i}{2}(\alpha_k-\alpha_l))}{\sinh(\gamma-\frac{i}{2}(\alpha_k-\alpha_l))}\qquad k=1,2,\cdots,n \tag{3.2.5}
$$

In this expression, n stands for the number of arrows reversed with respect to the reference ferroelectric state $|\uparrow\uparrow\cdots\uparrow\rangle$, in a row of of N vertical links. It is a conserved quantity since $S^z=\frac{1}{2}\sum_{j=1}^{N}\sigma_j^z$ commutes with $\tau(\theta)$.

In order to find the specific free energy, one needs the Bethe Ansatz Equations in the thermodynamic limit. To obtain these one first takes the logarithm of (3.2.5), which become

$$
p^0(\alpha_k)-\frac{1}{N}\sum_{l=1}^{n}\Theta(\alpha_k-\alpha_l)+2ih=\frac{2\pi}{N}I_k\qquad k=1,2,\cdots,n \tag{3.2.6}
$$

where I_k is half-odd (integer) if n is even (odd) and

$$
\Theta(\alpha)=-i\ln\left[\frac{\sinh(\gamma+\frac{i\alpha}{2})}{\sinh(\gamma-\frac{i\alpha}{2})}\right]
$$

is the so–called shift function. Also

$$
p^0(\alpha)=-i\ln\left[\frac{\sinh(\frac{\gamma}{2}+\frac{i\alpha}{2})}{\sinh(\frac{\gamma}{2}-\frac{i\alpha}{2})}\right]
$$

The cuts are chosen so that $\Theta(\alpha)$ is analytical in $-2\gamma<\Im(\alpha)<2\gamma$ and real, monotonically increasing when $\alpha\in[-2\pi,2\pi]$. Cuts are thus chosen to run from $i\gamma$ to $i\infty$ and from $-i\gamma$ to $-i\infty$ for $p^0(\alpha)$; from $2i\gamma$ to $i\infty$ and from $-2i\gamma$ to $-i\infty$ for $\Theta(\alpha)$. Moreover one takes $p^0(0)=\Theta(0)=0$. Notice from (3.2.5) that $\Re(\alpha)\in[-\pi,\pi]$ so $\Re(\alpha_k-\alpha_l)\in[-2\pi,2\pi]$.

In the thermodynamic limit, the roots of Bethe's equations form a continuum and lie on some curve C. Equation (3.2.6) becomes (Nolden, 1992)

$$
p^0(\alpha)-\frac{1}{2\pi}\int_C d\beta\Theta(\alpha-\beta)R(\beta)+2ih=2\pi x\qquad -\frac{1-y}{4}\le x\le\frac{1-y}{4} \tag{3.2.7}
$$

x is the real parameter of the curve C, y is the vertical polarization defined through

$$
y=\lim_{N\to\infty}\frac{2S^z}{N}=\lim_{N\to\infty}(1-\frac{2n}{N})=1-\frac{1}{\pi}\int_C d\alpha R(\alpha) \tag{3.2.8}
$$

and the rapidity density $R(\alpha_l)=\lim_{N\to\infty}\frac{2\pi}{N(\alpha_{l+1}-\alpha_l)}$ is determined by solving the integral equation

$$
\xi(\alpha)-\frac{1}{2\pi}\int_C d\beta K(\alpha-\beta)R(\beta)=R(\alpha) \tag{3.2.9}
$$

where

$$
\xi(\alpha)=\frac{dp^0(\alpha)}{d\alpha};\qquad K(\alpha)=\frac{d\Theta(\alpha)}{d\alpha}
$$

The factor 2π in the definition of the density $R(\alpha)$ is chosen for convenience.

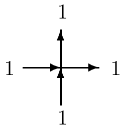

$$= e^{-h-v}\,\frac{\sinh(\gamma-\theta)}{\sinh\gamma} = S_{11}^{11}(\theta) = \text{vertex 1}$$

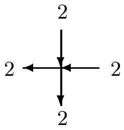

$$= e^{h+v}\,\frac{\sinh(\gamma-\theta)}{\sinh\gamma} = S_{22}^{22}(\theta) = \text{vertex 2}$$

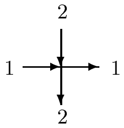

$$= e^{-h+v}\,\frac{\sinh\theta}{\sinh\gamma} = S_{22}^{11}(\theta) = \text{vertex 3}$$

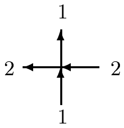

$$= e^{h-v}\,\frac{\sinh\theta}{\sinh\gamma} = S_{11}^{22}(\theta) = \text{vertex 4}$$

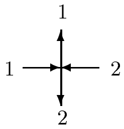

$$= 1 = S_{21}^{12}(\theta) = \text{vertex 5}$$

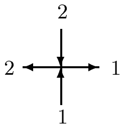

$$= 1 = S_{12}^{21}(\theta) = \text{vertex 6}$$

Figure 4. Boltzmann weights in the notation with spectral parameter θ. The physical region is corresponds to $0 < \theta < \gamma$.

The specific free energy is determined by the largest eigenvalue Λ_0 of the tranfer matrix (*cf.* discussion prior to eq. (B.1.14)) and is given by

$$f(\theta,\gamma,h,v) = -\lim_{N\to\infty}\frac{\ln\Lambda_0(\theta,\gamma,h,v)}{N}$$

whose value, as $N\to\infty$, is dominated by the largest of the two limits

$$\begin{aligned}\lim_{N\to\infty}\frac{1}{N}\ln\Lambda_{\mathrm{R}}(\theta) = F_{\mathrm{R}}(\theta,\gamma,h,y) + vy &= h + \ln\frac{\sinh(\gamma-\theta)}{\sinh\gamma} + vy \\ &\quad + \frac{1}{2\pi}\int_C d\alpha R(\alpha) f_{\mathrm{R}}(\alpha;\theta) \end{aligned} \tag{3.2.10}$$

$$\begin{aligned}\lim_{N\to\infty}\frac{1}{N}\ln\Lambda_{\mathrm{L}}(\theta) = F_{\mathrm{L}}(\theta,\gamma,h,y) + vy &= -h + \ln\frac{\sinh(\theta)}{\sinh\gamma} + vy \\ &\quad + \frac{1}{2\pi}\int_C d\alpha R(\alpha) f_{\mathrm{L}}(\alpha;\theta) \end{aligned} \tag{3.2.11}$$

where

$$f_{\mathrm{R}}(\alpha;\theta) = \ln\frac{\sinh(\frac{\gamma}{2}+\theta-\frac{i\alpha_j}{2})}{\sinh(\frac{\gamma}{2}-u+\frac{i\alpha_j}{2})} \tag{3.2.12}$$

$$f_{\mathrm{L}}(\alpha;\theta) \quad = \quad \ln \frac{\sinh(\frac{-3\gamma}{2} + \theta - \frac{i\alpha_j}{2})}{\sinh(\frac{\gamma}{2} - u + \frac{i\alpha_j}{2})} \tag{3.2.13}$$

If F_{R}, F_{L} are known, and one calls F the dominant one, the equilibrium value of y and the free energy are determined by the minimum condition

$$f(\theta,\gamma,h,v) = \min_{-1\leq y\leq 1}\{-F(\theta,\gamma,h,y) - vy\} \tag{3.2.14}$$

Before discussing the solution of the integral equations for arbitrary values of the fields, it is interesting first to discuss some already known facts about the physics of the asymmetric six–vertex model. The phase diagram and the nature of the phase transitions are well understood when $h = v = 0$ (symmetric six-vertex), or when $h = 0$ and $v \neq 0$ (Lieb and Wu, 1972; Baxter, 1982).

If $(h, v) \neq 0$, some general features of the phase diagram have been described by Sutherland, Yang and Yang (1967). The thoroughly derivation of their results was given by Nolden (1992). The $T = 0$ case is trivial, as can be seen in fig. 5 where schematic plots of the free energy in the (h, v)–plane and the (η_x, η_y)–plane (Andreev's fields) are depicted. In the former, the regions with their associated vertex configurations are indicated. The latter is analogous to the ECS of an fcc–crystal. Region $5 + 6$ corresponds to the (110) facet and other regions are accordingly indicated.

As the temperature is raised, thermal excitations bring about a rounding of edges (Jayaprakash and Saam, 1984). When $T \neq 0$ (γ finite) the free energy $f(h, v)$ remains constant as function of the field ('flat phase') in a region of the (h, v) plane containing $h = v = 0$, bounded by a curve Γ (Sutherland, Yang and Yang, *op. cit.*). Beyond this region the field is sufficiently strong to destroy the antiferroelectric order of the system, but not strong enough to impose ferroelectric order, and an incommensurate phase appears where the polarization (zero in the flat phase) changes continuously with the field. Here the spectrum of the transfer matrix is gapless with finite size corrections typical of the gaussian model (Noh and Kim, 1995). The curve Γ has been investigated only at a few points and the nature of the phase transition was found to be of a Pokrovskii–Talapov (PT) type (Pokrovskii and Talapov, 1980), whose more detailed description is given at the end of this chapter.

3.3 Solving the Bethe Ansatz Equations

At $h = 0$ the root distribution corresponding to the highest eigenvalue of the transfer matrix in each sector of fixed polarization $y = 1 - \frac{2n}{N}$ corresponds to a sequence of n consecutive numbers $\{I_k\}$ in (3.2.6) and symmetric around 0, running from $-\frac{n-1}{2}$ to $\frac{n-1}{2}$ (Yang and Yang, 1966). The rapidities $\{\alpha_j\}$ are real and distributed symmetrically around $\alpha = 0$. As $h \neq 0$, the rapidities move into the complex plane along a curve C. In order to tackle the integral equations, one has to have some preliminary information about the shape of C. One information can be extracted directly by looking more carefully into (3.2.5). The equations are invariant under $\alpha \to -\alpha^*$, and the curve C should reflect this symmetry. One may set accordingly $A = -a + ib$ and $B = a + ib$ to be the endpoints of the curve.

The location of C in the complex plane can be obtained by solving (3.2.5) numerically. One takes as initial solution the one composed of real roots and corresponding to the highest Λ at fixed y, for $h = 0$. According to the Perron–Frobenius theorem (Gantmacher, 1959; Yang and Yang, 1966), the relevant eigenstate remains the largest at fixed y even when $h \neq 0$, and it is real. For $h > 0$ ($h < 0$) numerical solutions of (3.2.5) show that the rapidities move into the lower (upper) half of the α–plane (see appendix C). Moreover, they indicate that, at fixed γ, h the real part of A (B) converges to π ($-\pi$) while the imaginary part converges to some value $b > -\gamma$.

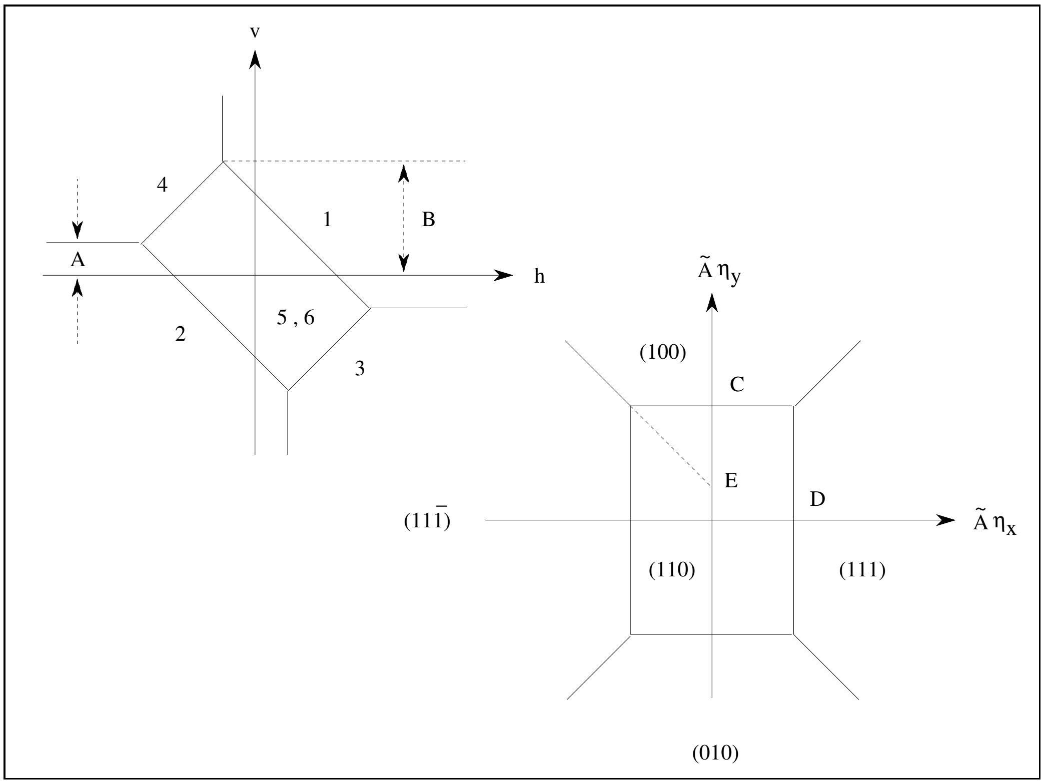

Figure 5. $T = 0$ view of the free energy in the (h, v)– and (η_x, η_y)–plane. The values of the parameters indicated read $A = \frac{J_1 - J_2}{2}$, $B = \frac{J_1 + J_2}{2}$, $C = J_1$, $D = J_2$ and $E = \sqrt{2}(J_1 - J_2)$; $\widetilde{A}$ is. the area of a vertex (*cf.* section 2.2.2)

When h reaches some critical value h_c, the end points are $a = \pi$ and $b = \gamma$. In the following tables the extrapolation for a and b are presented for different values of h. The data were obtained from numerical solutions of finite–size lattices, from $N = 8$ up to $N = 80$ sites. A standard VBS acceleration technique was used to extrapolate the data (van den Broeck and Schwarz, 1979). For shortness, only the first entries are given. The value of the anisotropy was chosen as $\cosh \gamma = 21$, where $\exp(2h_c) = 10.51787$. The first table is for $\exp(2h) = 9$. The second, for $h = h_c$.

Lattice size	a	b
8	2.226901585	1.186380535
12	2.522418777	1.215745628
16	2.674453171	1.227403536
20	2.766810718	1.233071106
24	2.828778340	1.236225697
28	2.873206253	1.238154458
32	2.906605731	1.239417236
36	2.932624180	1.240288031
40	2.953462078	1.240913442
Extrap. ∞	3.141592659(9)	1.243603723(1)
	$\pi = 3.141592653$	$\gamma = 3.737102242$

Lattice size	a	b
8	1.785583002	2.593887405
12	2.057980434	2.774837295
16	2.213907007	2.891216801
20	2.317825087	2.973733400
24	2.393340584	3.036075744
28	2.451377199	3.085293597
32	2.497766251	3.125418776
36	2.535938455	3.158941520
40	2.568060115	3.187492541
Extrap. ∞	3.141592655(2)	3.73710224(8)
	$\pi = 3.141592653$	$\gamma = 3.737102242$

Consider the curve for which $a = \pi$. In this case, since $R(\alpha)$ is 2π–periodic, (3.2.9) can be solved by Fourier transform. The solution is (Lieb and Wu, 1972)

$$R(\alpha) = \sum_n \frac{e^{-in\alpha}}{2\cosh \gamma n} \qquad -\gamma < \Im(\alpha) < \gamma \tag{3.3.1}$$

Hereafter sums are understood to run from $-\infty$ to ∞ unless otherwise stated. Strictly speaking $R(\alpha)$ is defined on C only, but (3.2.9) can be used to define it outside of this curve. If C is contained in the strip $-\gamma < \Im(\alpha) < \gamma$, then $R(\alpha)$ is analytic in $-\gamma < \Im(\alpha) < \gamma$, but it inherits the poles of $\xi(\alpha)$ at $\pm i\gamma$.

Equation (3.3.1) can be expressed using elliptic functions. Introducing the complete elliptic integrals of the first kind I (I') of modulus k (k'), with $k^2 + k'^2 = 1$ related to γ by (see Erdélyi *et al*, 1953)

$$\frac{I'(k)}{I(k)} = \frac{\gamma}{\pi}$$

the solution of (3.2.9) in a wider domain reads (Gaudin, 1983)

$$R(\alpha) = \frac{I(k)}{\pi}\mathsf{dn}\left(\frac{I(k)\alpha}{\pi}; k\right) \tag{3.3.2}$$

This expression is valid beyond the limits of the strip. However, the presence of a pole at $\alpha = \pm i\gamma$ prevents the convergence of (3.3.1) beyond the smaller domain.

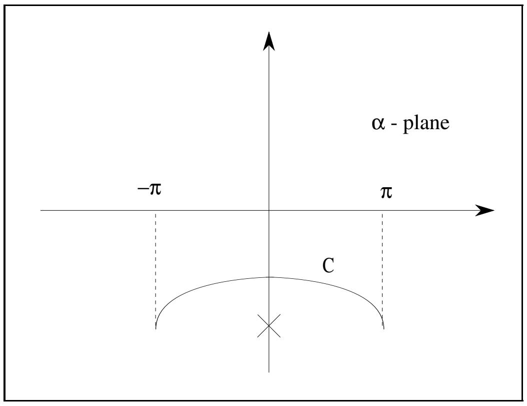

Figure 6. Integration path in the complex α–plane, with pole at $-i\gamma$.

Another important information which can be obtained concerns the precise position of the curve C. From the numerical studies, for fixed γ, h, v one obtains a curve whose endpoint changes with b. As it will be shown next, this allows one to obtain a parametric equation $h(b)$ and $v(b)$ which defines the boundaries of the region where the free energy is determined by the highest eigenvalue of the $y = 0$ polarization sector (the flat phase), and consequently the geometrical form of the (110) facet. In order to do so, one has to revert to (3.2.7). Since $\Theta(\alpha + 2\pi) = \Theta(\alpha) + 2\pi$, one may use the expansion

$$\Theta(\alpha) = \alpha + i \sum_{n \neq 0} \frac{e^{-in\alpha - 2\gamma|n|}}{n} \qquad -2\gamma < \Im(\alpha) < 2\gamma$$

and

$$p^0(\alpha) = \alpha + i \sum_{n \neq 0} \frac{e^{-in\alpha - \gamma|n|}}{n} \tag{3.3.3}$$

These series in (3.3.3) and (3.3.4) converge when $-\gamma < \Im(\alpha) < \gamma$ but also at $\alpha = \pm\pi \pm i\gamma$, because of the alternating sign. Introducing

$$p(\alpha) = \frac{\alpha}{2} + i \sum_{n \neq 0} \frac{e^{-in\alpha}}{2n \cosh \gamma n} = \mathsf{am}\left(\frac{I(k)\alpha}{\pi}; k\right) \tag{3.3.4}$$

from eq. (3.2.7) it follows that

$$p(\alpha) + \frac{ib}{2} + i \sum_{n \neq 0} (-)^n \frac{e^{nb}}{2n \cosh \gamma n} + 2ih = 2\pi x \qquad -\frac{1}{4} \leq x \leq \frac{1}{4}$$

Specialization to the endpoints permits relating the value of h to b (Lieb and Wu, 1972; Nolden, 1992)

$$h(b) = -\frac{b}{2} - \sum_{n=1}^{\infty} (-)^n \frac{\sinh nb}{n \cosh n\gamma} \tag{3.3.5}$$

so that the final equation of the curve is

$$p(\alpha) + ih = 2\pi x \qquad -\frac{1}{4} \leq x \leq \frac{1}{4}$$

One notices that the points on the curve are characterized by

$$\Im(p(\alpha)) + h = 0 \tag{3.3.6}$$

One might suspect that, when $h > h_c = h(b = -\gamma)$, the endpoints of C would remain at $a = \pi$ but with $b < -\gamma$ (or $b > \gamma$ if $h < -h_c$). If C does not cross the point $-i\gamma$ where $\xi(\alpha)$ has a pole, it can always be deformed to the real axis in (3.2.9)

$$R(\alpha) + \frac{1}{2\pi} \int_{-\pi}^{\pi} du K(\alpha - u) R(u) = \xi(\alpha) \tag{3.3.7}$$

so that the solution is still given by $\frac{I(k)}{\pi}\mathsf{dn}\left(\frac{I(k)}{\pi}\alpha; k\right)$, but the expansion (3.3.1) is no longer useful. In this integral $u = \Re(\beta)$. To find the $h(b)$ relation, one closes C in (3.2.7) to the real axis, and take $\alpha = A$

$$p^0(A) - \frac{1}{2\pi} \int_{-\pi}^{\pi} du \Theta(A - u) R(u) + \int_{-\pi}^{A} d\beta R(\beta) + 2ih = -\frac{\pi}{2} \tag{3.3.8}$$

The integral of $R(\alpha)$ is obtained by integrating both sides of (3.3.7), and from (3.3.8) one concludes

$$2h(b) = b + 2\ln\frac{\cosh\left(\frac{\gamma}{2}-\frac{b}{2}\right)}{\cosh\left(\frac{\gamma}{2}+\frac{b}{2}\right)} + 2\sum_{n>0}(-)^n\frac{e^{-2n\gamma}\sinh nb}{n\cosh n\gamma} \qquad (3.3.9)$$

which reduces to (3.3.5) when $|b| \leq \gamma$. Eq. (3.3.9) though cannot give the right dependence $h(b)$ at $|b| > \gamma$, because $h(b)$ decreases when $b < -\gamma$ and increases for $b > \gamma$, going back to the range of values it had as $b \in [-\gamma, \gamma]$. Clearly the initial assumption $a = \pi$ cannot be correct. To gain more insight one may resort as usual to the numerical solution of (3.2.5) which shows that, as $h > h_c$, the curve with $y = 0$ has endpoints at (see table below)

$$b = -\gamma \qquad a < \pi$$

This (new) result is used in the calculation of the free energy singularity in section 3.4. The following table shows the convergence of a and b for $e^{2h} = 18$ (*cf.* data for $h < h_c$ and $h = h_c$). As before, the extrapolated values were obtained from lattice sizes up to 80.

Lattice size	a	b
8	1.345603261	3.0497549071
12	1.479730321	3.2366686985
16	1.535932819	3.3472122872
20	1.564274277	3.4190538006
24	1.580405494	3.4690826450
28	1.590409443	3.5057653322
32	1.597021761	3.5337453681
36	1.601612009	3.5557588049
40	1.604924714	3.5735136386
Extrap. ∞	1.6193362(3)	3.737102232(7)
	$\pi = 3.141592653$	$\gamma = 3.737102242$

In the domain of interest, that is $-\pi < \Re(\alpha) < \pi$ and $0 < \theta < \gamma$, $f_{\rm R}(\alpha;\theta)$ has cuts in the α–plane from $i(\gamma - 2\theta)$ to $i\infty$ and from $-i(\gamma + 2\theta)$ to $-i\infty$, while $f_{\rm L}(\alpha;\theta)$ has cuts from $i(3\gamma - 2\theta)$ to $i\infty$ and from $i(\gamma - 2\theta)$ to $-i\infty$.

When $-h_c \leq h \leq h_c$ and for small enough values of v, the state defined by C $(a = \pi; -\gamma \leq b \leq \gamma)$ also yields the largest eigenvalue of the transfer matrix. The free energy [1]

$$f(\theta,\gamma,h,v) = -2\sum_{n=1}^{\infty}\frac{e^{-2\gamma n}}{n\cosh\gamma n}\sinh(n\theta)\sinh n(\gamma-\theta) \qquad (3.3.10)$$

is constant in a whole region of the (h, v) plane bounded by a curve Γ ('flat' phase). The parametric equation $(h(b), v(b))$ of Γ is given by (3.3.7) and by

$$v(b) = -\frac{\partial F}{\partial y}\bigg|_{\text{h fixed, y=0}}$$

[1]The only part in which the analysis present here differs from Nolden (1992) is that $\Lambda_{\rm R}$ is exponentially larger for $d < \gamma - 2\theta$ and $\Lambda_{\rm L}$ for $d > \gamma - 2\theta$ where id is the point in which C crosses the imaginary axis. A comparison of (3.3.10) with the cited author should take into account the different normalization of the Boltzmann weights.

which can be explicitly computed

$$2v(b) = \gamma - |\gamma - 2\theta + b| + 2\sum_{n=1}^{\infty} \frac{(-)^n}{n} \frac{\sinh[n(\gamma - |\gamma - 2\theta - b|)]}{\cosh n\gamma} \qquad -\gamma \le b \le \gamma \tag{3.3.11}$$

The other half of the curve Γ can be recovered from the symmetry $f(-h,-v) = f(h,v)$ of the free energy (see fig. 7). This topic is discussed briefly: under the action of the (unitary) charge conjugation operator

$$C = \prod_{k=1}^{N} \sigma_k^x \qquad C = C^\dagger = C^{-1}$$

which in the basis of the rapidities reads

$$\langle \underline{\alpha}, C\underline{\alpha}' \rangle = \prod_{k=1}^{N} \delta_{\alpha_k, -\alpha'_k}$$

the transfer matrix tranforms as

$$C\ \tau(\gamma,\theta,h,v)\ C\Big|_{\underline{\alpha},\underline{\alpha}'} = \tau(\gamma,\theta,-h,-v)\Big|_{\underline{\alpha},\underline{\alpha}'} \tag{3.3.12}$$

This follows directly from the definition (3.2.3) of the Botzmann weights. It implies moreover in the relation between spectra

$$\mathcal{S}_{TM}\{h,v,S^z\} = \mathcal{S}_{TM}\{-h,-v,-S^z\} \tag{3.3.13}$$

This symmetry manifests itself in the fact that the partition function satisfies

$$\mathbf{Z}(h,v) = \mathbf{Z}(-h,-v)$$

3.4 The Free Energy Singularity and Exponents of the ECS

As long as the field is bound to values within the region delimited by Γ, the free energy of the asymmetric six–vertex remains invariant, i.e. $f(h,v) = f(0,0)$ and the polarization remains at $y = 0$. It is noteworthy saying that the same holds for the associated spin chain (Albertini, Dahmen and Wehefritz, 1996a), in which case the ground state energy is independent of the strength of the field and belongs to the sector of zero magnetization $S^z = \frac{1}{2}\sum \sigma^z = 0$. As the field crosses the critical value of the Γ line (3.3.5), (3.3.11) the system enters a phase where horizontal and vertical polarizations change continuously. This is an incommensurate phase belonging to the universality class of the gaussian model (Noh and Kim, 1995). It is interesting to determine the singularity of the free energy as (h,v) approach Γ from the incommensurate regime.

It is widely believed that the free energy singularity should be governed by a universal exponent $\frac{3}{2}$ (van Beijeren, 1977; Nolden, 1992). An exact calculation has been done by Lieb and Wu (1972) only when $h = 0$, in which case

$$f \sim c(\gamma,\theta)\Big[v - v_c(\gamma,\theta,b=0)\Big]^{\frac{3}{2}}$$

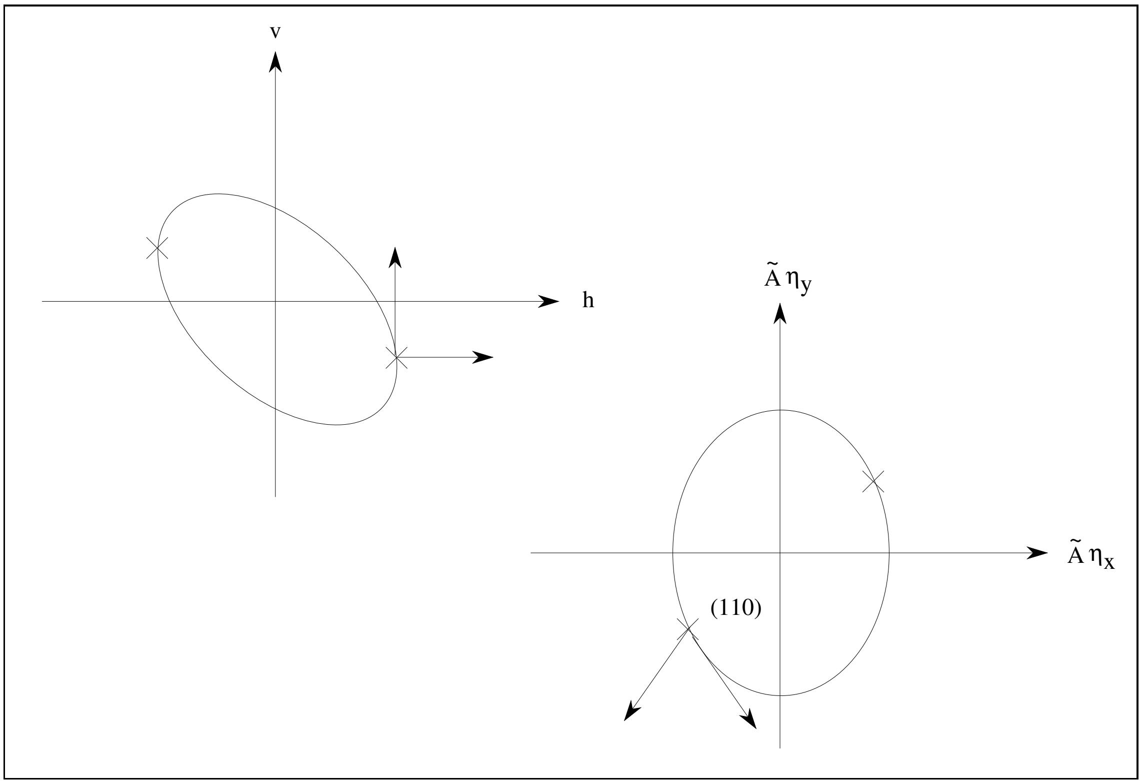

Figure 7. Parametric plot of Γ for $\cosh\gamma = 21$ and spectral parameter $\theta = \frac{1}{2}$ in the (h, v)– and (η_x, η_y)–plane respectively. The latter corresponds to the boundaries of the (110) fcc facet. In the first plot the special points (h_c, v_c) (lower half–plane) and $(-h_c, -v_c)$ (upper half-plane) are singled out. At these points the normal and tangent to the curve are parallel to the h and v axis respectively. Expansions of the free energy are performed in the vicinity of these points (*cf.* discussion in the next section).

Jayaprakash and Saam (1984) have performed a similar calculation in the (η_x, η_y)–plane for $\eta_y = 0$ and obtained

$$\overline{f} \sim \overline{f_0} + \mathsf{constant} \times (\eta_x - \eta_x^{crit})^{3/2} + \mathcal{O}(\delta\eta_x^2)$$

for the leading order terms in the expansion of Andreev's free energy. In terms of the ECS, this implies that

$$z = z_0 + \mathsf{constant} \times (x - x_0)^{3/2}$$

that is, the rounding-off of the edge where the (110) facet meets the other facets is governed by an exponent $\frac{3}{2}$ when approaching the surface in the normal direction. In this scenario, Lieb and Wu's result implies the same exponent, but when approaching the surface along the straight line $\eta_x = -\frac{\eta_y}{\sqrt{2}}$.

Is this however the whole picture? To answer this question, one must perform a series of Taylor expansions on the quantities leading to the free energy. The details of the calculation are lengthy but straightforward (Albertini, Dahmen and Wehefritz, 1996b).

Eqs. (3.2.7) and (3.2.8–3.2.11) determine, through the solution of (3.2.9), f, y and h as functions of A and B. Assuming this dependence to be analytic, that f, y and h can be expanded in powers of δA, δB as $A \to A + \delta A$, $B \to B + \delta B$ and making explicit the dependence of $R(\alpha)$ on A, B by writing $R(\alpha; A, B)$, one has, from (3.2.8)

$$\partial_A y(A, B) \quad = \quad -\frac{2}{2\pi}\int_A^B d\alpha \partial_A R(\alpha; A, B) + \frac{2}{2\pi} R(A; A, B)$$

$$\begin{aligned}
\partial_B y(A,B) &= -\frac{2}{2\pi}\int_A^B d\alpha \partial_B R(\alpha;A,B) - \frac{2}{2\pi}R(B;A,B) \\
\delta y &= \partial_A y(A,B)\delta A + \partial_B y(A,B)\delta B + \mathcal{O}(\delta A^2, \delta B^2, \delta A\delta B)
\end{aligned} \tag{3.4.1}$$

Likewise, the specific free energy is obtained by considering the expansion of $\frac{\ln \Lambda}{N}$. The cases Λ_{R} and Λ_{L} should be treated seperately, but one may limit oneself to the region where the first is dominant (when $d < \gamma - 2\theta$, id being the point where the curve C crosses the imaginary axis in the α–plane). So, the aim is to look for the variation of (see (3.2.14))

$$-\delta(F(\theta,\gamma,h,y) + vy) = -\delta F - \delta y(v_c + \delta v)$$

The expansion to be determined is that of (see (3.2.10))

$$G_{\mathrm{R}} = \frac{1}{2\pi}\int_A^B d\alpha R(\alpha) f_{\mathrm{R}}(\alpha;\theta)$$

In other words

$$\begin{aligned}
\partial_A G_{\mathrm{R}}(A,B) &= \frac{1}{2\pi}\int_A^B d\alpha f_{\mathrm{R}}(\alpha;\theta)\partial_A R(\alpha;A,B) - \frac{1}{2\pi} f_{\mathrm{R}}(A;\theta)R(A;A,B) \\
\partial_B G_{\mathrm{R}}(A,B) &= \frac{1}{2\pi}\int_A^B d\alpha f_{\mathrm{R}}(\alpha;\theta)\partial_B R(\alpha;A,B) + \frac{1}{2\pi} f_{\mathrm{R}}(B;\theta)R(A;A,B) \\
\delta G_{\mathrm{R}}(A,B) &= \partial_A G_{\mathrm{R}}(A,B)\delta A + \partial_B G_{\mathrm{R}}(A,B)\delta B + \mathcal{O}(\delta A^2, \delta B^2, \delta A\delta B)
\end{aligned} \tag{3.4.2}$$

Similar equations can be obtained for h, specializing (3.2.7) to the endpoints of the curve and taking the more symmetric expression

$$-4ih(A,B) = p^0(A) + p^0(B) - \frac{1}{2\pi}\int_A^B d\beta R(\beta;A,B)\Big[\Theta(A-\beta) + \Theta(B-\beta)\Big]$$

over eq. (3.2.7). After some straightforward calculation

$$\begin{aligned}
-4i\partial_A h(A,B) &= -\frac{1}{2\pi}\int_A^B d\beta \partial_A R(\beta;A,B)\Big[\Theta(A-\beta) + \Theta(B-\beta)\Big] \\
&\quad + R(A;A,B)\Big[1 + \frac{1}{2\pi}\Theta(B-A)\Big] \\
-4i\partial_B h(A,B) &= -\frac{1}{2\pi}\int_A^B d\beta \partial_B R(\beta;A,B)\Big[\Theta(A-\beta) + \Theta(B-\beta)\Big] \\
&\quad + R(B;A,B)\Big[1 + \frac{1}{2\pi}\Theta(B-A)\Big]
\end{aligned}$$

To determine these expansions one has to determine first those for the rapidity density. A detailed expansion of $R(\alpha)$ is presented in what follows. These results are used to obtain the expansion of y.

Perturbative Calculation of the Rapidity Density, eq. (3.2.9)

$R(\alpha;A,B)$ is assumed analytical in all variables. To simplify the notation, one may write $R(\alpha) = R(\alpha;A,B)$ and $R(A) = R(\alpha = A;A,B)$, the same being valid for $R(B)$.

First Order

$$\begin{aligned}
\partial_A R(\alpha) + \frac{1}{2\pi}\int_A^B d\beta K(\alpha-\beta)\partial_A R(\beta) &= \frac{1}{2\pi}K(\alpha-A)R(A) \\
\partial_B R(\alpha) + \frac{1}{2\pi}\int_A^B d\beta K(\alpha-\beta)\partial_B R(\beta) &= -\frac{1}{2\pi}K(\alpha-B)R(B)
\end{aligned} \tag{3.4.3}$$

Second Order

$$\begin{aligned}
\partial_A^2 R(\alpha) + \frac{1}{2\pi}\int_A^B d\beta K(\alpha-\beta)\partial_A^2 R(\beta) &= \frac{1}{2\pi}K(\alpha-A)\Big[2\partial_A R(A) + R'(A)\Big] \\
&- \frac{1}{2\pi}K'(\alpha-A)R(A) \\
\partial_B^2 R(\alpha) + \frac{1}{2\pi}\int_A^B d\beta K(\alpha-\beta)\partial_B^2 R(\beta) &= -\frac{1}{2\pi}K(\alpha-B)\Big[2\partial_B R(B) + R'(B)\Big] \\
&+ \frac{1}{2\pi}K'(\alpha-B)R(B) \\
\partial_A\partial_B R(\alpha) + \frac{1}{2\pi}\int_A^B d\beta K(\alpha-\beta)\partial_A\partial_B R(\beta) &= -\frac{1}{2\pi}K(\alpha-B)\partial_A R(B) \\
&+ \frac{1}{2\pi}K(\alpha-A)\partial_B R(A)
\end{aligned} \tag{3.4.4}$$

A prime indicates a derivative with respect to the variable α.

Third Order

$$\begin{aligned}
\partial_A^3 R(\alpha) + \frac{1}{2\pi}\int_A^B d\beta K(\alpha-\beta)\partial_A^3 R(\beta) &= \frac{1}{2\pi}K(\alpha-A) \\
&\times \Big[3\partial_A^2 R(A) + 3\partial_A R'(A) + R''(A)\Big] \\
&- \frac{1}{2\pi}K'(\alpha-A)\Big[3\partial_A R(A) + 2R'(A)\Big] \\
&+ \frac{1}{2\pi}K''(\alpha-A) \\
\partial_B^3 R(\alpha) + \frac{1}{2\pi}\int_A^B d\beta K(\alpha-\beta)\partial_B^3 R(\beta) &= -\frac{1}{2\pi}K(\alpha-B) \\
&\times \Big[3\partial_B^2 R(B) + 3\partial_B R'(B) + R''(B)\Big] \\
&+ \frac{1}{2\pi}K'(\alpha-B)\Big[3\partial_B R(B) + 2R'(B)\Big] \\
&- \frac{1}{2\pi}K''(\alpha-B) \\
\partial_B\partial_A^2 R(\alpha) + \frac{1}{2\pi}\int_A^B d\beta K(\alpha-\beta)\partial_B\partial_A^2 R(\beta) &= \frac{1}{2\pi}K(\alpha-A)\Big[2\partial_A\partial_B R(A) + \partial_B R'(A)\Big] \\
&- \frac{1}{2\pi}K(\alpha-B)\partial_A^2 R(B) \\
&- \frac{1}{2\pi}K'(\alpha-B)\partial_B R(A) \\
\partial_A\partial_B^2 R(\alpha) + \frac{1}{2\pi}\int_A^B d\beta K(\alpha-\beta)\partial_A\partial_B^2 R(\beta) &= -\frac{1}{2\pi}K(\alpha-B)\Big[2\partial_A\partial_B R(B) + \partial_A R'(B)\Big] \\
&+ \frac{1}{2\pi}K(\alpha-A)\partial_B^2 R(A) \\
&+ \frac{1}{2\pi}K'(\alpha-A)\partial_A R(B)
\end{aligned} \tag{3.4.5}$$

Finally, the derivatives with respect to the variable α are given by

$$\begin{aligned} R'(\alpha) + \frac{1}{2\pi}\int_A^B d\beta K(\alpha-\beta)R'(\beta) &= \xi'(\alpha) \\ &+ \frac{1}{2\pi}\Big[K(\alpha-B)R(B) - K(\alpha-A)R(A)\Big] \end{aligned} \tag{3.4.6}$$

$$\begin{aligned} R''(\alpha) + \frac{1}{2\pi}\int_A^B d\beta K(\alpha-\beta)R''(\beta) &= \xi''(\alpha) \\ &+ \frac{1}{2\pi}\Big[K(\alpha-B)R'(B) - K(\alpha-A)R'(A)\Big] \\ &+ \frac{1}{2\pi}\Big[K'(\alpha-B)R(B) - K'(\alpha-A)R(A)\Big] \end{aligned} \tag{3.4.7}$$

and so on.

Equations (3.4.3–3.4.7) must be specialized to the values $A = A_0 = -\pi - i\gamma$ and $B = B_0 = \pi - i\gamma$. $R(\alpha)$ is periodic of 2π and the last term of (3.4.7) cancels. It follows that $R'(\alpha)$ is also periodic. Hence, denoting $R(\alpha; A_0, B_0) = R_0(\alpha)$ one gets

$$R_0'(\alpha) + \frac{1}{2\pi}\int_A^B d\beta K(\alpha-\beta)R_0'(\beta) = \xi'(\alpha) \tag{3.4.8}$$

$$R_0''(\alpha) + \frac{1}{2\pi}\int_A^B d\beta K(\alpha-\beta)R_0''(\beta) = \xi''(\alpha) \tag{3.4.9}$$

One may now calculate (3.4.3–3.4.5) by noticing that $R_0(A_0) = R_0(B_0) = 0$ since the dn function has zeroes at $\pm I(k) \pm I'(k)$, where $\frac{I'(k)}{I(k)} = \frac{\gamma}{\pi}$ (see discussion prior to eq. (3.3.2)). Therefore, one has

First order

$$\partial_A R_0(\alpha) = \partial_B R_0(\alpha) = 0 \qquad \forall\alpha \tag{3.4.10}$$

since in the expression $\partial_A R(\alpha) + \frac{1}{2\pi}\int_{A_0}^{B_0} d\beta K(\alpha-\beta)\partial_A R(\beta) = 0$ the integral vanishes since both $K(\alpha-\beta)$ and $\partial_A R(\beta)$ are periodic.

Second order

One gets further

$$\begin{aligned} \partial_A^2 R_0(\alpha) + \frac{1}{2\pi}\int_{A_0}^{B_0} d\beta K(\alpha-\beta)\partial_A^2 R_0(\beta) &= \frac{1}{2\pi}K(\alpha-A_0)R'(A_0) \\ \partial_B^2 R_0(\alpha) + \frac{1}{2\pi}\int_{A_0}^{B_0} d\beta K(\alpha-\beta)\partial_B^2 R_0(\beta) &= -\frac{1}{2\pi}K(\alpha-B_0)R'(B_0) \\ \partial_A\partial_B R_0(\alpha) &= \partial_B\partial_A R_0(\alpha) = \quad 0 \end{aligned} \tag{3.4.11}$$

where the same property on the periodicity of the integral has been used, as in (3.4.9). Since both $\partial_A^2 R_0(\alpha)$ and $\partial_B^2 R_0(\alpha)$ are periodic of 2π it follows that

$$\partial_A^2 R_0(A_0) = \partial_A^2 R_0(B_0) \qquad \partial_B^2 R_0(A_0) = \partial_B^2 R_0(B_0)$$

as well as the periodicity of R_0' implies

$$\partial_A^2 R_0(\alpha) = -\partial_B^2 R_0(\alpha)$$

In the most general case, $\partial_A^2 R_0(A_0) \neq 0$ and one sets

$$\partial_A^2 R_0(A_0) = \partial_A^2 R_0(B_0) = -\partial_B^2 R_0(A_0) = -\partial_B^2 R_0(A_0) = r_3 \tag{3.4.12}$$

Third order

To obtain the equations at order 3 one needs $\partial_A R'(\alpha)$ and $\partial_B R'(\alpha)$ calculated at the endpoints of C. Since

$$\partial_A R_0'(\alpha) = \partial_B R_0'(\alpha) = 0 \qquad \forall\alpha$$

and the constants $R'(A_0) = R'(B_0)$ and $R''(A_0) = R''(B_0)$ can be obtained directly from the properties of the dn function,

$$\begin{aligned} R_0'(\alpha) &= \left(\frac{I(k)}{\pi}\right)^2 \mathsf{dn}'(\beta;k)\Big|_{\beta=\frac{I(k)}{\pi}\alpha} \\ R_0''(\alpha) &= \left(\frac{I(k)}{\pi}\right)^3 \mathsf{dn}''(\beta;k)\Big|_{\beta=\frac{I(k)}{\pi}\alpha} \end{aligned} \tag{3.4.13}$$

it is not difficult to see that

$$R_0''(A_0) = R_0''(B_0) = 0 \tag{3.4.14}$$

since dn'' vanishes where the dn function does (Erdélyi *et al*, 1953). However the same is not true for dn', so that $R_0'(A_0) = R_0'(B_0) \neq 0$. Setting

$$R_0'(A_0) = R_0'(B_0) = r_1 \tag{3.4.15}$$

One finally has

$$\begin{aligned} \partial_A^3 R_0(\alpha) + \frac{1}{2\pi}\int_{A_0}^{B_0} d\beta K(\alpha-\beta)\partial_A^3 R_0(\beta) &= \frac{3r_3}{2\pi}K(\alpha-A_0) - \frac{r_1}{\pi}K'(\alpha-A_0) \\ \partial_B^3 R_0(\alpha) + \frac{1}{2\pi}\int_{A_0}^{B_0} d\beta K(\alpha-\beta)\partial_B^3 R_0(\beta) &= \frac{3r_3}{2\pi}K(\alpha-B_0) + \frac{r_1}{\pi}K'(\alpha-B_0) \\ \partial_B\partial_A^2 R_0(\alpha) + \frac{1}{2\pi}\int_{A}^{B} d\beta K(\alpha-\beta)\partial_B\partial_A^2 R_0(\beta) &= -\frac{r_3}{2\pi}K(\alpha-B_0) \\ \partial_A\partial_B^2 R_0(\alpha) + \frac{1}{2\pi}\int_{A}^{B} d\beta K(\alpha-\beta)\partial_A\partial_B^2 R_0(\beta) &= -\frac{r_3}{2\pi}K(\alpha-A_0) \end{aligned} \tag{3.4.16}$$

One notices that $\partial_B\partial_A^2 R_0(\alpha) = \partial_A\partial_B^2 R_0(\alpha)$ $\forall\alpha$, since K is 2π–periodic.

All integrals can be treated in an analogous way. Integrands are periodic of 2π and the integration contour defined by C can be closed with the segment $[-\pi,\pi]$ of the real axis, by joining them through two straight segments parallel to the imaginary axis, that is $\Re(\alpha) = \pm\pi$ and $\Im(\alpha) \in [-\gamma, 0]$. Since no poles are inclosed, the contour integral is zero. The contribution from the two straight lines cancel since integrands are periodic. The integral over C is therefore reduced to an integral over the real axis, from $[-\pi,\pi]$. As an example, the first integral equation in (3.4.11) becomes

$$\partial_A^2 R_0(u) + \frac{1}{2\pi}\int_{-\pi}^{\pi} dv K(u-v)\partial_A^2 R_0(v) = \frac{r_1}{2\pi}K(u+\pi+i\gamma) \tag{3.4.17}$$

with $u = \Re(\alpha)$ and $v = \Re(\beta)$. The solution is obtained through Fourier transforms (Nolden, 1992)

$$\partial_A^2 R_0(\alpha) = -\partial_B^2 R_0(\alpha) = \frac{r_1}{2\pi} \sum_{n=-\infty}^{\infty} (-)^n e^{-in\alpha} \frac{e^{\gamma(n-|n|)}}{2\cosh(\gamma n)} \tag{3.4.18}$$

From this result and the fact that $r_3 = \partial_A^2 R_0(-\pi - i\gamma)$ one sees that both r_1 and r_3 are related

$$r_3 = \frac{r_1}{2\pi} \sum_{n=-\infty}^{\infty} \frac{e^{-\gamma|n|}}{2\cosh(\gamma n)} \tag{3.4.19}$$

One is thus led to

$$\begin{aligned}
\partial_A^3 R_0(\alpha) &= \frac{1}{2\pi} \sum_{n=-\infty}^{\infty} (-)^n e^{-in\alpha} \frac{e^{\gamma(n-|n|)}}{2\cosh(\gamma n)} (3r_3 + 2inr_1) && (3.4.20)\\
\partial_B^3 R_0(\alpha) &= \frac{1}{2\pi} \sum_{n=-\infty}^{\infty} (-)^n e^{-in\alpha} \frac{e^{\gamma(n-|n|)}}{2\cosh(\gamma n)} (3r_3 - 2inr_1) && (3.4.21)\\
\partial_A \partial_B^2 R_0(\alpha) &= \partial_B \partial_A^2 R_0(\alpha) = -\frac{r_3}{2\pi} \sum_{n=-\infty}^{\infty} (-)^n e^{-in\alpha} \frac{e^{\gamma(n-|n|)}}{2\cosh(\gamma n)} && (3.4.22)
\end{aligned}$$

With this result one may now proceed to get the expansion of the polarization y.

Perturbative Calculation of the Polarization

The first order expansion of y is given by (3.4.1). Since the expansion is especialized to the zeroes of the dn function, from (3.4.10) it follows that

$$\partial_A y_0 = \partial_B y_0 = 0 \tag{3.4.23}$$

The second order terms follow accordingly

$$\begin{aligned}
\partial_A^2 y(A,B) &= -\frac{1}{\pi} \int_A^B d\alpha \partial_A^2 R(\alpha) + \frac{2}{\pi} \partial_A R(A) + \frac{1}{\pi} R'(A)\\
\partial_B^2 y(A,B) &= -\frac{1}{\pi} \int_A^B d\alpha \partial_B^2 R(\alpha) - \frac{2}{\pi} \partial_B R(B) - \frac{1}{\pi} R'(B)\\
\partial_A \partial_B y(A,B) &= -\frac{1}{\pi} \int_A^B d\alpha \partial_A \partial_B R(\alpha) - \frac{1}{\pi} \partial_A R(B) + \frac{1}{\pi} \partial_B R(A)\\
\partial_B \partial_A y(A,B) &= -\frac{1}{\pi} \int_A^B d\alpha \partial_B \partial_A R(\alpha) + \frac{1}{\pi} \partial_A R(B) - \frac{1}{\pi} \partial_B R(A) && (3.4.24)
\end{aligned}$$

Considering the previous results one has, after especializing the expressions for A_0 and B_0

$$\begin{aligned}
\partial_A^2 y_0 &= -\frac{1}{\pi} \int_{A_0}^{B_0} d\alpha \partial_A^2 R_0(\alpha) + \frac{1}{\pi} \underbrace{R'(A_0)}_{r_1}\\
&= -\frac{r_1}{\pi} \sum_n (-)^n \frac{e^{\gamma(n-|n|)}}{2\cosh\gamma} \underbrace{\frac{1}{2\pi} \int_{-\pi}^{\pi} du e^{-inu}}_{\delta_{n,0}} + \frac{r_1}{\pi}\\
&= \frac{r_1}{2\pi}\\
&= -\partial_B^2 y_0 && (3.4.25)
\end{aligned}$$

It is straighforward to show that

$$\partial_A \partial_B y_0 = \partial_B \partial_A y_0 = 0 \tag{3.4.26}$$

Considering the third order terms in the expansion of y we have

$$\begin{aligned}
\partial_A^3 y(A,B) &= -\frac{1}{\pi}\int_A^B d\alpha \partial_A^3 R(\alpha) + \frac{3}{\pi}\partial_A^2 R(A) + \frac{3}{\pi}\partial_A R'(A) + \frac{1}{\pi}R''(A) \\
\partial_B^3 y(A,B) &= -\frac{1}{\pi}\int_A^B d\alpha \partial_B^3 R(\alpha) - \frac{3}{\pi}\partial_B^2 R(B) - \frac{3}{\pi}\partial_B R'(B) - \frac{1}{\pi}R''(B) \\
\partial_A \partial_B^2 y(A,B) &= -\frac{1}{\pi}\int_A^B d\alpha \partial_A \partial_B^2 R(\alpha) - \frac{1}{\pi}\partial_B^2 R(B) - \frac{2}{\pi}\partial_A \partial_B R(B) - \frac{1}{\pi}\partial_A R'(B) \\
\partial_B \partial_A^2 y(A,B) &= -\frac{1}{\pi}\int_A^B d\alpha \partial_B \partial_A^2 R(\alpha) + \frac{1}{\pi}\partial_B^2 R(A) + \frac{2}{\pi}\partial_B \partial_A R(A) + \frac{1}{\pi}\partial_B R'(A)
\end{aligned} \tag{3.4.27}$$

At the endpoints of the curve C we have

$$\begin{aligned}
\partial_A^3 y_0 &= -\frac{1}{\pi}\int_{A_0}^{B_0} d\alpha \partial_A^3 R_0(\alpha) + \frac{3}{\pi}\underbrace{\partial_A^2 R(A_0)}_{=r_3} + \frac{3}{\pi}\underbrace{\partial_A R'(A_0)}_{\partial_A r_1 = 0} + \frac{1}{\pi}\underbrace{R''(A_0)}_{=0} \\
&= -\frac{3r_3}{2\pi} + \frac{3r_3}{\pi} \\
&= \frac{3r_3}{2\pi} \\
&= \partial_B^3 y_0
\end{aligned} \tag{3.4.28}$$

Finally

$$\begin{aligned}
\partial_A \partial_B^2 y_0 &= \frac{1}{\pi}\int_{A_0}^{B_0} d\alpha \partial_A \partial_B^2 R_0(\alpha) - \frac{1}{\pi}\underbrace{\partial_B^2 R(B_0)}_{=0} - \frac{2}{\pi}\underbrace{\partial_A \partial_B R(B_0)}_{=0} - \frac{1}{\pi}\underbrace{\partial_A R'(B_0)}_{=0} \\
&= -\frac{r_3}{2\pi} \\
&= \partial_B \partial_A^2 y_0
\end{aligned} \tag{3.4.29}$$

All remaining expansions have been carried out up to the third order in $\delta A, \delta B$. In principle they can be used for any A, B with $a = \pi, |b| \leq \gamma$, and the integrals computed by Fourier transform. However, as it is already evident from the first order terms and the above results for y, the expansions for h and f also simplify considerably when carried out around $A_0 = -\pi \pm i\gamma, B_0 = \pi \pm i\gamma$. These points correspond, through (3.3.5) and (3.3.11), to the critical point (h_c, v_c). In the (h,v)–plane this point has also the property that δh and δv are exactly normal and tangential to the curve Γ respectively (see fig. 8). Writing

$$\delta A = -\delta a + i\delta b \qquad \delta B = \delta a + i\delta b$$

and considering first the expansion around $A_0 = -\pi - i\gamma, B_0 = \pi - i\gamma$, one has

$$\delta f = 2c_2[(\delta a)^3 - 3\delta a(\delta b)^2] - \delta v \delta y + \ldots \tag{3.4.30}$$

$$\delta y = -\frac{c_1}{\pi}\delta a \delta b + \frac{c_3}{\pi}\delta b(\delta a)^2 + \ldots \tag{3.4.31}$$

$$\delta h = \frac{c_1}{2}[(\delta a)^2 - (\delta b)^2] + \frac{c_3}{3}(\delta a)^3 + \ldots \tag{3.4.32}$$

with

$$\begin{aligned}
c_1 &= k'(\frac{I(k)}{\pi})^2 > 0 \\
\frac{c_2}{c_1} &= \frac{1}{6\pi}\left[\frac{1}{2} + \sum_{n>0} \frac{(-1)^n \cosh(\gamma(n-2\theta))}{\cosh(n\gamma)}\right] > 0 \\
\frac{c_3}{c_1} &= \frac{1}{\pi}\sum_n \frac{\exp(-|n|\gamma)}{2\cosh\gamma n} > 0
\end{aligned}$$

It is important to notice that $\delta y = 0 = \delta f$ when $\delta a = 0$, as it should, since by taking $\delta a = 0$ and $\delta b > 0$ one reenters the 'flat phase'. It is also important to check that if $\delta a = 0$ there is no way to increase h by changing b. An increase in h, when keeping y fixed at $y = 0$, can instead be achieved by $\delta a < 0, \delta b = 0$, which confirms the numerical findings already discussed. A variation $\delta a > 0$ is ruled out *a priori*, because the periodicity of (3.2.5) in the real direction implies that rapidities are contained in the strip $-\pi \leq \Re(\alpha) \leq \pi$ and a cannot exceed π.

Another point to discuss is the reliability of (3.4.30)–(3.4.32) when $n > N/2$, that is $\delta y < 0$. The Bethe-ansatz equations for the symmetric six vertex model are always discussed keeping $n \leq N/2$, since the arrow reversal symmetry guarantees that the spectrum is the same when $N/2 < n \leq N$. It is not immediately clear what happens to (3.2.4) when $n > N/2$. As an example, consider the one dimensional sector $S^z = -N$ $(n = N)$, whose only eigenstate is $|\downarrow\downarrow\downarrow\cdots\downarrow\rangle$. It is not obvious that (3.2.4) should have only one solution when the number of unknowns is N. To be on the safe side one must trust (3.4.30)–(3.4.32) only for $n \leq \frac{N}{2}$ $(y \geq 0)$. In this case $\delta b \geq 0$ and $\delta a \leq 0$. To deal with the states at $n > \frac{N}{2}$ $(y < 0)$, one must resort to the symmetry properties of f, which imply

$$f(\gamma, h_c + \delta h, v_c + \delta v, -y) = f(\gamma, -h_c - \delta h, -v - \delta v, y) \tag{3.4.33}$$

Hence it is necessary to consider also an expansion around $h = -h_c, y = 0$. This can be done by evaluating (3.4.1) and the following equations at the endpoints $A_0' = -\pi + i\gamma, B_0' = \pi + i\gamma$. The result is that (3.4.30)–(3.4.32) still hold, with $\delta b > 0$ (< 0) if $\delta y > 0$ (< 0). A final observation about (3.4.30)–(3.4.32) is that it is legitimate to neglect higher order terms in (3.4.31) and (3.4.32). The parameters δa and δb are independent and there is no control over their relative magnitude, but the second order term in (3.4.32) is dominant unless $\delta a \simeq \pm\delta b$, in which case the third order term is certainly larger than all possible fourth order terms. Likewise, in (3.4.31) no term δa^n or δb^n is allowed since $\delta y = 0$ if $\delta a = 0$ or $\delta b = 0$. Consequently, all higher order terms can certainly be neglected and one can further limit the expansion to

$$\delta y = -\frac{c_1}{\pi}\delta a \delta b$$

Suppose now that h is kept fixed at h_c and $\delta v \neq 0$. Then, from (3.4.32),

$$\delta b = \mp \delta a$$

where the upper (lower) sign holds for $\delta y > 0$ (< 0). Consider first $\delta y > 0$. Then

$$\begin{aligned}
\delta y &= \frac{c_1}{\pi}(\delta a)^2 \\
\delta f(\delta a) &= -4c_2(\delta a)^3 - \frac{c_1 \delta v}{\pi}(\delta a)^2
\end{aligned}$$

which has a minimum, when $\delta v > 0$, at

$$\delta a_0 = -\frac{\delta v c_1}{6\pi c_2}$$

that yields

$$\delta f(h = h_c, \delta v > 0) = -\frac{2}{c_2^2}\left(\frac{c_1 \delta v}{6\pi}\right)^3$$

No minimum occurs if $\delta v < 0$. Instead, if $\delta y < 0$, one has a minimum at

$$\delta a_0 = \frac{\delta v c_1}{6\pi c_2}$$

that yields

$$\delta f(h_c, \delta v < 0) = \frac{2}{c_2^2}\left(\frac{c_1 \delta v}{6\pi}\right)^3$$

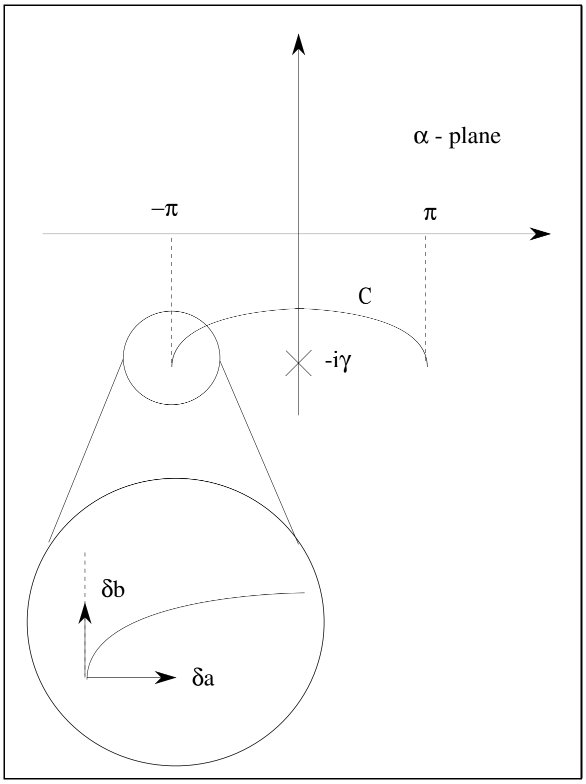

Figure 8. The increments δa and δb at one of the endpoints of the curve C. This point corresponds to (h_c, v_c) in the parametric plot of Γ, see fig. 7.

Consequently,

$$\begin{aligned} f(h_c, v_c + \delta v) &= f(h = h_c, v = v_c) - \frac{2}{c_2^2}\left(\frac{c_1}{6\pi}\right)^3 |\delta v|^3 \\ \delta y &= \mathsf{sign}(\delta v)\frac{c_1}{\pi}\left(\frac{c_1 \delta v}{6\pi c_2}\right)^2 \end{aligned}$$

is the free energy singularity as one approaches the point (h_c, v_c) along the v direction.

The case $\delta v = 0, \delta h \neq 0$ is more involved. One wants $\delta h > 0$, in order to move into the incommensurate phase. From (3.4.30)–(3.4.32)

$$\begin{aligned}
\delta b &= \pm\sqrt{g(\delta a)} \qquad g(\delta a) = \delta a^2 + \frac{2}{3}\frac{c_3}{c_1}\delta a^3 - \frac{2}{c_1}\delta h && (3.4.34)\\
\delta y &= -\frac{c_1}{\pi}\delta a(\pm\sqrt{g(\delta a)}) && (3.4.35)\\
\delta f(\delta a) &= 2c_2\delta a\Big(-2(\delta a)^2 - 2\frac{c_3}{c_1}(\delta a)^3 + \frac{6}{c_1}\delta h\Big) && (3.4.36)
\end{aligned}$$

where the sign in (3.4.35) depends on whether one wants $\delta y > 0$ or $\delta y < 0$. The variation δa must be negative and contained in a range where $g(\delta a)$ is non negative, so if

$$g(\delta a_0) = 0 \qquad \delta a_0 = -\sqrt{\frac{2}{c_1}}(\delta h)^{1/2} + O(\delta h)$$

one considers

$$\delta a \leq \delta a_0$$

It is not difficult to see that there is a left neighborhood of δa_0 (of the order $\delta h^{1/2}$) where

i. $g(\delta a)$ is positive

ii. $\delta y(\delta a)$ is monotonic

iii. $\delta f(\delta a)$ is decreasing

Consequently, regardless of the sign in (3.4.35), $\delta a = \delta a_0$ is a local minimum of $\delta f(\delta a)$, which, incidentally, corresponds to $\delta y = 0$. Inserting δa_0 in (3.4.36)

$$f(h_c + \delta h, v_c) = f(h_c, v_c) - 2c_2\left(\frac{2}{c_1}\delta h\right)^{3/2} \tag{3.4.37}$$

Although it is not obvious from the previous proof, $\delta y = 0$ is actually a stationary point for $\delta f(\delta y)$. In fact

$$\frac{\partial \delta f}{\partial \delta y} = \frac{\frac{\partial \delta e_0}{\partial \delta a}|_{\delta a_0}}{\frac{\partial \delta y}{\partial \delta a}|_{\delta a_0}}$$

and

$$\frac{\partial \delta y}{\partial \delta a} = \pm\Big(-\frac{c_1}{\pi}\sqrt{f(\delta a)} - \frac{c_1}{2\pi}\delta a\frac{f'(\delta a)}{\sqrt{f(\delta a)}}\Big)$$

becomes infinite at δa_0.

The conclusion is therefore that the leading singularities of the free energy when approaching (h_c, v_c) from the incommensurate phase are

$$\begin{aligned}
f(\theta, \gamma, h_c + \delta h, v_c) &= f(\theta, \gamma, h_c, v_c) - 2c_2\left(\frac{2}{c_1}\delta h\right)^{3/2}\\
f(th, \gamma, h_c, v_c + \delta v) &= f(\theta, \gamma, h_c, v_c) - \frac{2}{c_2^2}\left(\frac{c_1}{6\pi}\right)^3 |\delta v|^3
\end{aligned}$$

3.5 Discussion and Experimental Setup

The leading singularity with the exponent 3 is certainly surprising, since in the ECS picture it implies the existence of a *new* rounding exponent of the (110) edge. The results, together with those of previous authors (Lieb and Wu, 1972; Jayaprakash and Saam, 1984) are also a strong indicative that the leading exponent which describes the slope of the edge is indeed $\frac{3}{2}$ unless one approaches the surface tangentially, in which case one then observes the slope exponent 3. Even though the transformation from the (h, v) to the (η_x, η_y)–plane is not orthogonal, the definition of the tangent does not depend on the parametrization of the Γ boundary (as the normal does). This result can be easily extended to the bcc geometry, where the (h, v) and (η_x, η_y) planes are related throught a simple rotation of $\frac{\pi}{4}$. The existence of this new exponent is also supported by recent calculations done by Kim (1996).

The fundamental question is however whether this exponent is a feature only of the special point studied in this work or a general feature of the whole boundary Γ. The point (h_c, v_c) itself is particular in the sense that one may enter the massless phase keeping the polarization at $y = 0$, as discussed in the preceeding sections. In the ECS language, it corresponds to the point where three different facets meet (fig. 5, facets 1, 3 and 5–6). Moving parallel to h (normally to the point in question) means running along the edge between faces 1 and 3. Intuitively one could thus argue that the new exponent should be particular to this point (as well as to all other geometrically equivalent 3–corner edges) and to no other. A proof however is lacking, either for the confirmation or dismissal of this conjecture. Numerical tries remained unsuccesfull since a study of any other point of the boundary not only is hindered by the fact that the polarization changes infinitesimally as one leaves Γ, but also by the fact that one does not know beforehand how to handle δh and δv at the same time. The first point makes it difficult to define an appropriate numerical limit while keeping the value of y fixed (the choice of one y should also be judicial) while the second point is related to how both increments should be added together to define an overall variation away from the boundary. To settle this question one possibility is to resort to an experimental measurement as described below.

Experimental Verification of Slope Exponents

Since the exponents are related to the behavior of the equilibrium crystal shapes close to the boundary of the (110) facet of an fcc crystal, by measuring slopes one should in principle be able to observe them experimentally. In spite of some experimental hindrances, several authors have been able to measure the exponent $\frac{3}{2}$. There is enough experimental evidence that there exists a 'measurement window' between the length scale below which the finite size effects cannot be left aside and the long time scales necessary to reach equilibrium. Rottman *et al* (1984) measured an exponent of 1.60 ± 0.15 in an experiment with small droplets of lead ($\sim$ 2–10μm) grown over a graphite substrate. Carmi, Lipson and Polturak (1987) studied rather large ^4He crystals ($\sim$ 5mm) in equilibrium with its superfluid at $1K$ and observed an exponent of 1.55 ± 0.06 (*hcp* lattice). Ohachi and Taniguchi (1985) found an exponent of 1.45 for plastic crystalline $AgCl$.

If one considers these successes it seems that such an undertaking is feasible, strengthening one's belief that the new exponent found in this work can also be measured. If this is achieved, it would not only confirm the exactness of the method but would also give the six–vertex model a renewed confirmation of its validity as a physical model. A successful experiment would also settle the question regarding the validity of 3 on the particular point or all over the boundary in a irrevocable manner.

The Nature of the Phase transition

It is interesting to speculate about the nature of the phase transition at (h_c, v_c) and compare it with what happens at the other points of Γ. The exponent $\frac{3}{2}$ characterizes what one calls the Pokrovskii–Talapov transition. The PT transition is due to level–crossings in the spectrum of the system. It is also characteristic of the PT line that gaps between the the highest and next–to–highest eigenvalues of the transfer matrix scale as N^{-2}, where N is the linear horizontal dimension of the system.

The results presented here were obtained under the assumption that a complete set of eigenstates of the transfer matrix exists. It is well known then that the correlation function of 2 vertical arrows can be analysed through a spectral decomposition (Johnson, Krinsky and Mccoy, 1973). For the correlator of two vertical arrows along the same column one has, on a $N \times M$ lattice

$$\langle \alpha_{0,0}\ \alpha_{0,n} \rangle = \frac{Tr(\sigma_0^z \tau^n \sigma_0^z \tau^{M-n})}{Tr\ \tau^M} \stackrel{M\to\infty}{\longrightarrow} \sum_k \left| \langle 0|\sigma_0^z|k\rangle \right|^2 \left(\frac{\Lambda_k}{\Lambda_0}\right)^n \tag{3.5.1}$$

and for the correlation function along the horizontal direction

$$\langle \alpha_{0,0}\ \alpha_{n,0} \rangle = \frac{Tr(\sigma_0^z \sigma_n^z \tau^M)}{Tr\ \tau^M} \stackrel{M\to\infty}{\longrightarrow} \langle 0|\sigma_0^z \sigma_n^z|0\rangle \tag{3.5.2}$$

where we have denoted with $|0\rangle$ the eigenstate of the largest eigenvalue of the transfer matrix on a finite lattice of width N. Here $\sum_k$ denotes the sum over a complete set of eigenvectors of the transfer matrix. It is useful to consider first what happens at $h = 0$. Since, obviously

$$\left[\sigma_n^z, \sum_{j=1}^N \sigma_j^z\right] = 0$$

and the ground state lies in the sector $y = 0$, only this sector contributes to (3.5.1) and (3.5.2). Furthermore, v does not change the spectrum within a sector of fixed polarization and it does not modify the eigenvectors which depend on γ and h only, as explicitly seen from the Bethe Ansatz Equations.

One concludes that v has no effect whatsoever on the correlators, which remain those of the symmetric six–vertex model, until the level–crossing transition takes place at $v = v(\gamma, \theta, b = 0)$ (as given by (3.3.11)). Here the system moves into the gaussian phase, and the ground state even for small $\delta v = v - v(\gamma, \theta, b = 0)$ falls into a sector at $y \neq 0$ (Lieb and Wu, 1972). The transition occurs without divergence of the correlation length which jumps from the (finite) value of the symmetric six–vertex to infinity. It is the conjecture of the present work that this picture does not change when $-h_c < h < h_c$, and the PT transition persists along all Γ, up to the points (h_c, v_c) or $(-h_c, -v_c)$. This is in accordance with numerical studies performed.

At these particular points, the correlation length should diverge according to the following argument. In the sector $y = 0$, the fact (numerically found)

$$\lim_{h\to h_c^-} \Delta \ln \Lambda(y = 0, h, v_c) = 0$$

is, by itself, not sufficient to prove the divergence of the correlation length ξ_1 in the vertical direction. The fact that Λ_k in (3.5.1) are generally complex forces one to sum over a whole band of them because oscillations can affect the behavior of ξ_1 (Johnson, Krinsky and McCoy, 1973). This in not doable until it is clarified what takes the place of strings as solutions of the Bethe Ansatz equations in the sector under consideration. Nevertheless, one can look at the horizontal correlation function in (3.5.2). As discussed in section 3.4, it is possible to enter the gaussian phase at (h_c, v_c) keeping the ground state at $y = 0$. Therefore it is tempting to conjecture that the ground state remains at $y = 0$, and this is confirmed by preliminary numerical studies performed. Hence no level crossing occurs at these points, because the Perron–Frobenius theorem prevents it from happening in a sector of fixed y, and the expectation value in (3.5.2) is taken with the same Bethe–Ansatz eigenvector in the 2 phases. Since in the gaussian phase the horizontal correlation lenght ξ_2 is infinite, $\xi_2(h)$ must diverge as $h \to \pm h_c$. It should be recalled that, if indeed (h_c, v_c) is critical in the sense of diverging correlation length, it cannot be classified in terms of conformal field theory as shown by the anomalous scaling of $N^{-\frac{1}{2}}$ instead of N^{-1} as our numerical results indicate.

Conclusion and Perspectives

The main result of this section is the existence of a new exponent in the scaling of the free energy of the asymmetric six–vertex model. This exponent should be experimentally verifiable, since, as shown, it can be interpreted as the slope exponent of the rounded edge where the (110) facet of an fcc crystal meets the other crystallographic facets. Moreover, the second exponent of $\frac{3}{2}$ confirms the long held belief that the phase transition presented by the model is of a Prokovski–Talapov type. Nonetheless, it is shown that there exist special points along the phase boundary where the transition is not more of a PT type (level–crossings), as confirmed by the anomalous finite–size scaling observed in numerical studies. At the moment it is not clear what kind of transition this is, and this warrants a further investigation of the phase transition at issue. Another point which should be investigated in more detail regards the universality of the exponent 3. By now the question regarding the universality of $\frac{3}{2}$ seems to be closed, but not of course for the new exponent. It is not known, presently, whether this new exponent is model dependent or not, and it would certainly be desirable to study some other microscopic models to see if it is also present.

Part II

Reaction–Diffusion Processes

Chapter 4

Quantum Chains and Diffusion–Reaction Processes

4.1 Introduction

In this chapter the problem of finding the set of chemical reactions associated to a given quantum chain is addressed. In section 4.2 the master equation approach for continuous times and discrete stochastic variables is presented. In section 4.3 the method is applied in a study–case. Section 4.4 brings the Perk–Schultz chains and section 4.5 is devoted to the extension to more general PS chains.

4.2 The Master Equation and Quantum Chains

Consider a one-dimensional lattice with L sites and open boundaries. At each site j one defines a variable β_j taking N integer values $(0, 1, 2, ..., N-1)$. To each possible configuration $\{\beta\} = \{\beta_1, ..., \beta_L\}$ of the lattice realized at time t one attaches a probability distribution $P(\{\beta\}, t)$ whose time evolution is given by the master equation

$$\begin{aligned} \frac{\partial P(\{\beta\},t)}{\partial t} &= \sum_{k=1}^{L-1} \Big\{ -\Omega_{\beta_k,\beta_{k+1}} P(\beta_1,\ldots,\beta_L;t) \\ &+ \sum_{l,m=0}^{L-1}{}' \Gamma^{\beta_k+l,\beta_{k+1}+m}_{\beta_k,\beta_{k+1}} P(\beta_1,\ldots,\beta_k+l,\beta_{k+1}+m,\ldots,\beta_L;t) \Big\} \end{aligned} \tag{4.2.1}$$

Here and henceforth the prime in a sum over l and m indicates exclusion of the pair $l = m = 0$. The $\Gamma^{a,b}_{c,d}$ are transition rates which equal the probability that, in a unit time step and at any site j,$j+1$ a state $(\beta_j, \beta_{j+1}) = (a, b)$ changes to a state $(\beta'_j, \beta'_{j+1}) = (c, d)$, pictorically $a + b \to c + d$ It is assumed throughout this work that the transition rates depend only on links (nearest-neighbor interaction) and are homogeneous, i.e. site independent. The $\Omega_{a,b}$ are related to the probability that a state (a, b) will not change after a unit time step. Conservation of probability implies

$$\Omega_{a,b} = \sum_{r,s}{}' \Gamma^{a,b}_{r,s} \tag{4.2.2}$$

It is possible to write the master equation in matrix form. In order to do so, one introduces the standard basis of matrices E^{kl} defined by

$$(E^{kl})_{a,b} = \delta_{k,a}\delta_{l,b}$$

One may thus rewrite the master equation (4.2.1) as

$$\frac{\partial\,|P\rangle}{\partial t} = -H\,|P\rangle \tag{4.2.3}$$

if one identifies $|P\rangle$ as the probability $P(\{\beta\},t)$ and H as

$$\begin{aligned} H &= \sum_{j=1}^{L-1} H_j = \sum_{j=1}^{L-1}(U_j - T_j) \\ U_j &= \sum_{a,b=0}^{N-1} \Omega_{a,b} E_j^{aa} E_{j+1}^{bb} \\ T_j &= {\sum_{a,b,c,d=0}^{N-1}}' \Gamma_{c,d}^{a,b} E_j^{ca} E_{j+1}^{db} \end{aligned} \tag{4.2.4}$$

Since H is regular, from the general theory of matrices (Gantmacher, 1959) it is known that the system whose dynamics is governed by (4.2.3) will eventually evolve towards a stationary state (the ground state of H). To identify the Hamiltonians of these chemical processes to those of known integrable quantum chains one must find the appropriate set of rates so that H can be recast as

$$H = H^0 + \sum_{j=1}^{L-1}(h_i + h_{i+1} + g_i - g_{i+1}) + H^1 \tag{4.2.5}$$

where H^0 is the integrable Hamiltonian and the terms under the summation sign are a field and a surface contribution respectively. The spectrum of H is independent of H^1. In what follows only those chemical processes whose spectrum is equivalent to that of some quantum chain shall be dealt with, therefore guaranteeing the equality of the phase diagram. The wave functions however are not the same. For a *non-degenerate* spectrum it is in principle possible to define a similarity transformation of the form $A(\lambda)$ such that

$$A(\lambda)HA^{-1}(\lambda) = H^0 + \sum_{j=1}^{L-1}(h_i + h_{i+1} + g_i - g_{i+1}) + H^{1'}(\lambda) \tag{4.2.6}$$

such that for some given value $\lambda = \lambda_0$ one has $H^{1'}(\lambda_0) = 0$. If such a transformation were found, then the wave functions of the chemical problem could be obtained from that of the quantum chain.

The ket $|P\rangle$ is defined as follows (Kadanoff and Swift, 1968; Halperin, Hohenberg and Ma, 1974; Grassberger and Scheunert, 1980): consider an orthogonal basis in $\{\beta\}$, that is

$$|\{\beta\}\rangle = |\beta_1, \beta_2, \cdots, \beta_{\mathrm{L}}\rangle \qquad \langle\{\beta'\}|\,|\{\beta\}\rangle = \delta_{\{\beta'\},\{\beta\}}$$

Then,

$$|P\rangle = \sum_{\{\beta\}} P(\{\beta\};t)\,|\{\beta\}\rangle$$

Since one is dealing with a stochastic process, some initial condition in the form of a $t=0$ probability distribution $P_0(\{\beta\})$ is required

$$|P_0\rangle = \sum_{\{\beta\}} P_0(\{\beta\})\,|\{\beta\}\rangle$$

The non hermiticity of H plus the conservation of probabilities imply

$$\langle 0| H = 0 \tag{4.2.7}$$

where the bra ground state is defined through

$$\langle 0| = \sum_{\{\beta\}} \langle \{\beta\}|$$

From this remarkable property (4.2.7) it follows that the ground state energy must be zero (it is the stationary state of the system). Moreover, averages can be computed straighforwardly

$$\begin{aligned} < X > (t) &= \sum_{\{\beta\}} X(\{\beta\}) P(\{\beta\};t) \\ &= \langle 0| X |P\rangle \\ &= \langle 0| X \exp(-Ht) |P_0\rangle \end{aligned}$$

where one should note that in contradistinction to quantum mechanics, in nonequilibrium problems the 'wave function' is already a probability.

It is important to note also that all the physics comes into the rates $\Gamma^{a,b}_{c,d}$. For instance if the N–state model is Z_N–symmetric, then only those rates given by

$$\Gamma^{a,b}_{c,d} \qquad \text{such that} \qquad a+b=c+d \quad \text{(modulo N)}$$

are nonzero. Moreover, left–right symmetric rates (parity invariance in the quantum chain language) implies

$$\Gamma^{a,b}_{c,d} = \Gamma^{b,a}_{d,c}$$

and so on. Another important symmetry among the ones mentioned above is the $U(1)$ particle–conservation symmetry. For instance, the trapping reaction has a $U(1)$–symmetry since the number of particles A (or B) is conserved. The two–species annihilation $A + B \to \emptyset + \emptyset$ has also a $U(1)$ symmetry since the difference in the number of particles A and B is conserved. Of course those non vacuum–driven processes have either a $U(1)$ or a $U(1) \otimes U(1)$ symmetry.

4.3 A Case Study

In what follows particles are identified with $A = 1$, $B = 2$ and inert state (or vacancy) $= \emptyset$. The boundaries are open. Only left-right symmetric processes are considered at first, that is particles A and B diffuse symmetrically with rates equal to unity: $\Gamma^{1,0}_{0,1} = \Gamma^{0,1}_{1,0} = \Gamma^{2,0}_{0,2} = \Gamma^{0,2}_{2,0} = 1$. In addition, particles are also allowed to react according to the following vacuum-driven rates:

(i) Annihilation with rates $\Gamma^{1,1}_{0,0}$, $\Gamma^{2,2}_{0,0}$, $\Gamma^{1,2}_{0,0} = \Gamma^{2,1}_{0,0}$

(ii) Coagulation with rates $\Gamma^{1,1}_{1,0} = \Gamma^{1,1}_{0,1}$ and $\Gamma^{2,2}_{2,0} = \Gamma^{2,2}_{0,2}$

(iii) Death with rates $\Gamma^{1,0}_{0,0} = \Gamma^{0,1}_{0,0}$ and $\Gamma^{2,0}_{0,0} = \Gamma^{0,2}_{0,0}$

(iv) Polymerisation (Spouge, 1988) with rates $\Gamma^{1,1}_{2,0} = \Gamma^{1,1}_{0,2}$ and $\Gamma^{2,2}_{1,0} = \Gamma^{2,2}_{0,1}$

(v) Trapping with rates $\Gamma^{1,2}_{1,0} = \Gamma^{1,2}_{0,1} = \Gamma^{2,1}_{1,0} = \Gamma^{2,1}_{0,1}$ and $\Gamma^{1,2}_{2,0} = \Gamma^{2,1}_{0,2} = \Gamma^{1,2}_{0,2} = \Gamma^{2,1}_{2,0}$ (Chopard *et al*, 1993; Rodriguez *et al*, 1993)

The aim is to find the associated quantum Hamiltonian and use its known properties as a workbench for the interpretation of the physics underlying the chemical process.

With these definitions one can use (4.2.2)–(4.2.4) to find the parity–invariant chemical Hamiltonian corresponding to the rates defined above. It is given by

$$
\begin{aligned}
H &= H^0 + H^1 \\
&= \sum_{i=1}^{L-1} \left(H^0_{i,i+1} + H^1_{i,i+1} \right)
\end{aligned}
\tag{4.3.1}
$$

where $H^0_{i,i+1}$ is given by

$$
H^0_{i,i+1} = \begin{pmatrix}
0 &&&&&&&& \\
& \Gamma^{0,1}_{0,0}+1 && -1 &&&&& \\
&& \Gamma^{0,2}_{0,0}+1 &&&& -1 && \\
& -1 && \Gamma^{0,1}_{0,0}+1 &&&&& \\
&&&& \begin{matrix}\Gamma^{1,1}_{0,0}+2\Gamma^{1,1}_{0,1}\\ +2\Gamma^{1,1}_{0,2}\end{matrix} &&&& \\
&&&&& \begin{matrix}\Gamma^{1,2}_{0,0}+2\Gamma^{1,2}_{0,1}\\ +2\Gamma^{1,2}_{0,2}\end{matrix} &&& \\
&& -1 &&&& \Gamma^{0,2}_{0,0}+1 && \\
&&&&&&& \begin{matrix}\Gamma^{1,2}_{0,0}+2\Gamma^{1,2}_{0,1}\\ +2\Gamma^{1,2}_{0,2}\end{matrix} & \\
&&&&&&&& \begin{matrix}\Gamma^{2,2}_{0,0}+2\Gamma^{2,2}_{0,1}\\ +2\Gamma^{2,2}_{0,2}\end{matrix}
\end{pmatrix}
$$

and $H^1_{i,i+1}$ reads

$$
H^1_{i,i+1} = \begin{pmatrix}
0 & \Gamma^{0,1}_{0,0} & \Gamma^{0,2}_{0,0} & \Gamma^{0,1}_{0,0} & \Gamma^{1,1}_{0,0} & \Gamma^{1,2}_{0,0} & \Gamma^{0,2}_{0,0} & \Gamma^{1,2}_{1,0} & \Gamma^{2,2}_{0,1} \\
& 0 &&& \Gamma^{1,1}_{0,1} & \Gamma^{1,2}_{0,1} && \Gamma^{1,2}_{0,1} & \Gamma^{2,2}_{0,1} \\
&& 0 && \Gamma^{1,1}_{0,2} & \Gamma^{1,2}_{0,2} && \Gamma^{1,2}_{0,2} & \Gamma^{2,2}_{0,2} \\
&&& 0 & \Gamma^{1,1}_{0,1} & \Gamma^{1,2}_{0,1} && \Gamma^{1,2}_{0,1} & \Gamma^{2,2}_{0,1} \\
&&&& 0 &&&& \\
&&&&& 0 &&& \\
&&&& \Gamma^{1,1}_{0,2} & \Gamma^{1,2}_{0,2} & 0 & \Gamma^{1,2}_{0,2} & \Gamma^{2,2}_{0,2} \\
&&&&&&& 0 & \\
&&&&&&&& 0
\end{pmatrix}
$$

All matrix elements not explicitly shown are zero. It is important to note that the spectrum of H coincides with that of H^0. This feature is encountered in many nonhermitian chains and can be understood as follows: H^0 conserves the total number n_A of A particles and n_B of B particles separately and can therefore be brought into a block diagonal form. On the other hand, H^1 reduces the total particle number n_A+n_B by one or two since it is made up of vacuum-driven processes. From linear algebra it is known that the spectrum of matrices of the type $H = H^0 + H^1$ is independent of H^1, as long as this properties hold. This has an important physical consequence: since the spectrum does not depend on each parameter of H^1 sepatately but only on their combinations which enter in H^0, the number of effective parameters is reduced to eight. [2].

In order to write this Hamiltonian in a more enlightening form, first define some shorter notation by regrouping processes of the same category as follows

[2]Due to conservation of probability each diagonal element of a Hamiltonian must equal the sum of the nondiagonal entries in that same column. One can see this if one lookds at the definitions of rates in in section 4.2 and realizes that the conservation of the probabilities implies in a relation among rates which can be written as $\sum_{k\neq l} H_{kl} = H_{ll}$.

notation	definition	processes
A_i	$\Gamma^{i,i}_{0,0}$	annihilation
$A^{\pm}_{1,2}$	$\Gamma^{1,2}_{0,0} \pm \Gamma^{2,1}_{0,0}$	annihilation
$D^{\pm}_i$	$\Gamma^{0,i}_{0,0} \pm \Gamma^{i,0}_{0,0}$	death
C^{+}_i	$\Gamma^{i,i}_{i,0} + \Gamma^{i,i}_{0,i}$	coagulation
P^{+}_1	$\Gamma^{1,1}_{0,2} + \Gamma^{1,1}_{2,0}$	polymerisation
P^{+}_2	$\Gamma^{2,2}_{0,1} + \Gamma^{2,2}_{1,0}$	polymerisation
$T^{\pm}$	$[\Gamma^{1,2}_{1,0} \pm \Gamma^{2,1}_{0,1}] + [\Gamma^{1,2}_{0,1} \pm \Gamma^{2,1}_{1,0}] + [\Gamma^{1,2}_{2,0} \pm \Gamma^{2,1}_{0,2}] + [\Gamma^{1,2}_{0,2} \pm \Gamma^{2,1}_{2,0}]$	trapping

In this table $i = 1, 2$. For the present problem only the symmetric combinations are nonzero. The more general definitions are given however for later use.

Using the matricial basis E^{kl} and the following identifications

$$\begin{aligned} v &= A_1 + C_1^+ + P_1^+ - D_1^+ - 2 \\ w &= \frac{D_1^+ + D_2^+}{4} + 1 \end{aligned} \tag{4.3.2}$$

together with three constraints on the rates, namely

$$\begin{aligned} 2w + v &= A_2 + C_2^+ + P_2^+ \\ 4w + 2v &= A_{12}^+ + T^+ \\ D_1^+ &= D_2^+ \end{aligned} \tag{4.3.3}$$

one may rewrite H^0 of (4.3.1) as

$$\begin{aligned} H^0 &= \sum_{i=1}^{L-1} -\left(E_i^{01}E_{i+1}^{10} + E_i^{10}E_{i+1}^{01} + E_i^{02}E_{i+1}^{20} + E_i^{20}E_{i+1}^{02}\right) \\ &\quad + w(\varepsilon_i^0 + \varepsilon_{i+1}^0) + v\varepsilon_i^0\varepsilon_{i+1}^0 \\ \varepsilon^0 &= E^{11} + E^{22} \qquad \varepsilon^z = E^{11} - E^{22} \end{aligned} \tag{4.3.4}$$

Adding a surface term to this Hamiltonian, one gets a new $\widetilde{H^0}$ (Alcaraz *et al, op. cit.*)

$$\widetilde{H^0} = H^0 + a\left(\varepsilon_i^0 - \varepsilon_{i+1}^0\right) \tag{4.3.5}$$

which is $U_q\widehat{SU}(2)$ invariant and has the spectrum (apart from degeneracies) and phase diagram of the spin-$\frac{1}{2}$ XXZ model with an external field and a surface term, which reads

$$H^{XXZ} = -\frac{1}{2}\sum_{i}^{L-1}\left\{\sigma_i^x\sigma_{i+1}^x + \sigma_i^y\sigma_{i+1}^y + \Delta\sigma_i^z\sigma_{i+1}^z + h\left(\sigma_i^z + \sigma_{i+1}^z\right) + a\left(\sigma_i^z - \sigma_{i+1}^z\right) + \beta\right\} \tag{4.3.6}$$

The equivalence between $\widetilde{H^0}$ and H^{XXZ} can be established by rewriting the latter in the basis of E^{kl} matrices

$$\begin{aligned} H^{XXZ} &= -\sum_{i=1}^{L-1}\left(E_i^{01}E_{i+1}^{10} + E_i^{10}E_{i+1}^{01}\right) + vE_i^{11}E_{i+1}^{11} \\ &\quad + w\left(E_i^{11} + E_{i+1}^{11}\right) + a\left(E_i^{11} - E_{i+1}^{11}\right) + b \end{aligned} \tag{4.3.7}$$

where

$$v = -2\Delta, \quad w = \Delta + h, \quad b = -(\frac{\Delta+\beta}{2} + h) \tag{4.3.8}$$

$\widetilde{H^0}$ is obtained from H^{XXZ} by adding the matrix elements $E_i^{02}E_{i+1}^{20}$ and $E_i^{20}E_{i+1}^{02}$ which do not affect the spectrum (only degeneracies). The diagonal terms are extended accordingly. The wave functions of $\widetilde{H^0}$ have been calculated but the effect of H_1' on the phase diagram has not yet been studied.

This equivalence is also crucial since the phase diagram for the XXZ chain has been known for many years (Johnson, McCoy, 1972) and one can, through the mapping, interpret it in the language of reaction diffusion processes. For $h = 0$ this model has a massless and conformal invariant phase when $-1 \leq \Delta \leq 1$ and a massive antiferromagnetic (ferromagnetic) phase for $\Delta < -1$ ($\Delta > 1$). When $h \neq 0$ the system is massive commensurate for $\Delta > 1 - h$ and massless incommensurate otherwise, the line $\Delta = 1 - h$ corresponding to PT phase transition between these two regimes (Prokovskii and Talapov,*op. cit.*). The physical mechanism behing this transition has been discussed in chapter 3. Comparing H^0 with $\widetilde{H^0}$ in (4.3.5) one concludes that they have both the same phase diagram since the term in H_0' having the parameter a as coefficient is a surface contribution. To interpret the phase diagram in the language of reaction-diffusion processes, it suffices to identify the parameters of the Heisenberg chain with the rates of the chemical model. These are

$$\begin{aligned} h &= \frac{A_1 + C_1^+ + P_1^+}{2} \\ \Delta &= 1 + \frac{D_1^+ - \left(A_1 + C_1^+ + P_1^+\right)}{2} \\ \beta &= -1 - \frac{A_1 + C_1^+ + P_1^+ + D_1^+}{2} \end{aligned} \tag{4.3.9}$$

The analysis is straightforward. $h = 0$ implies that all rates vanish **but** death. In this situation

$$\begin{aligned} \Delta &= 1 + \frac{D_1^+}{2} \\ \beta &= -\Delta \end{aligned} \tag{4.3.10}$$

By varying the death rate one goes from a massive regime to a massless one, that is the time evolution for the concentration of particles has an exponential or algebraic fall-off respectively. This can be understood on physical grounds: being a 'one-particle' process, death happens irrespectively of any other processes ocurring in the system, i.e. it is not diffusion-limited since any particle can die alone. It therefore outruns the characteristic time scale set by diffusion and brings about a quicker decay. With an external field we have

$$\Delta + h - 1 = \frac{D_1^+}{2} \tag{4.3.11}$$

If death has a non-zero probability, then from the equation above one sees that the system is massive ferromagnetic. If one identifies an upturned spin in the Heisenberg model as a vacancy in the chemical model, this means that the ground state is a state with no particles. By varying the rate of death one approaches the line on the phase diagram given by $\Delta + h = 1$. The system undergoes a PT transition where the energy of the state with just one particle equals that of the state with no particles and it becomes the ground state. There is a level-crossing: since death is absent the system can evolve to a final steady state where only one particle is left. It is noteworthy observing that in the massless regime (absence of death) many reactions besides diffusion still coexist, namely annihilation, coagulation, polymerisation and trapping. This is so because the time-scale set by diffusion cannot be outrun, since all the remaining processes are 2-particle interactions. In other words, in a situation where the particles are some lattice spacings apart, they need first to diffuse before they reach each other and react – the processes are diffusion–limited. This observation is confirmed by results obtained in other studies where the time-decay of the concentration of particles was shown to be algebraic in time, for instance for pure annihilation where $c_j \sim t^{1/4}$ (Toussaint and Wilczek, 1983; Kang and Redner, 1984). It also allows one to say that qualitatively the massless regime remains even if the other three reactions are present, as the equations above show.

4.4 The $U_qSU(3/0)$, $U_qSU(2/1)$ and $U_qSU(1/2)$ chains

It is well known that the Hamiltonian of the 6-vertex model is also the time-evolution operator for the two-state asymmetric diffusion process (Kandel, Domany and Nienhuis, 1990). Recently this idea has been extended (Alcaraz *et al*,1994b) to encompass the Perk-Schultz Hamiltonians as the corresponding operators for higher-state diffusive systems. Intuitively one can understand this if one recalls that the quantum PS chains are obtained from the transfer–matrix of higher-state vertex models which obeying the ice-rule in the $\tau-$ continuum limit (Sutherland, 1975; Perk and Schultz, 1983; Schultz, 1983. See Appendix B).

The $(P+M)$-state $U_qSU(P/M)$-invariant Perk-Schultz models are defined through the one–dimensional Hamiltonians

$$
\begin{aligned}
H_{\{\epsilon_1,\cdots,\epsilon_{P+M}\}} \;=\; & \sum_{j=1}^{L-1}\Bigg\{\frac{q+q^{-1}}{2}-\Bigg[\sum_{\alpha\neq\beta=0}^{P+M-1} E_j^{\alpha\beta}E_{j+1}^{\beta\alpha}+\frac{q+q^{-1}}{2}\sum_{\alpha=0}^{P+M-1}\epsilon_\alpha E_j^{\alpha\alpha}E_{j+1}^{\alpha\alpha} \\
& +\frac{q-q^{-1}}{2}\sum_{\alpha\neq\beta=0}^{P+M-1} sign\,(\alpha-\beta)\,E_j^{\alpha\alpha}E_{j+1}^{\beta\beta}\Bigg]\Bigg\}
\end{aligned}
\tag{4.4.1}
$$

where, besides the anisotropy parameter q, one has an extra set of parameters $\{\epsilon_\alpha\}$ such that $\epsilon_0=\epsilon_1=\ldots=\epsilon_{P-1}=-\epsilon_P=-\epsilon_{P+1}=\ldots=-\epsilon_{P+M-1}=1$. Their role can be better understood in the original 2-dimensional formulation of the Perk-Schultz models, namely the multicolor ice–models (number of colors $=P+M$). In these models ferroelectric configurations (all links of a vertex having the same color) are favored for colors a having $\epsilon_a=+1$ and for colors b with $\epsilon_b=-1$ the corresponding vertex weights favor alternating colored configurations. Each possible set $\{\epsilon_\alpha\}$ defines therefore a completely different physical system (Martin and Rittenberg, 1992).

This picture is however far from complete and can be extended to encompass more general chemical systems if one reinterprets the additional reactions on chemical Hamiltonians as external fields in the PS chains they are mapped onto. For the sake of completeness, the results without external fields are presented first. The generalization to the models given by $(P/M)=(3/0)$ and $(P/M)=(2/1)$ with fields follows.

Consider a system in which particles A and B diffuse on the lattice with rate Γ_R if the particle jumps to the right or Γ_L otherwise. For the interchange process rates are defined accordingly if B replaces A to the right or to the left. With the rates so defined the Hamiltonian obtained reads

$$
\begin{aligned}
H &= \sum_{i=1}^{L-1} H_i \\
H_i &= \begin{pmatrix}
0 &&&&&&&& \\
& \Gamma_L && -\Gamma_R &&&&& \\
&& \Gamma_L &&&& -\Gamma_R && \\
& -\Gamma_L && \Gamma_R &&&&& \\
&&&& 0 &&&& \\
&&&&& \Gamma_L && -\Gamma_R & \\
&& -\Gamma_L &&&& \Gamma_R && \\
&&&&& -\Gamma_L && \Gamma_R & \\
&&&&&&&& 0
\end{pmatrix}
\end{aligned}
\tag{4.4.2}
$$

Defining $\sqrt{\frac{\Gamma_L}{\Gamma_R}}=q$, which measures the asymmetry of the diffusion, and the diffusion constant

$\sqrt{\Gamma_L \Gamma_R} = \mathcal{D}$, which sets the time scale of the problem, this can be rewritten as

$$\frac{H_i}{\mathcal{D}} = \begin{pmatrix} 0 & & & & & & & & \\ & q & & -q^{-1} & & & & & \\ & & q & & & & -q^{-1} & & \\ & -q & & q^{-1} & & & & & \\ & & & & 0 & & & & \\ & & & & & q & & -q^{-1} & \\ & & -q & & & & q^{-1} & & \\ & & & & & -q & & q^{-1} & \\ & & & & & & & & 0 \end{pmatrix} \tag{4.4.3}$$

This nonhermitian (q is real) Hamiltonian is $U_qSU(3/0)$-invariant (cf. eq. (4.4.1)). Considering only a new set of processes corresponding to coagulation of B ($B + B \to B + \emptyset$ with rate $\Gamma^{2,2}_{2,0}$ and $B + B \to \emptyset + B$ with $\Gamma^{2,2}_{0,2}$) such that $\Gamma^{2,2}_{2,0} + \Gamma^{2,2}_{0,2} = \mathcal{D}(q + q^{-1})$ plus coagulation of A ($A + A \to A + \emptyset$ with $\Gamma^{1,1}_{1,0}$ and $A + A \to \emptyset + A$ with $\Gamma^{1,1}_{0,1}$) with the restriction $\Gamma^{11}_{10} + \Gamma^{11}_{01} = \mathcal{D}(q + q^{-1})$, the nonhermitian $U_qSU(2/1)$-invariant and $U_qSU(1/2)$-invariant chains are obtained (Alcaraz *et al*, 1994b).

Another interesting remark is that for the $U_qSU(2/0)$ chain (the XXZ model with open boundaries), a similarity transformation which brings this nonhermitian Hamiltonian over to a hermitian one (plus volume–dependent boundary conditions in the case of periodic chains) was long known (Alcaraz and Wreszinski, 1990). For higher–state models such transformation was expected to exist (Reshetikhin, 1989) but its exact form was still lacking. This motivated the present work in trying to find this similarity transformation. In contradistinction to the 2–state case it is given by a nonlocal matrix which reads (Dahmen, 1994)

$$\mathcal{F} = \sum_{\alpha_1, \alpha_2, \cdots, \alpha_L = 0}^{2} q^{\frac{1}{2} \sum_{j>i=1}^{L} sign(\alpha_j - \alpha_i)} E^{\alpha_1 \alpha_1} \otimes E^{\alpha_2 \alpha_2} \otimes \cdots \otimes E^{\alpha_L \alpha_L} \tag{4.4.4}$$

The physical features this matrix induces are also completely novel (see chapter 5).

It is instructive noting that the two last chains present a particular feature. From the spectrum of the (2/1) chain, the spectrum of the (1/2) can be obtained in a straighforward manner: one reverses the sign of the whole spectrum of the (2/1) model and add an overall constant equal to $(L-1)(q + q^{-1})$, which is the highest energy of the (2/1) chain. This value is indeed the highest energy for all L-site (P/M) chains with q real and non-zero P and M and an outline proof was given by Martin and Rittenberg (1992). In the chemical scenario however, they correspond to different physical pictures and the reason is the positivity of the spectrum.

4.5 The Chains with External Fields

The results presented are generalized to include the most general set of vacuum-driven processes which can be written as a pure nonhermitian Hamiltonian H^1 which does not affect the spectrum of the PS chains. Beyond the rates in the first section of this chapter (no left-right symmetry) one can include one more set of reactions, namely those corresponding to mutation and transmutation of A. The corresponding rates are $\Gamma^{1,0}_{2,0}$, $\Gamma^{0,1}_{0,2}$, $\Gamma^{1,0}_{0,2}$ and $\Gamma^{0,1}_{2,0}$. For these reactions one defines the following combination

$$\begin{aligned} M_1^{\pm} &= \Gamma^{0,1}_{0,2} \pm \Gamma^{1,0}_{2,0} \\ X_1^{\pm} &= \Gamma^{0,1}_{2,0} \pm \Gamma^{1,0}_{0,2} \end{aligned} \tag{4.5.1}$$

The master equation approach yields in this case a Hamiltonian which can be written as follows

$$\frac{H'}{\mathcal{D}} = \frac{H}{\mathcal{D}} + \sum_{i=1}^{L-1} (h_i + h_{i+1} + g_i - g_{i+1}) + H^1 \tag{4.5.2}$$

where H is given by (4.4.3) and $H^1 = \sum_i H_i^1$ being the same in all cases, reads

$$H_i^1 = \begin{pmatrix} 0 & \Gamma^{0,1}_{0,0} & \Gamma^{0,2}_{0,0} & \Gamma^{1,0}_{0,0} & \Gamma^{1,1}_{0,0} & \Gamma^{1,2}_{0,0} & \Gamma^{2,0}_{0,0} & \Gamma^{2,1}_{0,0} & \Gamma^{2,2}_{0,0} \\ & 0 & & & \Gamma^{1,1}_{0,1} & \Gamma^{1,2}_{0,1} & & \Gamma^{2,1}_{0,1} & \Gamma^{2,2}_{0,1} \\ & \Gamma^{0,1}_{0,2} & 0 & \Gamma^{1,0}_{0,2} & \Gamma^{1,1}_{0,2} & \Gamma^{1,2}_{0,2} & & \Gamma^{2,1}_{0,2} & \Gamma^{2,2}_{0,2} \\ & & & 0 & \Gamma^{1,1}_{1,0} & \Gamma^{1,2}_{1,0} & & \Gamma^{2,1}_{1,0} & \Gamma^{2,2}_{1,0} \\ & & & & 0 & & & & \\ & & & & & 0 & & & \\ & \Gamma^{0,1}_{2,0} & & \Gamma^{1,0}_{2,0} & \Gamma^{1,1}_{2,0} & \Gamma^{1,2}_{2,0} & 0 & \Gamma^{2,1}_{2,0} & \Gamma^{2,2}_{2,0} \\ & & & & & & & 0 & \\ & & & & & & & & 0 \end{pmatrix} \tag{4.5.3}$$

It is important to note, as in the last section, that the spectrum of H' depends on H^1 only through the h's and g's which are diagonal contributions arising due to conservation of probabilities. They commute with H, playing the role of external fields and surface terms respectively. Their values differ for each particular chain as can be seen in the following table:

Model	h_1	h_2	g_1	g_2	constraints
$U_qSU(3/0)$	$\frac{M_1^+ + X_1^+ + D_1^+}{2\mathcal{D}}$	$\frac{D_2^+}{2\mathcal{D}}$	$-\frac{M_1^- + X_1^- + D_1^-}{2\mathcal{D}}$	$-\frac{D_2^-}{2\mathcal{D}}$	$M_1^+ + T_1^+ + D_1^+ = C_1^+ + P_1^+ + A_1$ $D_2^+ = C_2^+ + P_2^+ + A_2$ $A_{12}^+ + T^+ = M_1^+ + X_1^+ + D_1^+ + D_2^+$ $A_{12}^- + T^- = D_2^- - M_1^- - X_1^- - D_1^-$
$U_qSU(2/1)$	$\frac{M_1^+ + X_1^+ + D_1^+}{2\mathcal{D}}$	$-\frac{D_2^+}{2\mathcal{D}}$	$-\frac{M_1^- + X_1^- + D_1^-}{2\mathcal{D}}$	$-\frac{D_2^-}{2\mathcal{D}}$	$M_1^+ + T_1^+ + D_1^+ = C_1^+ + P_1^+ + A_1$ $D_2^+ = C_2^+ + P_2^+ + A_2 - \mathcal{D}(q+q^{-1})$ $A_{12}^+ + T^+ = M_1^+ + X_1^+ + D_1^+ + D_2^+$ $A_{12}^- + T^- = D_2^- - M_1^- - X_1^- - D_1^-$
$U_qSU(1/2)$	$-\frac{M_1^+ + X_1^+ + D_1^+}{2\mathcal{D}}$	$-\frac{D_2^+}{2\mathcal{D}}$	$-\frac{M_1^- + X_1^- + D_1^-}{2\mathcal{D}}$	$-\frac{D_2^-}{2\mathcal{D}}$	$M_1^+ + T_1^+ + D_1^+ = C_1^+ + P_1^+ + A_1 -$ $\mathcal{D}(q+q^{-1})$ $D_2^+ = C_2^+ + P_2^+ + A_2 - \mathcal{D}(q+q^{-1})$ $A_{12}^+ + T^+ = M_1^+ + X_1^+ + D_1^+ + D_2^+$ $A_{12}^- + T^- = D_2^- - M_1^- - X_1^- - D_1^-$

The constraints arise from the fact the number of parameters in the original chemical problem exceeds those of the quantum chains they are mapped onto and must therefore be related. Due to the symmetry properties of the PS chains, the field (and surface contribution) is decomposed into 3 independent variables h_α (g_α), one for each conserved particle of type α. Since one of our particles is an inert state, one may take the corresponding variables $h_0 = g_0 = 0$.

Unfortunately little is known about the phase diagram of the PS chains on an external field. Since the field commutes with the particle number operators, its effect on the spectrum is trivial and one may use the Bethe Ansatz equations to obtain reliable finite-size data and consequently determine the phase diagram. Apart from the difficulties in analysing these equations, there is an additional subtlety: the nonhermitian chemical Hamiltonians are related under $\mathcal{F}$ to PS chains with different properties, whether the boundaries in the original formulation are open or periodic. This reflects the fact that the chemistry of reaction-diffusion models is boundary dependent (see the discussion in the introduction of this paper) and in the case presented here this is brought about by the nonlocality of $\mathcal{F}$. The Bethe Ansatz equations are given by (Lopes, 1992; Dahmen, 1994)

$$
\begin{aligned}
e^{\gamma(N_0+N_1)}\epsilon_1^{M_1}\left(\frac{sinh(\lambda_k^{(0)}+\epsilon_0\gamma/2)}{\sinh(\lambda_k^{(0)}-\epsilon_0\gamma/2)}\right)^N &= \prod_{\alpha=1}^{M_0}\frac{\sinh(\lambda_k^{(0)}-\lambda_\alpha^{(0)}+\epsilon_1\gamma)}{sinh(\lambda_k^{(0)}-\lambda_\alpha^{(0)}-\epsilon_0\gamma)} \\
&\times \prod_{\alpha=1}^{M_1}\frac{sinh(\lambda_k^{(0)}-\lambda_\alpha^{(1)}-\epsilon_1\gamma/2)}{sinh(\lambda_k^{(0)}-\lambda_\alpha^{(1)}+\epsilon_1\gamma/2)} \\
e^{\gamma(N_1+N_2)}\epsilon_2^{M_2}\epsilon_0^{M_0} &= \prod_{\alpha=1}^{M_0}\frac{sinh(\lambda_\alpha^{(0)}-\lambda_l^{(1)}+\epsilon_1\gamma/2)}{sinh(\lambda_\alpha^{(0)}-\lambda_l^{(1)}-\epsilon_1\gamma/2)} \\
&\times \prod_{\alpha=1}^{M_1}\frac{sinh(\lambda_\alpha^{(1)}-\lambda_l^{(1)}-\epsilon_2\gamma)}{sinh(\lambda_\alpha^{(1)}-\lambda_l^{(1)}+\epsilon_1\gamma)}
\end{aligned}
\tag{4.5.4}
$$

where $\{\epsilon_\alpha\}$ are the parameters of the Perk-Schultz chains, as defined in section 4.4. γ is related to q through $q = exp(\gamma)$. The N_i's correspond to the particular number of particles of type i in each charge sector and the M_i's equal the number of roots of the set of coupled equations. They are obtained from the N_i's through

$$M_i = L - (N_0 + N_1 + \cdots + N_i) \tag{4.5.5}$$

where L is the lattice size. Up to the present date there is no known solutions, either numerical or analytical, of these Bethe Ansatz Equations.

Chapter 5

Similarity Transformation and Boundary Conditions

5.1 Introduction

In this chapter a detailed description of the transformation given by the matrix $\mathcal{F}$ introduced in the last chapter is given. Two points are addressed: the first regards the extention of $\mathcal{F}$ not only to higher-state models but also to multi-parameter diffusion processes, i.e. those characterized by a larger set $\{q\} = \{q_1, q_2, \cdots\}$ of parameters in contradistinction to the one-parameter diffusion we dealt with so far. The second regards the effect of $\mathcal{F}$ on periodic chains and the physical features it induces.

5.2 Multi-parameter and Higher-State Diffusion Processes

As before, consider a system in which $(N-1)$ different species diffuse and interchange places on a one-dimensional lattice with open boundary conditions with rates

$$A_x + A_y \rightleftharpoons A_y + A_x \quad \Gamma^{A_x,A_y}_{A_y,A_x}; \Gamma^{A_y,A_x}_{A_x,A_y} \quad x > y = 0, 1, \cdots, N-1 \tag{5.2.1}$$

from which one defines $\frac{N(N-1)}{2}$ parameters q_{xy}

$$\sqrt{\frac{\Gamma^{A_y,A_x}_{A_x,A_y}}{\Gamma^{A_x,A_y}_{A_y,A_x}}} = q_{xy} \tag{5.2.2}$$

with $q_{xy} = q_{yx}^{-1}$. A homogeneous time scale is imposed

$$\sqrt{\Gamma^{0,A_1}_{A_1,0}\Gamma^{A_1,0}_{0,A_1}} = \sqrt{\Gamma^{0,A_2}_{A_2,0}\Gamma^{A_2,0}_{0,A_2}} = \cdots = \sqrt{\Gamma^{A_{N-2},A_{N-1}}_{A_{N-1},A_{N-2}}\Gamma^{A_{N-1},A_{N-2}}_{A_{N-2},A_{N-1}}} = \mathcal{D} \tag{5.2.3}$$

and obtain a nonhermitian Hamiltonian

$$\frac{H}{\mathcal{D}} = \sum_{k=1}^{L-1}\left\{\sum_{x\neq y=0}^{N-1} q_{xy}\left(E_k^{xx}E_{k+1}^{yy} - E_k^{xy}E_{k+1}^{yx}\right)\right\} \tag{5.2.4}$$

which governs the time-evolution of the chemical system above defined. The goal is to find a similarity transformation which makes H hermitian. The (nonlocal!) similarity transformation which accomplishes this reads

$$\mathcal{F} = \sum_{\alpha_1,\alpha_2,\cdots,\alpha_L=0}^{N-1}\left(\prod_{x>y=0}^{N-1}(q_{xy})^{f_{xy}(\alpha_1,\alpha_2,\cdots,\alpha_L)}\right)E^{\alpha_1\alpha_1}\otimes E^{\alpha_2\alpha_2}\otimes\cdots\otimes E^{\alpha_L\alpha_L} \tag{5.2.5}$$

with the functions f_{xy} given by

$$f_{xy}(\alpha_1, \alpha_2, \cdots, \alpha_L) = \frac{1}{2} \sum_{n>m=1}^{L} (\delta_{\alpha_n,x}\delta_{\alpha_m,y} - \delta_{\alpha_n,y}\delta_{\alpha_m,x}) \tag{5.2.6}$$

It is important to notice that in the expression above the order of the arguments in the function is very important since they index the sites on the chain, that is $f(\cdots, \alpha_j, \alpha_{j+1}, \cdots) \neq f(\cdots, \alpha_{j+1}, \alpha_j, \cdots)$.

Proof

For clarity, one may consider the diagonal and nondiagonal parts of the Hamiltonian separately. Since $\mathcal{F}(\sum_j H_{j,j+1})\mathcal{F}^{-1} = \sum_j \mathcal{F}H_{j,j+1}\mathcal{F}^{-1}$, it suffices to consider the action of S on the 2-site operator $H_{j,j+1}$.

Starting with the action of $\mathcal{F}$ on the diagonal piece of the Hamiltonian, one has

$$\begin{aligned}
\mathcal{F}\frac{H_{j,j+1}^{diag}}{\mathcal{D}}\mathcal{F}^{-1} &= \sum_{\{\alpha\}=0}^{N-1} \prod_{x>y}^{N-1} \left(q_{xy}^{f_{xy}(\alpha_1,\alpha_2,\cdots,\alpha_L)} E^{\alpha_1\alpha_1} \otimes E^{\alpha_2\alpha_2} \otimes \cdots \otimes E^{\alpha_L\alpha_L} \right) \\
&\times \left(\sum_{a\neq b=0}^{N-1} q_{ab} E_j^{aa} E_{j+1}^{bb} \right) \\
&\times \sum_{\{\beta\}=0}^{N-1} \prod_{w>z}^{N-1} \left(q_{wz}^{-f_{wz}(\beta_1,\beta_2,\cdots,\beta_L)} E^{\beta_1\beta_1} \otimes E^{\beta_2\beta_2} \otimes \cdots \otimes E^{\beta_L\beta_L} \right)
\end{aligned} \tag{5.2.7}$$

Reordering the terms leads to

$$\begin{aligned}
\mathcal{F}\frac{H_{j,j+1}^{(diag)}}{\mathcal{D}}\mathcal{F}^{-1} &= \sum_{\{\alpha\}}^{N-1} \sum_{\{\beta\}}^{N-1} \prod_{x>y=0}^{N-1} \prod_{w>z=0}^{N-1} \left(q_{xy}^{f_{xy}(\alpha_1,\alpha_2,\cdots,\alpha_L)} q_{wz}^{-f_{wz}(\beta_1,\beta_2,\cdots,\beta_L)} \right) \\
&\times E^{\alpha_1\alpha_1}E^{\beta_1\beta_1} \otimes E^{\alpha_2\alpha_2}E^{\beta_2\beta_2} \otimes \cdots \otimes \mathbf{1}^{(j)} \otimes \mathbf{1}^{(j+1)} \otimes \cdots \otimes E^{\alpha_L\alpha_L}E^{\beta_L\beta_L} \\
&\times \sum_{\substack{\alpha_j,\alpha_{j+1} \\ \beta_j,\beta_{j+1}}} \sum_{a\neq b=0}^{N-1} (q_{ab} E^{\alpha_j\alpha_j} E_j^{aa} E^{\beta_j\beta_j} \otimes E^{\alpha_{j+1}\alpha_{j+1}} E_{j+1}^{bb} E^{\beta_{j+1}\beta_{j+1}})
\end{aligned} \tag{5.2.8}$$

Since x, y, w and z serve only to index the same set $\{q\}$ of diffusion parameters, one may take $x = w$, $y = z$. Using the multiplication properties of the matrices $E^{\alpha\beta}$, namely

$$E^{pq}E^{rs} = \delta_{q,r}E^{ps} \tag{5.2.9}$$

the expression reduces to

$$\begin{aligned}
\mathcal{F}\frac{H_{j,j+1}^{(diag)}}{\mathcal{D}}\mathcal{F}^{-1} &= \sum_{\{\alpha\}}^{N-1} \sum_{\{\beta\}}^{N-1} \prod_{x>y=0}^{N-1} \left(q_{xy}^{f_{xy}(\alpha_1,\alpha_2,\cdots,\alpha_L) - f_{xy}(\beta_1,\beta_2,\cdots,\beta_L)} \right) \\
&\times E^{\alpha_1\alpha_1}\delta_{\alpha_1,\beta_1} \otimes E^{\alpha_2\alpha_2}\delta_{\alpha_2,\beta_2} \otimes \cdots \otimes \mathbf{1}^{(j)} \otimes \mathbf{1}^{(j+1)} \otimes \cdots \otimes E^{\alpha_L\alpha_L}\delta_{\alpha_L,\beta_L} \\
&\times \sum_{\substack{\alpha_j,\alpha_{j+1} \\ \beta_j,\beta_{j+1}}} \sum_{a\neq b=0}^{N-1} \left(q_{ab} E_j^{aa} E_{j+1}^{bb} \delta_{\alpha_j,a}\delta_{\alpha_{j+1},b}\delta_{\alpha_j,\beta_j}\delta_{\alpha_{j+1},\beta_{j+1}} \right)
\end{aligned} \tag{5.2.10}$$

Taking into account the Kronecker deltas one has further

$$\begin{aligned}\mathcal{F}\frac{H_{j,j+1}^{(diag)}}{\mathcal{D}}\mathcal{F}^{-1} &= \sum_{\{\alpha\}}^{N-1}\prod_{x>y=0}^{N-1} q_{xy}^{f_{xy}(\alpha_1,\alpha_2,\cdots,\alpha_L)-f_{xy}(\alpha_1,\alpha_2,\cdots,\alpha_L)}\left(\sum_{a\neq b=0}^{N-1} q_{ab}E_j^{aa}E_{j+1}^{bb}\right)\\ &\times\; E^{\alpha_1\alpha_1}\otimes E^{\alpha_2\alpha_2}\otimes\cdots\otimes\mathbf{1}^{(j)}\otimes\mathbf{1}^{(j+1)}\otimes\cdots\otimes E^{\alpha_L\alpha_L}\end{aligned} \tag{5.2.11}$$

The exponent of q_{xy} is clearly zero. Summing over $\{\alpha\}$ one finally obtains

$$\begin{aligned}\mathcal{F}\frac{H_{j,j+1}^{(diag)}}{\mathcal{D}}\mathcal{F}^{-1} &= \sum_{a\neq b=0}^{N-1} q_{ab}\mathbf{1}\otimes\mathbf{1}\otimes\cdots\otimes E_{(j)}^{aa}\otimes E_{(j+1)}^{bb}\otimes\cdots\otimes\mathbf{1}\\ &= \frac{H_{j,j+1}^{(diag)}}{\mathcal{D}}\end{aligned} \tag{5.2.12}$$

This shows that the diagonal elements of the Hamiltonian are not changed by the transformation generated by $\mathcal{F}$.

To see the effect of $\mathcal{F}$ on the nondiagonal part, consider only the 2-body operator for a given value of the pair (a,b). One has

$$\mathcal{F}\frac{H_{j,j+1}^{(nond)}}{\mathcal{D}}\mathcal{F}^{-1} = \mathcal{F}\left(q_{ab}E_j^{ab}E_{j+1}^{ba} + q_{ab}^{-1}E_j^{ba}E_{j+1}^{ab}\right)_{a>b}\mathcal{F}^{-1} \tag{5.2.13}$$

As in the diagonal case, after multiplying the $E^{\alpha\beta}$ matrices on each site, one is left with

$$\begin{aligned}\mathcal{F}\frac{H_{j,j+1}^{(nond)}}{\mathcal{D}}\mathcal{F}^{-1} &= \sum_{\{\alpha\}}^{N-1}\sum_{\{\beta\}}^{N-1}\prod_{x>y=0}^{N-1}\left(q_{xy}^{f_{xy}(\alpha_1,\alpha_2,\cdots,\alpha_L)-f_{xy}(\beta_1,\beta_2,\cdots,\beta_L)}\right)\\ &\times\; E^{\alpha_1\alpha_1}\delta_{\alpha_1,\beta_1}\otimes\cdots\otimes\mathbf{1}^{(j)}\otimes\mathbf{1}^{(j+1)}\otimes\cdots\otimes E^{\alpha_L\alpha_L}\delta_{\alpha_L,\beta_L}\\ &\times \sum_{\substack{\alpha_j,\alpha_{j+1}\\ \beta_j,\beta_{j+1}}}\left(q_{ab}E_j^{ab}E_{j+1}^{ab}\delta_{\alpha_j,a}\delta_{\beta_j,b} + q_{ab}^{-1}E_j^{ba}E_{j+1}^{ab}\delta_{\alpha_j,b}\delta_{\beta_j,a}\right)_{a>b}\\ &\times\; \delta_{\alpha_{j+1},\beta_j}\delta_{\alpha_j,\beta_{j+1}}\end{aligned} \tag{5.2.14}$$

which reduces to

$$\begin{aligned}\mathcal{F}\frac{H_{j,j+1}^{(nond)}}{\mathcal{D}}\mathcal{F}^{-1} &= \sum_{\{\alpha\}}^{N-1}\prod_{x>y=0}^{N-1} q_{xy}^{f_{xy}(\alpha_1,\cdots,\alpha_j,\alpha_{j+1},\cdots,\alpha_L)-f_{xy}(\alpha_1,\cdots,\alpha_{j+1},\alpha_j,\cdots,\alpha_L)}\\ &\times\; E^{\alpha_1\alpha_1}\otimes E^{\alpha_2\alpha_2}\otimes\cdots\otimes\mathbf{1}^{(j)}\otimes\mathbf{1}^{(j+1)}\otimes\cdots\otimes E^{\alpha_L\alpha_L}\\ &\times\left(q_{ab}E_j^{ab}E_{j+1}^{ab}\delta_{\alpha_j,a}\delta_{\alpha_{j+1},b} + q_{ab}^{-1}E_j^{ba}E_{j+1}^{ab}\delta_{\alpha_j,b}\delta_{\alpha_{j+1},a}\right)_{a>b}\end{aligned} \tag{5.2.15}$$

Note the interchanged arguments in the exponent of q_{xy}, that is

$$\begin{aligned} f_{xy}(\alpha_1,\cdots,\alpha_j,\alpha_{j+1},\cdots,\alpha_L) &- f_{xy}(\alpha_1,\cdots,\alpha_{j+1},\alpha_j,\cdots,\alpha_L) = \\ \frac{1}{2}(\delta_{\alpha_{j+1},x}\delta_{\alpha_j,y} - \delta_{\alpha_{j+1},y}\delta_{\alpha_j,x}) &- \frac{1}{2}(\delta_{\alpha_j,x}\delta_{\alpha_{j+1},y} - \delta_{\alpha_j,y}\delta_{\alpha_{j+1},x})\\ &= \delta_{\alpha_{j+1},x}\delta_{\alpha_j,y} - \delta_{\alpha_{j+1},y}\delta_{\alpha_j,x}\end{aligned} \tag{5.2.16}$$

Substituting this expression on (5.2.15) yields

$$
\begin{aligned}
\mathcal{F}\frac{H^{(nond)}_{j,j+1}}{\mathcal{D}}\mathcal{F}^{-1} &= \sum_{\{\alpha\}}^{N-1}\prod_{x>y=0}^{N-1} q_{xy}^{\delta_{\alpha_{j+1},x}\delta_{\alpha_j,y}-\delta_{\alpha_{j+1},y}\delta_{\alpha_j,x}} \\
&\times \left(q_{ab}E_j^{ab}E_{j+1}^{ab}\delta_{\alpha_j,a}\delta_{\alpha_{j+1},b}+q_{ab}^{-1}E_j^{ba}E_{j+1}^{ab}\delta_{\alpha_j,b}\delta_{\alpha_{j+1},a}\right)_{a>b} \\
&\times E^{\alpha_1\alpha_1}\otimes E^{\alpha_2\alpha_2}\otimes\cdots\otimes\mathbf{1}^{(j)}\otimes\mathbf{1}^{(j+1)}\otimes\cdots\otimes E^{\alpha_L\alpha_L}
\end{aligned}
\tag{5.2.17}
$$

Summing over $\{\alpha\}$ gives an identity matrix on each site. Taking into account the Kronecker delta and the sum over α_j,α_{j+1}, one is left with

$$
\begin{aligned}
\mathcal{F}\frac{H^{(nond)}_{j,j+1}}{\mathcal{D}}\mathcal{F}^{-1} &= \prod_{x>y=0}^{N-1}\left(q_{xy}^{\delta_{b,x}\delta_{a,y}-\delta_{a,x}\delta_{b,y}}q_{ab}E_j^{ab}E_{j+1}^{ba}+q_{xy}^{\delta_{a,x}\delta_{b,y}-\delta_{a,y}\delta_{b,x}}q_{ab}^{-1}E_j^{ba}E_{j+1}^{ab}\right)_{a>b} \\
&= \left(q_{ab}^{-1}q_{ab}E_j^{ab}E_{j+1}^{ba}+q_{ab}q_{ab}^{-1}E_j^{ba}E_{j+1}^{ab}\right)_{a>b} \\
&= (E_j^{ab}E_{j+1}^{ba}+E_j^{ba}E_{j+1}^{ab})_{a>b}
\end{aligned}
\tag{5.2.18}
$$

The above term is clearly hermitian. This concludes the proof.

To finish it is instructive to indicate how in the one-parameter N-state diffusion process this expression simplifies. The rates are defined according to

$$A_x + A_y \rightleftharpoons A_y + A_x \quad \Gamma_R, \Gamma_L \quad x > y = 0, 1, \cdots, N-1 \tag{5.2.19}$$

for which the L-site Perk–Schultz Hamiltonia reads

$$
\begin{aligned}
\frac{H}{\mathcal{D}} = \sum_{k=1}^{L-1}\Bigg\{&\frac{q+q^{-1}}{2}-\Bigg[q^{-1}\sum_{\alpha>\beta=0}^{N-1}E_k^{\alpha\beta}E_{k+1}^{\beta\alpha}+q\sum_{\alpha<\beta=0}^{N-1}E_k^{\alpha\beta}E_{k+1}^{\beta\alpha} \\
&+\frac{q+q^{-1}}{2}\sum_{\alpha=0}^{N-1}E_k^{\alpha\alpha}E_{k+1}^{\alpha\alpha}+\frac{q-q^{-1}}{2}\sum_{\alpha\neq\beta=0}^{N-1}sign(\alpha-\beta)E_k^{\alpha\alpha}E_{k+1}^{\beta\beta}\Bigg]\Bigg\}
\end{aligned}
\tag{5.2.20}
$$

In this situation the operator $\mathcal{F}$ from eq. (5.2.5) with $q_{xy}=q$ reduces to a much simpler form. By observing that in this case one has

$$f_1(\alpha_1,\alpha_2,\cdots,\alpha_L)+\cdots+f_{N-1}(\alpha_1,\alpha_2,\cdots,\alpha_L)=\frac{1}{2}\sum_{n>m=1}^{L}sign(\alpha_n-\alpha_m) \tag{5.2.21}$$

then the similarity transformation $\mathcal{F}$ is reduced to (see section 4)

$$\mathcal{F}=\sum_{\alpha_1,\alpha_2,\cdots,\alpha_L=0}^{N-1}q^{\frac{1}{2}\sum_{n>m=1}^{L}sign(\alpha_n-\alpha_m)}E^{\alpha_1\alpha_1}\otimes E^{\alpha_2\alpha_2}\otimes\cdots\otimes E^{\alpha_L\alpha_L} \tag{5.2.22}$$

The results presented here hold for any of the $U_qSU(P/M)$-invariant PS chains with $P+M=N$.

5.3 Periodic Boundary Conditions

Due to the nonlocality of the similarity transformation, the chemical chains with free or periodic boundaries transform differently under $\mathcal{F}$. In the first case the nonhermitian chemical Hamiltonian is transformed into a hermitian PS chain. In the second case, the Hamiltonian is similar under $\mathcal{F}$ to a quantum chain with nontrivial bulk interactions. In the 2-state model this simplifies to a volume dependent boundary interaction which, on its turn, was understood to arise from a Dzialoshinsky-Moriya interaction in the bulk (Henkel and Schütz, 1993; Schütz, 1993; Alcaraz, 1994).

Consider as before particles diffusing on a one-dimensional lattice with **periodic** boundaries. The rates are given by

$$A + \emptyset \rightleftharpoons \emptyset + A \quad \Gamma_R, \Gamma_L \tag{5.3.1}$$

where $\mathcal{D}$ and q are defined in the usual way. The Hamiltonian thus generated reads

$$\begin{aligned}\frac{H}{\mathcal{D}} &= \sum_{k=1}^{L} \left\{ \frac{q+q^{-1}}{2} - \frac{q+q^{-1}}{2} \sum_{\alpha=0}^{1} E_k^{\alpha\alpha} E_{k+1}^{\alpha\alpha} - \frac{q-q^{-1}}{2} \sum_{\alpha \neq \beta = 0}^{1} sign(\alpha-\beta) E_k^{\alpha\alpha} E_{k+1}^{\beta\beta} \right. \\ & \left. -q^{-1} E_k^{10} E_{k+1}^{01} - q E_k^{01} E_{k+1}^{10} \right\} \end{aligned} \tag{5.3.2}$$

It is convenient to change to the more familiar basis of Pauli matrices, by making the identification

$$\begin{aligned} E^{00} &= \frac{\mathbf{1}+\sigma^z}{2} \\ E^{11} &= \frac{\mathbf{1}-\sigma^z}{2} \\ E^{01} &= \sigma^+ \\ E^{10} &= \sigma^- \end{aligned} \tag{5.3.3}$$

In this basis the Hamiltonian can be written as

$$\frac{H}{\mathcal{D}} = -\frac{1}{2} \sum_{k=1}^{L} \left\{ 2q^{-1} \sigma_k^+ \sigma_{k+1}^- + 2q \sigma_k^- \sigma_{k+1}^+ + \frac{q+q^{-1}}{2} \sigma_k^z \sigma_{k+1}^z - \frac{q-q^{-1}}{4} \right\} \tag{5.3.4}$$

The constant term is irrelevant to the present discussion and one may drop it for the time being. Applying eq. (5.2.22) to the remaining terms in the chain yields

$$\begin{aligned} \mathcal{F} \frac{H}{\mathcal{D}} \mathcal{F}^{-1} = \frac{\widetilde{H}}{\mathcal{D}} &= -\frac{1}{2} \sum_{k=1}^{L-1} \left\{ 2\sigma_k^+ \sigma_{k+1}^- + 2\sigma_k^- \sigma_{k+1}^+ + \frac{q+q^{-1}}{2} \sigma_k^z \sigma_{k+1}^z \right\} \\ & -\frac{1}{2} \left\{ 2q^L \sigma_L^+ \sigma_1^- + 2q^{-L} \sigma_L^- \sigma_1^+ + \frac{q+q^{-1}}{2} \sigma_L^z \sigma_1^z \right\} \end{aligned} \tag{5.3.5}$$

Since q is real, one has a boundary term which is proportional to the volume of the system, changing the whole structure of the problem. In other words, the dynamics of diffusion processes in a chain with open boundaries are different from that of a periodic chain.

To see explicitly the Dzialoshinsky-Moryia interaction in (5.3.4), one must redefine q as a function of a new variable η as

$$q = \sqrt{\frac{1-\eta}{1+\eta}} \tag{5.3.6}$$

in terms of which $\Gamma_R = \frac{1+\eta}{2}$ and $\Gamma_L = \frac{1-\eta}{2}$. After some simple algebraic manipulation one can write (5.3.4), apart from the constant term, as

$$\frac{H}{\mathcal{D}} = -\frac{1}{2}\sum_{k=1}^{L}\left\{2\sigma_k^+\sigma_{k+1}^- + 2\sigma_k^-\sigma_{k+1}^+ + \frac{q+q^{-1}}{2}\sigma_k^z\sigma_{k+1}^z + 2\eta\left(\sigma_k^+\sigma_{k+1}^- - \sigma_k^-\sigma_{k+1}^+\right)\right\} \tag{5.3.7}$$

The Dzialoshinsky-Moryia interaction term is clearly recognizable as the last term in this summation.

For higher-state diffusion models on periodic lattices, after applying $\mathcal{F}$ one gets interactions other than the ones obtained in the 2–state case. To see this first note that the whole effect of $\mathcal{F}$ is to change the off-diagonal terms of the 2-body chemical Hamiltonian at the boundary, namely $E_L^{ab}E_1^{ba}$ and $E_L^{ba}E_1^{ab}$. In the 2-state case there are only two possibilities for the pair (a,b): $(1,0)$ and $(0,1)$. Since opposite pairs are related by an inversion of the power of q, one has effectively one result which is q^L. In higher-state cases, the power depends on the particular (a,b) chosen. The results for the 3-state model and the for the general N-state case are presented next.

i) 3-state diffusion process

Here one has $(a,b) = (0,1); (0,2); (1,2)$ together with the reversed pairs. The action of $\mathcal{F}$ yields

$$\begin{aligned} \mathcal{F}\{q^{-1}E_1^{01}E_L^{10}\}\mathcal{F}^{-1} &= q^{-2}E_1^{01}\otimes M_1\otimes M_1\otimes\cdots\otimes M_1\otimes E_L^{10} \\ M_1 &= \begin{pmatrix} q & & \\ & q & \\ & & 1\end{pmatrix} \end{aligned} \tag{5.3.8}$$

for $(a,b) = (0,1)$. Exchanging a with b leads to the same structure where however q is replaced by q^{-1} as expected. For the pair $(a,b) = (1,2)$ one may easily show that

$$\begin{aligned} \mathcal{F}\{q^{-1}E_1^{12}E_L^{21}\}\mathcal{F}^{-1} &= q^{-2}E_1^{12}\otimes M_2\otimes M_2\otimes\cdots\otimes M_2\otimes E_L^{21} \\ M_2 &= \begin{pmatrix} 1 & & \\ & q & \\ & & q\end{pmatrix} \end{aligned} \tag{5.3.9}$$

Finally for $(a,b) = (0,2)$ it follows that

$$\mathcal{F}\{q^{-1}E_1^{02}E_L^{20}\}\mathcal{F}^{-1} = q^{-2}E_1^{02}\otimes M_1M_2\otimes M_1M_2\otimes\cdots\otimes M_1M_2\otimes E_L^{21} \tag{5.3.10}$$

In conclusion, the effect of the transformation cannot be understood in terms of boundary interactions, in contradistinction to the 2-state problem - the interaction is 'spread' over the bulk. The structure is analogous in higher-state models as it is shown next.

ii) N-state diffusion process

Assume that $(a,b) = (i,j)$ such that $i < j = 0,1,\cdots,N-1$. In this case then

$$\mathcal{F}\{q^{-1}E_1^{ij}E_L^{ji}\}\mathcal{F}^{-1} = q^{-2}E_1^{ij}\otimes M\otimes M\otimes\cdots\otimes M\otimes E_L^{ji} \tag{5.3.11}$$

where M is an $N \times N$ matrix which reads

$$M = \begin{pmatrix} 1 & & & & & & & & & & \\ & \ddots & & & & & & & & & \\ & & 1 & & & & & & & & \\ & & & q & & & & & & & \\ & & & & q^2 & & & & & & \\ & & & & & \ddots & & & & & \\ & & & & & & q^2 & & & & \\ & & & & & & & q & & & \\ & & & & & & & & 1 & & \\ & & & & & & & & & \ddots & \\ & & & & & & & & & & 1 \end{pmatrix} \tag{5.3.12}$$

where q appears at the i-th and j-th positions in the diagonal. All other M_{kk} are equal to 1 for $k < i$ and $k > j$ and equal to q^2 in the case $i < k < j$. The interaction is spread along the bulk since, as one may see from (5.3.11), it is impossible to factorize the matrix M.

5.4 Conclusions

In the last two chapters two results have been presented: (i) the Hamiltonian obtained from the master equation of general three-state diffusion–reaction systems is related to two known integrable chains, namely the $U_q\widehat{SU(2)}$-invariant model and the Perk-Schultz Hamiltonian with external fields. It was shown that it is a fundamental characteristic of such mappings that the rates governing chemical processes are bound to satisfy some constraints relating them. These arise ultimately from the fact that the parameters in the chemical problem exceeds the number of those in the quantum chains they are mapped onto. For the $U_q\widehat{SU(2)}$–model these constraints are contained in equations (5.2.9)–(5.2.11), while for the Perk–Schultz hamiltonians they are reproduced in table 1, section 5.3. (ii) The asymmetry in the diffusion rates for 3– and higher–state systems reflects itself in the structure of the related quantum chains, which under the similarity transformation (5.3.4) manifests itself throught the appearance of a non–local bias–dependent interaction term, in contradistinction to the 2 –state case, where such asymmetry leads only to a volume-dependent boundary term. This novel interaction can be understood as an extension of a Dzialoshinsky-Moryia interaction for higher–state chains, as explained in the last section of this chapter.

The mapping here defined preserves the spectrum of the chains, implying that the phase diagram of the chemical model is completely settled by that of the integrable chain. As an example, it was shown in chapter 4 how the massless and massive regimes of the $U_q\widehat{SU(2)}$–model, whose phase diagram is identical to that of the XXZ chain with an external field, can be interpreted in terms of the time-dependence for the decay of the particles' concentration. In the Perk-Schultz models with external fields the present work went beyond the mapping by deriving the Bethe Ansatz Equations for the 3-state chemical processes taking place on a lattice with periodic boundaries. These are related, through a similarity transformation, to chains with novel bulk interactions. As to what regards the Bethe Ansatz Equations, these are too complex to solve and a treatment (numerical and/or analytical) remains an open problem.

Part III

Appendices

Appendix A

The Coordinate Bethe Ansatz and the Asymmetric XXZ Chain

A.1 Introduction

This appendix is concerned with the coordinate variant of the Bethe Ansatz technique (Bethe, 1931; Orbach, 1958) as applied to the asymmetric XXZ Model. This chain is defined by the Hamiltonian

$$H(\psi,\Delta,N) = -\frac{1}{2}\sum_{n=1}^{N}\left(2e^{\psi}\sigma_n^+\sigma_{n+1}^- + 2e^{-\psi}\sigma_n^-\sigma_{n+1}^+ + \Delta\left(\sigma_n^z\sigma_{n+1}^z - 1\right)\right) \tag{A.1}$$

where $2\sigma^\pm = \sigma^x \pm i\sigma^y$ and $\psi \in R$. ψ breaks parity invariance and makes H non hermitian. The Pauli matrices $\sigma^x, \sigma^y, \sigma^z$ are defined as usual

$$\sigma^x = \begin{pmatrix} 0 & 1 \\ 1 & 0 \end{pmatrix} \qquad \sigma^y = \begin{pmatrix} 0 & -i \\ i & 0 \end{pmatrix} \qquad \sigma^z = \begin{pmatrix} 1 & 0 \\ 0 & -1 \end{pmatrix} \tag{A.2}$$

Along the stochastic line $\Delta = \cosh\psi$ this hamiltonian can be seen as the evolution operator of 2–state diffusive systems in one dimension. ψ is related to the probability of particles hopping to the right (or left) lattice sites (see part II of this dissertation and Alcaraz *et al*, 1994b).

The detailed derivation of the Bethe Ansatz Equations are presented in what follows. Through an expansion of the wave function in a properly chosen basis (Bethe's hypothesis), an equation on the coefficients of this expansion is obtained. After solving it for the one–, two– and three–magnon cases, the form of the amplitudes for the general M–magnon problem is derived. The compatibility conditions one has to impose if the appearance of two excitations on the same lattice site is to be avoided, together with the periodicity of the lattice lead to the so–called Bethe Ansatz Equations (BAE).

A.2 The Ansatz of Bethe

A more thoroughly look into the structure of (A.1) reveals three important features of this operator

- the z–component of the total spin $S^z = \sum_{k=1}^{N}\sigma_k^z$ is a conserved charge.
- there is a trivial ferromagnetic eigenstate with all spins pointing in the same direction $|S^z = N\rangle = |\uparrow\uparrow\cdots\uparrow\rangle \equiv |0\rangle$
- this trivial eigenstate is *scale invariant*

Together these features imply that one may decompose the 2^N–dimensional Hilbert space into $(N+1)$ disjoint charge sectors, which can be labelled by the spin deviation w.r.t. $|0\rangle$, *i.e.* by the number of down–turned spins relative to the ordered state $|0\rangle$. Therefore, one may span the subspace of n spin deviations ($S^z = N - 2n$) in a set of orthogonal kets defined accordingly as [1]

$$|x_1\, x_2\, x_3\, \cdots\, x_n\rangle = \sigma^-_{x_1}\sigma^-_{x_2}\sigma^-_{x_3}\cdots\sigma^-_{x_n}\,|0\rangle \tag{A.2.1}$$

where x_i is the cartesian coordinate fo the i–th atom whose electron has a spin projection $-\frac{1}{2}$. In conclusion, due to the linear character of the chain one may characterize a given spin configuration by ordering the position of the down–turned spins under the restriction

$$1 \leq x_1 < x_2 < \cdots < x_n \leq N \tag{A.2.2}$$

The $U(1)$–charge conservation, the scale–invariance of the reference state $|0\rangle$ and the ordering (A.2.2) of the spin deviations are fundamental ingredients behind Bethe's hypothesis. This Ansatz consists in the assumption that the wave–function of a state in the sector with n spin deviates is given by a linear combination of kets of type (A.2.1)

$$|n\rangle = \sum_{\{x\}} a\,(x_1, x_2, \cdots, x_n)\,|x_1\, x_2\, \cdots\, x_n\rangle \tag{A.2.3}$$

where the sum runs over all the $C^N_n = \begin{pmatrix} N \\ n \end{pmatrix}$ distinct arrangements of coordinates $\{x_1, x_2, \cdots, x_n\} \equiv \{x\}$ among N sites subject to (A.2.2). Periodic boundary conditions further imply [2]

$$a\,(x_1, x_2, \cdots, x_n) = a\,(x_2, x_3, \cdots, x_n, x_1 + N) \tag{A.2.4}$$

Solving the Bethe Ansatz means finding an analytic expression for the coefficients $a(\{x\})$, *i.e.* to determine and solve the equations these coefficients fulfill. These defining equations are found by operating with $H(\psi, \Delta, N)$ on $|n\rangle$ and requiring this ket to be an eigenstate of this Hamiltonian.

A.3 The defining equation

To determine the equation satisfied by the $a(\{x\})$'s, one first needs a representation for the ket $|x_1\, x_2\, \cdots\, x_n\rangle$. The natural choice is the tensor product space spanned by the vectors $\begin{pmatrix} 0 \\ 1 \end{pmatrix} = |\downarrow\rangle$ and $\begin{pmatrix} 1 \\ 0 \end{pmatrix} = |\uparrow\rangle$, *i.e.*

$$|x_1\, x_2\, \cdots\, x_n\rangle \equiv \begin{pmatrix} 1 \\ 0 \end{pmatrix} \otimes \begin{pmatrix} 1 \\ 0 \end{pmatrix} \otimes \cdots \otimes \begin{pmatrix} 1 \\ 0 \end{pmatrix} \otimes \underbrace{\begin{pmatrix} 0 \\ 1 \end{pmatrix}}_{x_1\text{-th site}} \otimes \begin{pmatrix} 1 \\ 0 \end{pmatrix} \otimes \cdots \otimes \begin{pmatrix} 1 \\ 0 \end{pmatrix} \tag{A.3.1}$$

We consider the diagonal and off–diagonal contributions separately. The diagonal contribution from $H(\psi, \Delta, N)$ gives

$$\langle\{x'\}| - \sum_{n=1}^{N} \Delta\,(\sigma^z_n\sigma^z_{n+1} - 1)\,|\{x\}\rangle = N_a\Delta \times \delta_{\{x'\},\{x\}} \tag{A.3.2}$$

[1] For the symmetric $\psi = 0$ case, the sector with n and $N - n$ spin deviates have the same energy. In the general case, these energies are related through complex conjugation.

[2] We would like to point out that the 'generalized' boundary formulation of the asymmetric chain would enter in the above expression in the form $a(x_1, x_2, \cdots, x_n) = e^{\psi}a(x_2, x_3, \cdots, x_n, x_1 + N)$

where N_a is the number of antiparallel spin pairs $|\downarrow\uparrow\rangle$ and $|\uparrow\downarrow\rangle$ in $\{x\}$ and δ is the Kronecker symbol. The off–diagonal elements require a more careful analysis. The action of the raising and lowering operators in $H(\psi,\Delta,N)$ gives rise to transitions $|x_1\, x_2\, \cdots\, x_n\rangle \longrightarrow |x'_1\, x'_2\, \cdots\, x'_n\rangle$ where $\{x'\}$ may differ from $\{x\}$ by the interchange of at most one pair of antiparallel spins, *i.e.*

$$x'_1 = x_1 \ , \ x'_2 = x_2 \ , \ \cdots \ , \ x'_\alpha = x_\alpha \pm 1 \ , \ \cdots \ , \ x'_n = x_n \tag{A.3.3}$$

Therefore

$$H^{od}(\psi, N)\,|\{x\}\rangle = -e^{\psi} \sum_{\{x'\}_{\mathrm{R}}} |\{x'\}\rangle - e^{\psi} \sum_{\{x''\}_{\mathrm{L}}} |\{x''\}\rangle \tag{A.3.4}$$

where H^{od} stands for the off-diagonal part of $H(\psi,\Delta,N)$ and the sums are restricted to those sets of coordinates having one position displaced to the right or to the left w.r.t. the initial arrangement $\{x_1\, x_2\, \cdots\, x_n\}$, *i.e.*

$$x'_\alpha = x_\alpha + 1 \qquad x''_\alpha = x_\alpha - 1 \tag{A.3.5}$$

for some α. Considering both contributions (A.3.2) and (A.3.4), the Ansatz $H(\psi,\Delta,N)\,|n\rangle = E\,|n\rangle$ yields

$$\begin{aligned} Ea\,(x_1, x_2, \cdots, x_n) &= N_a \Delta a\,(x_1, x_2, \cdots, x_n) - e^{\psi} \sum_{\{x'\}_{\mathrm{R}}} a\,(x'_1, x'_2, \cdots, x'_n) \\ &- e^{-\psi} \sum_{\{x''\}_{\mathrm{L}}} a\,(x''_1, x''_2, \cdots, x''_n) \end{aligned} \tag{A.3.6}$$

This is the defining equation for the coefficients. Solving this for general n spin deviates is not a straighforward task. The idea is then to consider the simplest case, namely the sector with one down–turned spin and proceed to higher sectors, in the hope this will shed some light into the structure of the general solution. It turns out this is indeed the case and one may find an expression for the $a(\{x\})$'s, hence determining the wave–function.

I. One–Magnon Sector

If $n = 1$ there is just one positon x in (A.3.6), which reduces to the finite–diference equation

$$Ea(x) = 2\Delta a(x) - e^{\psi} a(x+1) - e^{-\psi} a(x-1) \tag{A.3.7}$$

whose solution reads

$$a(x) = e^{ikx} \tag{A.3.8}$$

Substituting this solution for $a(x)$ back into (A.3.7) gives the energy of the one–magnon problem

$$E = 2\Delta - 2\cos\,(k - i\psi) \tag{A.3.9}$$

Notice that the wave–number k is shifted by a complex amount in comparison to the $\psi = 0$ symmetric case. From the boundary conditions follow the quantization of k,

$$a(x+N) = a(x) \longrightarrow k = \frac{2\pi}{N} l \ , \qquad l = 0, \pm 1, \cdots, \pm \frac{N-1}{2} \tag{A.3.10}$$

The normalized wave–function reads

$$|1\rangle = \frac{1}{\sqrt{N}} \sum_{x=1}^{N} e^{ikx}\,|x\rangle \tag{A.3.11}$$

This is simply the wave–function of a free magnon on a periodic one–dimensional box of length N (the lattice spacing in this case being taken equal to 1).

II. Two–Magnon Sector

There are two distinct situations for the positions x_1 and x_2 of the spin deviates to consider, namely whether both magnons are nearest neighbors or not.

i) case $x_2 \neq x_1 + 1$. If the down–turned spins are not nearest neighbors, we have from (A.3.6) the defining equation

$$\begin{aligned} Ea(x_1, x_2) &= 4\Delta a(x_1, x_2) - e^{\psi} a(x_1 + 1, x_2) - e^{\psi} a(x_1, x_2 + 1) \\ &- e^{-\psi} a(x_1 - 1, x_2) - e^{-\psi} a(x_1, x_2 - 1) \end{aligned} \tag{A.3.12}$$

The solution $a(x_1, x_2)$ is a combination of a direct plus an exchange term

$$a(x_1, x_2) = A_{12} e^{ik_1 x_1 + ik_2 x_2} + A_{21} e^{ik_2 x_1 + ik_1 x_2} \tag{A.3.13}$$

The energy of the two–magnon state follows by setting this solution back into the defining equation (A.3.12),

$$E = 2\left[\Delta - \cos\left(k_1 - i\psi\right)\right] + 2\left[\Delta - \cos\left(k_2 - i\psi\right)\right] \tag{A.3.14}$$

Notice that the energy of the two–magnon state is the sum of one–magnon energies. This quasi–particle feature of the spectrum is valid for arbitrary number of spin deviates, as we shall show, and is typical for all systems solvable through the Bethe Ansatz.

ii) case $x_2 = x_1 + 1$. In this situation the equation for the $a(\{x\})$'s reads

$$\begin{aligned} Ea(x, x+1) &= 2\Delta a(x, x+1) - e^{\psi} a(x+1, x+1) - e^{\psi} a(x, x+2) \\ &- e^{-\psi} a(x-1, x+1) - e^{-\psi} a(x, x) \end{aligned} \tag{A.3.15}$$

This equation however must be compatible with the equation for the previous situation. This imposes some restrictions on the possible values of A_{12} and A_{21}, leading, together with the periodicity of the boundaries, to the so–called *Bethe Ansatz Equations.* To have (A.3.12) reproduce (A.3.15) we set $x_2 = x_1 + 1$ in the former. This yields three extra terms which must be set to zero if both equations are to be the same, that is

$$2\Delta a(x, x+1) - e^{\psi} a(x+1, x+1) - e^{-\psi} a(x, x) = 0 \tag{A.3.16}$$

Substituting the Ansatz (A.3.13) back into the above equation we obtain a condition on A_{12} and A_{21}, namely

$$\frac{A_{12}}{A_{21}} = \frac{1 - 2\Delta e^{i(k_1 - i\psi)} + e^{i(k_1 + k_2 - 2i\psi)}}{1 - 2\Delta e^{i(k_2 - i\psi)} + e^{i(k_1 + k_2 - 2i\psi)}} \tag{A.3.17}$$

It turns out it is convenient to define the shifted wave number $p = k - i\psi$ for later comparison with the literature on the symmetric XXZ model. Then

$$\frac{A_{12}}{A_{21}} = \frac{1 - 2\Delta e^{ip_1} + e^{i(p_1 + p_2)}}{1 - 2\Delta e^{ip_2} + e^{i(p_1 + p_2)}} = \exp\left[-i\Theta(p_1, p_2)\right] \tag{A.3.18}$$

where the *shift function* $\Theta(p_1, p_2)$ is defined as

$$\Theta(p_1, p_2) = 2\tan^{-1}\left[\frac{\Delta \sin(\frac{p_1 - p_2}{2})}{\cos(\frac{p_1 + p_2}{2}) - \Delta\cos(\frac{p_1 - p_2}{2})}\right] \tag{A.3.19}$$

The boundary condition $a(x_1, x_2) = a(x_2, x_1 + N)$ leads to two extra conditions on A_{12} and A_{21}, namely

$$\frac{A_{12}}{A_{21}} = e^{ik_1 N} = e^{ip_1 N - N\psi} \tag{A.3.20}$$
$$\frac{A_{21}}{A_{12}} = e^{ik_2 N} = e^{ip_2 N - N\psi} \tag{A.3.21}$$

Comparison between these expressions and eq. (A.3.17) yields a set of equations coupling the shifted momenta p_1 and p_2, the Bethe Ansatz Equations for the two–magnon problem,

$$e^{ip_1 N - N\psi} = -\frac{1 - 2\Delta e^{ip_1} + e^{i(p_1+p_2)}}{1 - 2\Delta e^{ip_2} + e^{i(p_1+p_2)}} \tag{A.3.22}$$
$$e^{ip_2 N - N\psi} = -\frac{1 - 2\Delta e^{ip_2} + e^{i(p_1+p_2)}}{1 - 2\Delta e^{ip_1} + e^{i(p_1+p_2)}} \tag{A.3.23}$$

One remark on condition (A.3.16), which leads to the above equations is noteworthy. One could have required the unphysical coefficients $a(x, x)$ to be identically zero from the onset of the problem. However, the two–magnon problem can be solved exactly for the general *isotropic* spin–S Heisenberg model through an analogous two-spin deviate basis state (Mattis, 1981)

$$|x_i\ x_j\rangle = S_i^- S_j^-\ |0\rangle \tag{A.3.24}$$

where S^- are higher–spin $SU(2)$ matrices, $|0\rangle$ is the ferromagnetic reference state and *there is no* restriction of the type $i \neq j$. In this situation, with an Ansatz

$$|2\rangle = \sum_{x_1 \leq x_2} a(x_1, x_2)\, |x_1\ x_2\rangle \tag{A.3.25}$$

one gets an equation similar to (A.3.12) where now coefficients of the type $a(x, x)$ cannot be discarded since they represent physically well defined amplitudes. Therefore, on consistency grounds, one does not require $a(x, x)$ to be zero in the spin $S = \frac{1}{2}$ case but only their combination as expressed in (A.3.16).

III. The Three–Magnon Sector

There are four different situations to consider.

i) case $x_2 \neq x_1 + 1$; $x_3 \neq x_2 + 1$. The fundamental equation reads

$$\begin{aligned} Ea(x_1, x_2, x_3) &= 6\Delta a(x_1, x_2, x_3) \\ &- e^{\psi}\left[a(x_1+1, x_2, x_3) + a(x_1, x_2+1, x_3) + a(x_1, x_2, x_3+1)\right] \\ &- e^{-\psi}\left[a(x_1-1, x_2, x_3) + a(x_1, x_2-1, x_3) + a(x_1, x_2, x_3-1)\right] \end{aligned} \tag{A.3.26}$$

The solution is given by a superposition of all permutations among momenta and positions

$$\begin{aligned} a(x_1, x_2, x_3) &= \\ A_{123} e^{i(k_1 x_1 + k_2 x_2 + k_3 x_3)} &+ A_{132} e^{i(k_1 x_1 + k_3 x_2 + k_2 x_3)} + A_{213} e^{i(k_2 x_1 + k_1 x_2 + k_3 x_3)} \\ + A_{321} e^{i(k_3 x_1 + k_2 x_2 + k_1 x_3)} &+ A_{312} e^{i(k_3 x_1 + k_1 x_2 + k_2 x_3)} + A_{231} e^{i(k_2 x_1 + k_3 x_2 + k_1 x_3)} \end{aligned} \tag{A.3.27}$$

This solution gives for the energy

$$E = 2\left[\Delta - \cos(k_1 - i\psi)\right] + 2\left[\Delta - \cos(k_2 - i\psi)\right] + 2\left[\Delta - \cos(k_3 - i\psi)\right] \tag{A.3.28}$$

ii) case $x_2 = x_1 + 1$; $x_3 \neq x_2 + 1$. If the first and second down–turned spins are nearest neighbors we have, as defining equation, the following expression

$$\begin{aligned} Ea(x, x+1, x') &= 4\Delta a(x, x+1, x') \\ &- e^{\psi}\left[a(x, x+2, x') + a(x, x+1, x'+1)\right] \\ &- e^{-\psi}\left[a(x-1, x+1, x') + a(x, x+1, x'-1)\right] \end{aligned} \tag{A.3.29}$$

As in the two–magnon case, compatibility in both situations yields

$$2\Delta a(x, x+1, x') - e^{\psi} a(x+1, x+1, x') - e^{-\psi} a(x, x, x') = 0 \tag{A.3.30}$$

This equation, after the substitution of the Ansatz (A.3.27), gives some relations to be satisfied by the A_{ijk}'s, namely

$$\frac{A_{123}}{A_{213}} = -e^{-i\Theta(p_1,p_2)}, \quad \frac{A_{132}}{A_{321}} = -e^{-i\Theta(p_1,p_3)}, \quad \frac{A_{231}}{A_{321}} = -e^{-i\Theta(p_2,p_3)} \tag{A.3.31}$$

with $\Theta(p_i, p_j)$ defined in (A.3.19).

iii) case $x_2 \neq x_1 + 1$; $x_3 = x_2 + 1$. In this situation, compatibility between the Ansätze can be expressed through

$$2\Delta a(x', x, x+1) - e^{\psi} a(x', x+1, x+1) - e^{-\psi} a(x', x, x) = 0 \tag{A.3.32}$$

This equation renders three more relations, namely

$$\frac{A_{123}}{A_{132}} = -e^{-i\Theta(p_2,p_3)}, \quad \frac{A_{213}}{A_{231}} = -e^{-i\Theta(p_1,p_3)}, \quad \frac{A_{312}}{A_{321}} = -e^{-i\Theta(p_1,p_2)} \tag{A.3.33}$$

iv) here $x_2 = x_1 + 1$; $x_3 = x_2 + 1$. The equation defining the amplitudes reads

$$\begin{aligned} Ea(x, x+1, x+2) &= 2\Delta a(x, x+1, x+2) - e^{\psi} a(x, x+1, x+3) \\ &- e^{-\psi} a(x-1, x+1, x+2) \end{aligned} \tag{A.3.34}$$

and it does not lead to any new relations among the coefficients A_{ijk} Setting finally the Ansatz (A.3.27) into the boundary condition $a(x_1, x_2, x_3) = a(x_2, x_3, x_1 + N)$ we obtain the following conditions on the rates

$$\frac{A_{123}}{A_{231}} = e^{ip_1 N - N\psi}, \quad \frac{A_{213}}{A_{132}} = e^{ip_2 N - N\psi}, \quad \frac{A_{312}}{A_{123}} = e^{ip_3 N - N\psi} \tag{A.3.35}$$

from which the Bethe Ansatz Equations for the three momenta p_1,p_2 and p_3 follow

$$e^{ip_l N - N\psi} = \prod_{j \neq l} - \frac{1 - 2\Delta e^{ip_l} + e^{i(p_l + p_j)}}{1 - 2\Delta e^{ip_j} + e^{i(p_l + p_j)}} \qquad j, l = 1, 2, 3 \tag{A.3.36}$$

IV. n–Magnon Sector

The structure of the one–, two– and three–magnon solutions for the coefficients $a(\{x\})$ allows us to write the coefficient for the general n–magnon sector. The defining equation for the amplitudes read, in this case

$$\begin{aligned} Ea(x_1, x_2, \cdots, x_{\mathrm{n}}) &= N_a \Delta a(x_1, x_2, \cdots, x_{\mathrm{n}}) - e^{\psi} \sum_{\alpha=1}^{n} a(x_1, x_2, \cdots, x_\alpha + 1, \cdots, x_{\mathrm{n}}) \\ &- e^{-\psi} \sum_{\alpha=1}^{n} a(x_1, x_2, \cdots, x_\alpha - 1, \cdots, x_{\mathrm{n}}) \end{aligned} \tag{A.3.37}$$

By enforcing compatibility conditions arising from configurations with neighboring spin deviates, we obtain some conditions on the unphysical amplitudes $a(\cdots,x,x,\cdots)$. These conditions can be read off directly from the above equation and read

$$2\Delta a(\cdots,x_\alpha,x_\alpha+1,\cdots)-e^{\psi}a(\cdots,x_\alpha+1,x_\alpha+1,\cdots)-e^{-\psi}a(\cdots,x_\alpha,x_\alpha,\cdots)=0 \qquad \text{(A.3.38)}$$

with $1\le\alpha\le n$. From these equations one obtains ratios among the coefficients A_{P} coming from the Ansatz

$$a(x_1,x_2,\cdots,x_n)=\sum_{\mathrm{P}}A_{\mathrm{P}}\exp\left(i\sum_{j=1}^{n}k_{\mathrm{P}_j}x_j\right) \qquad \text{(A.3.39)}$$

where P is some permutation of $(1,2,\cdots,n)$. These ratios are of the form

$$\frac{A_{\mathrm{P}}}{A_{\mathrm{I}}}=\pm\prod e^{-i\Theta(p_j,p_k)} \qquad \text{(A.3.40)}$$

The product runs over all pairs (j,k) which have to be interchanged in going from the identity permutation $A_{\mathrm{I}}=a_{1234\cdots n}$ to any A_{P}. The $\pm$ sign comes from the parity of the number of permutations necessary to go from A_{I} to a given A_{P}.

Finally, eq. (A.3.40) together with the boundary condition eq. (A.2.4) yield the Bethe Ansatz Equations for the shifted wave vectors $p_1,p_2,\cdots,p_n$. They read

$$e^{ip_lN-N\psi}=\prod_{j\neq l=1}^{n}-\frac{1-2\Delta e^{ip_l}+e^{i(p_l+p_j)}}{1-2\Delta e^{ip_j}+e^{i(p_l+p_j)}} \qquad j,l=1,2,\cdots,n \qquad \text{(A.3.41)}$$

The energy of the n–magnon state with quasi momenta $p_1,p_2,\cdot,p_n$ reads

$$E=\sum_{j=1}^{n}2\left[\Delta-\cos\left(k_j-i\psi\right)\right]=\sum_{j=1}^{n}2\left[\Delta-\cos p_j\right] \qquad \text{(A.3.42)}$$

In the literature one usually finds the BAE parametrized in terms of the variables λ_j (rapidities) in place of the momenta p_j. This parametrization was originally introduced by Orbach (1958) and carries his name. It depends on the different regimes of anisotropy Δ.

Δ	p_j	$\Theta(\lambda_j-\lambda_l)$	Energy	λ_j
$\Delta=\cosh\gamma$	$2\tan^{-1}(\coth\frac{\gamma}{2}\tan\lambda_j)$	$2\tan^{-1}[\coth\gamma\tan(\lambda_j-\lambda_l)]$	$\Lambda=\lambda$	$\lvert Re(\lambda_j)\rvert\le 2\pi$ **Equation I with** $\eta=i\frac{\gamma}{2}$
$\Delta=1$	$2\cot^{-1}(2\lambda_j)$	$2\tan^{-1}(\lambda_j-\lambda_l))$	$\Lambda=\lambda$	$-\infty<\lambda_j<\infty$ **Equation II**
$\Delta=-\cos\gamma$	$2\tan^{-1}(\cot\frac{\gamma}{2}\tanh\lambda_j)$	$2\tan^{-1}[\cot\gamma\tanh(\lambda_j-\lambda_l)]$	$\Lambda=i\lambda+\frac{\pi}{2}$	$-\infty<\lambda_j<\infty$ **Equation I with** $\eta=\frac{\pi}{2}-\frac{\gamma}{2}$
$\Delta=-1$	$2\tan^{-1}(2\lambda_j)$	$2\tan^{-1}(\lambda_j-\lambda_l))$	$\Lambda=\lambda$	$-\infty<\lambda_j<\infty$ **Equation II**
$\Delta=-\cosh\gamma$	$2\tan^{-1}(\coth\frac{\gamma}{2}\tan\lambda_j)$	$2\tan^{-1}[\coth\gamma\tan(\lambda_j-\lambda_l)]$	$\Lambda=\lambda+\frac{\pi}{2}$	$\lvert Re(\lambda_j)\rvert\le 2\pi$ **Equation I with** $\eta=\frac{\pi}{2}+i\frac{\gamma}{2}$

In the first column the different regimes of anisotropy are given. In the second the functional dependence of p in terms of λ is shown. The third colums gives the shift function Θ as a function of the rapidities. The energy in the fourth column is given by the expressions below (Energy I and II) with the appropriate substitution of Λ. The last column gives the range of the rapidities λ and the appropriate Bethe Ansatz Equation for that regime (Equation I and II).

Equation I
$$\left[\frac{\sin(\lambda_j+\eta)}{\sin(\lambda_j-\eta)}\right]^N e^{\psi N} = \prod_{l\neq j=1}^{n} \frac{\sin(\lambda_j-\lambda_l+2\eta)}{\sin(\lambda_j-\lambda_l-2\eta)} \tag{A.3.43}$$

Energy I
$$E = -\sum_{j=1}^{n} \frac{2\sin^2 2\eta}{\cos 2\eta - \cos 2\Lambda_j} \tag{A.3.44}$$

Equation II
$$\left[\frac{\lambda_j+\frac{i}{2}}{\lambda_j-\frac{i}{2}}\right]^N e^{\psi N} = \prod_{l\neq j=1}^{n} \frac{\lambda_j-\lambda_l+i}{\lambda_j-\lambda_l-i} \tag{A.3.45}$$

Energy II
$$E = \mathrm{sign}(\Delta)\sum_{j=1}^{n} \frac{1}{{\Lambda_j}^2+\frac{1}{4}} \tag{A.3.46}$$

In all cases the total momentum of a state is given by the sum of the individual momenta p_j. The Bethe Equations of chapter 3 are regained from I under the substitution $\eta = i\frac{\gamma}{2}$, $\lambda_j = \frac{\alpha_j}{2}$ and $\psi = 2h$.

In its coordinate version, the Bethe Ansatz is only of limited applicability: there are many interesting one–dimensional models which require a non trivial generalization of Bethe's method, for instance the XYZ hamiltonian (Baxter, 1972). This breaking down of the original method can be understood as follows: Bethe's original ideia consists of the decomposition of the exponents of the wave functions into phase shifts which depend on two wave–vectors only. This essential feature of the model can be seen in (A.3.40), that is the factorization of the n–particle scattering into $\frac{n(n-1)}{2}$ two–body scatterings. If more than two excitations are allowed on a given site (*i.e.* models with more than two states per site), this decomposition might not hold any longer. A factorization condition (the Yang–Baxter Equation) is required, and it is the starting point for the derivation of the Algebraic Bethe Ansatz (Yang, 1968; Baxter 1972).

Appendix B

The Algebraic Bethe Ansatz and the Six–Vertex Model

B.1 Integrability in two dimensions

In this appendix the algebraic version of the Bethe's technique is applied to obtain the transfer matrix spectrum of the asymmetric six–vertex model. We introduce the factorizable S–matrix and the factorization equation, as a sufficient condition for the integrability of a scattering theory in two space–time dimensions. The formal connection between the elements of the S–matrix and the Boltzmann weights of a statistical model on the lattice leads naturally from the field theoretical to the statistical mechanical formulation of integrability: The factorization equation of the multiparticle S–matrix becomes the Yang–Baxter Equation (YBE), which implies in the commutation of the one–parameter family of transfer matrices, through the existence of the $\check{R}$–matrix, from whose algebraic structure the Bethe Ansatz Equations are regained.

The transition from two–dimensional classical vertex–models to one–dimensional quantum chains is done via the extremely anisotropic limit of the transfer matrix, following Baxter's definition. From the commutation of the tranfer matrix with the Hamiltonian, it follows that they are diagonalized by the same Bethe Ansatz and the connection with Appendix A is established.

B.1.1 $(1+1)$–d Field Theoretical Formulation: the S–matrix and the Factorization Equation

According to Liouville's theorem, a system with n degrees of freedom is said to be integrable if it possesses n independent first integrals (constants of motion).

In integrable $(1+1)$–dimensional quantum field theories, there being an infinite number of degrees of freedom, Liouville's theorem implies the existence of an infinite number of conserved charges. This imposes severe constraints on the scattering process (Zamolodchikov, Zamolodchikov, 1979). Consider a scattering theory whose underlying relativistic dynamics is governed by infinitely many conservation laws, the symmetry generators Q_n $(n = 0, 1, \cdots, \mathrm{inf})$ being diagonal in one–particle states

$$Q_n \left|p_1, p_2, \cdots, p_k\right\rangle_{in} = \sum_{j=1}^{k} (p_j)^n \left|p_1, p_2, \cdots, p_k\right\rangle_{in} \tag{B.1.1}$$

$$Q_n \left|p'_1, p'_2, \cdots, p'_l\right\rangle_{out} = \sum_{j=1}^{l} \left(p'_j\right)^n \left|p'_1, p'_2, \cdots, p'_l\right\rangle_{out} \tag{B.1.2}$$

where p_i (p'_i) is the momentum of the i–th incoming (outgoing) particle. Since $\frac{dQ}{dt} = 0$, the expectation value of the charge must be the same in both cases, i.e.

$$\sum_{j=1}^{k} (p_j)^n = \sum_{j=1}^{l} \left(p'_j\right)^n \tag{B.1.3}$$

This equality can only be satisfied for all n if $k = l$: there can be no particle production and each individual momentum is conserved. The scattering consists of an exchange of quantum numbers only. If this is the case, using general field–theoretical arguments, it can be proven that the many–body scattering–matrix is given by the product of all possible 2–particle S–matrices (Iagolnitzer, 1978), and these must satisfy a *factorization equation*.

In order to study the S–matrix it is convenient to parametrize energy and momentum of a particle of mass m in terms of the rapidity (or spectral parameter) θ through

$$p^\mu = \left(p^0, p^1\right) = (m\cosh\theta, m\sinh\theta) \tag{B.1.4}$$

Consider the 2–particle scattering $(i,j) \to (k,l)$ where $i, j, \cdots$ are quantum numbers labelling particle states with rapidities θ_1, θ_2. Relativistic invariance constrains the matrix $S_{j\to l}^{i\to k} = S_{jl}^{ik}$ of such process to depend only on the difference of rapidities $S_{jl}^{ik} = S_{jl}^{ik}(\theta_1 - \theta_2)$. The scattering amplitudes for in– and outgoing particles are related through

$$A_i(\theta_1)A_j(\theta_2) = S_{jl}^{ik}(\theta_1 - \theta_2)A_k(\theta_1)A_l(\theta_2) \tag{B.1.5}$$

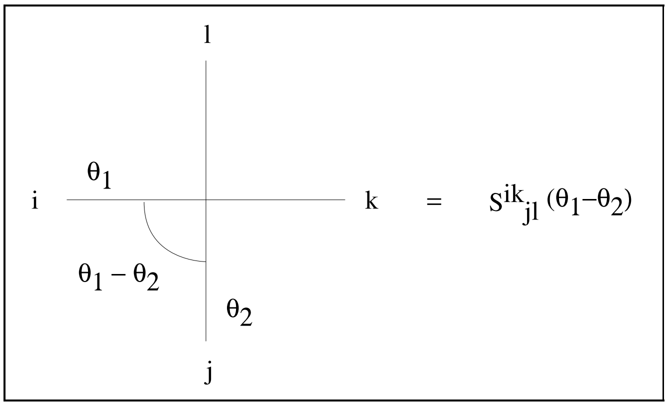

Figure 9. The scattering matrix S.

Considering the 3–body process $(i,j,k) \to (p,q,r)$, there are *a priori* two inequivalent ways (temporal ordering) of describing the scattering in terms of 2–body S–matrices: first, i scatters with j and then k, followed by j with k. Reversing the order, j interacts with k, followed by k with i and then i with j. From this factorization condition follows the *factorization equation*, which reads

$$\sum_{\alpha\beta\gamma} S_{\gamma r}^{\beta q}(\theta')\, S_{k\gamma}^{\alpha p}(\theta+\theta')\, S_{j\beta}^{i\alpha}(\theta) = \sum_{\alpha\beta\gamma} S_{\beta q}^{\alpha p}(\theta)\, S_{\gamma r}^{i\alpha}(\theta+\theta')\, S_{k\gamma}^{j\beta}(\theta') \tag{B.1.6}$$

Note that upon 'shifting' one line through the vertices, the angles have to be preserved.

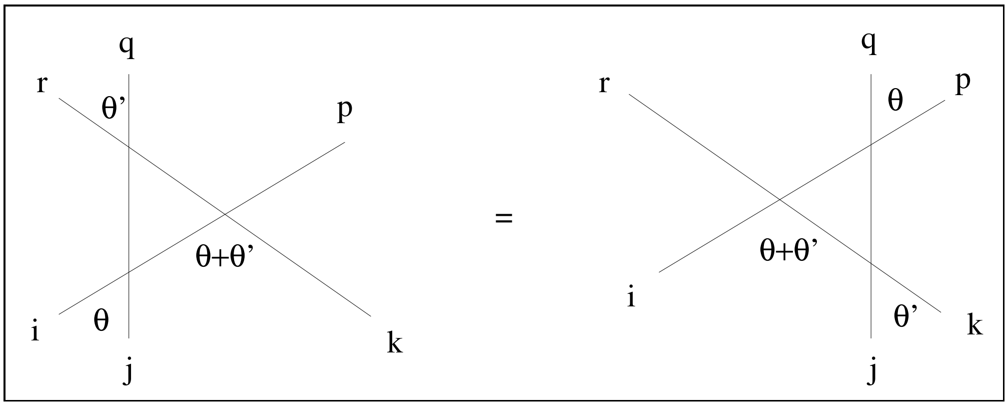

Figure 10. The factorization equation (time flows upwards).

B.1.2 The transition to Statistical Mechanics: Vertex–Models

Any factorizable S–matrix can be interpreted as the Boltzmann weight of a 2–dimensional vertex–model. The factorization equation turns out to be the commutativity condition for the row–to–row transfer matrix of the model for different values of the spectral parameter.

Consider a square lattice of horizontal width N and vertical width M. We attach to each link a variable (spin, color, ...) taking the values $-s, -s+1, \cdots, s-1, s$. The configuration space of a row of N vertical links is spanned by the states belonging to the vector space $\mathcal{V}^{(1)} \otimes \mathcal{V}^{(2)} \otimes \cdots \mathcal{V}^{(N-1)} \otimes \mathcal{V}^{(N)} = \mathcal{V}^{\otimes N}$, where $\mathcal{V}$ is the 1–body vector space V $= \mathcal{C}^{2s+1}$. To each configuration (i, j, k, l) around a vertex we assign a statistical weight $w(ij|kl)$ which is a function of a temperature–dependent coupling paramater θ and may also depend on some other variables (as in the case when external fields are present). The lattice and the weight $w(ij|kl)$ are depicted below.

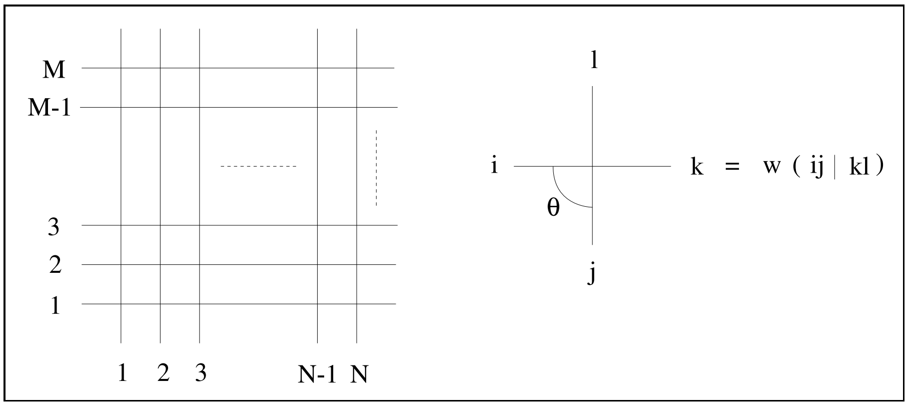

Figure 11. Boltzmann weight and the corresponding lattice configuration.

If $s = \frac{1}{2}$, there are at most 16 different configurations. The six–vertex model is obtained through the implementation of a selection rule, the *ice condition*: representing the two possible states on each horizontal (vertical) link by a left or right (up or down) pointing arrow, we allow only those vertices for which the number of incoming arrows in a vertex equals that of outgoing ones. This is achieved by assigning all other configurations an infinite energy. The choice of Boltzmann weights associated to the six remaining vertices (figure 4) defines the so–called asymmetric six–vertex model, which is the natural extension of the symmetric ($h = v = 0$) model [1].

[1]Note also that since our model is defined on a torus, periodicity in the horizontal direction implies that vertices

One may further define a parameter Δ through

$$\Delta = \frac{1}{2}\left(e^{\beta(J_2-J_1)} + e^{-\beta(J_2-J_1)} - e^{-\beta(J_1+J_2)}\right) = \kappa\cosh\gamma \tag{B.1.7}$$

where $\kappa = \pm 1$. This parameter is the anisotropy of the associated asymmetric XXZ chain.

The connection between the statistical mechanical and the field theoretical formalism follows by giving the Boltzmann weights the values of the S–matrix elements

$$w(ij|kl) = S_{jl}^{ik}(\theta) \tag{B.1.8}$$

where[2]

$$S(\theta) = \begin{pmatrix} a_1(\theta) & & & \\ & c_1(\theta) & b_1(\theta) & \\ & b_2(\theta) & c_2(\theta) & \\ & & & a_2(\theta) \end{pmatrix} \tag{B.1.9}$$

B.1.3 The Transfer Matrix

The partition function $\mathbf{Z}$ is defined as the sum over all possible configurations of the lattice, each configuration having a weight given by the product of all weights over the lattice

$$\mathbf{Z} = \sum_{\text{config.}} \prod_{\text{vert.}} w(ij|kl) \tag{B.1.10}$$

The question which naturally arises is whether the formal connection between Boltzmann weights and elements of a factorizable S–matrix allows one to rewrite the partition function so as to make use of the *factorization equation*. This question can be answered through the introduction of the *transfer matrix* (Kramers and Wannier, 1941). The idea behind the transfer matrix is to consider the vertical direction of the two–dimensional lattice as being a time–like variable, such that the k–th row of N vertical links on a $N \times M$ lattice can be seen as a configuration of the $(k-1)$–th row at a later time, time being discrete. The transfer matrix is an operator which takes one row of links to another such that all selection rules (ice condition, symmetries, etc.), if present, are obeyed.

Let $\{\alpha^{(i)}\}$ be a short-hand notation for the set of states $\{\alpha_1\alpha_2\cdots\alpha_N\}$ in the i-th row of vertical links and $\{a_{r,r+1}\}$ the set of N horizontal states between $\{\alpha^{(r)}\}$ and $\{\alpha^{(r+1)}\}$. Assuming periodic boundary conditions in the horizontal direction one has

$$\begin{aligned} \mathbf{Z} &= \sum_{conf.} \prod_{vert.} S_{jl}^{ik}(\theta) = \sum_{\{\alpha^{(1)}\}} \sum_{\{\alpha^{(2)}\}} \cdots \sum_{\{\alpha^{(M)}\}} \left[\tau^{[N]}(\{a_{1,2}\},\theta)\,|_{\{\alpha^{(1)}\}}^{\{\alpha^{(2)}\}}\right] \\ & \left[\tau^{[N]}(\{a_{2,3}\},\theta)\,|_{\{\alpha^{(2)}\}}^{\{\alpha^{(3)}\}}\right] \cdots \left[\tau^{[N]}(\{a_{M,M+1},\theta\})\,|_{\{\alpha^{(M)}\}}^{\{\alpha^{(M+1)}\}}\right] \end{aligned} \tag{B.1.11}$$

where the transfer matrix $\tau^{[N]}(\{a\},\theta)$ is defined by

$$\begin{aligned} \langle\alpha_1,\cdots,\alpha_N|\,\tau^{[N]}(\{a\},\theta)\,|\beta_1,\cdots,\beta_N\rangle &= \sum_{\{a\}=-s}^{s} S_{\alpha_1\beta_1}^{\overbrace{aa_1}^{\text{horizontal}}}(\theta)\, S^{a_1a_2}_{\underbrace{\alpha_2\beta_2}_{\text{vertical}}}(\theta)\cdots \\ & \cdots S_{\alpha_{N-1}\beta_{N-1}}^{a_{N-2}a_{N-1}}(\theta)\, S_{\alpha_N\beta_N}^{a_{N-1}a}(\theta) \end{aligned} \tag{B.1.12}$$

5 and 6 always appear in pairs. Therefore one may take the energies e_5 and and e_6 to be equal, since they will only enter in the partition function through the combination e_5+e_6. Thus $e_5 = e_6$ means no restriction at all. The choice of their Boltzmann weights as unity is due to the arbitrariness in choosing the zero of the energy.

[2] a_1 =vertex 1, a_2 =vertex 2, c_1 =vertex 3, c_2 =vertex 4, b_1 =vertex 5, b_2 =vertex 6.

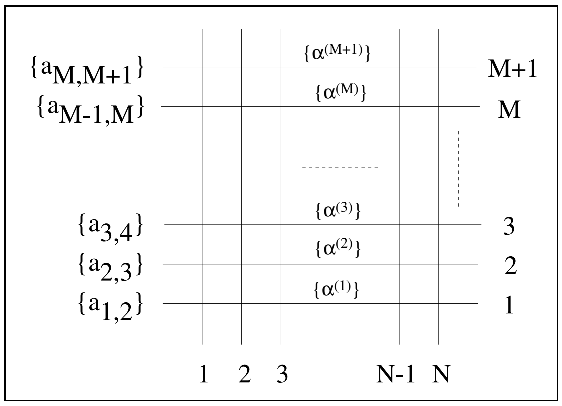

Figure 12. The lattice.

and the S–matrix is defined in (B.1.9). In what follows we shall drop the $\{a\}$ in the notation of the transfer matrix since these variables are summed over. Assuming periodic boundary conditions in the the vertical direction one has, for the partition function,

$$Z = Tr_{\mathcal{V}} \left[\tau^{[N]} (\theta) \right]^M \tag{B.1.13}$$

where the trace is over the vertical space, also called *quantum* space. The free energy follows straightforwardly

$$\begin{aligned} f &= - \lim_{N,M \to \inf} \frac{1}{NM} \ln Z \\ &= - \lim_{N,M \to \inf} \frac{1}{NM} \ln \left[\Lambda_0 (\theta, N) \right]^M \\ &= - \lim_{N \to \inf} \frac{1}{N} \ln \Lambda_0 (\theta, N) \end{aligned} \tag{B.1.14}$$

where $\Lambda_0(\theta, N)$ is the largest eigenvalue of τ (the dominant one when N, $M \to \infty$). We introduce next an operator called *Monodromy Matrix* $T^{[N]}_{ab}(\theta)$ as a tensor product over the $\mathcal{V}^{\otimes N}$ space

$$T^{[N]}_{ab} (\theta) = \sum_{a_1, a_2, \cdots, a_{N-1} = -s}^{s} t^{(1)}_{a,a_1}(\theta) \otimes t^{(2)}_{a_1,a_2}(\theta) \otimes \cdots \otimes t^{(N-1)}_{a_{N-2},a_{N-1}}(\theta) \otimes t^{(N)}_{a_{N-1},b}(\theta) \tag{B.1.15}$$

In this equation we have a standard matrix multiplication over the horizontal (also called *auxiliary*) space and a tensor product over the vertical (*quantum*) space. The $(2s+1) \times (2s+1)$ matrix $t^{(j)}_{a_{j-1},a_j}(\theta)$ acts on the vertical space $\mathcal{V}$ associated to the j–th column of the lattice. It reads

$$t_{a,b} (\theta) = \sum_{cd} S^{ab}_{cd} (\theta) E^{cd} \tag{B.1.16}$$

where E^{cd} are matrices whose entry (i, j) is defined by

$$\left(E^{nm} \right)_{ij} = \delta_{ni} \delta_{mj} \tag{B.1.17}$$

Therefore the t–matrices read[3]

$$\begin{aligned} t_{11}(\theta) &= \begin{pmatrix} a_1(\theta) & 0 \\ 0 & c_1(\theta) \end{pmatrix} \qquad t_{21}(\theta) = \begin{pmatrix} 0 & 0 \\ b_1(\theta) & 0 \end{pmatrix} \\ t_{22}(\theta) &= \begin{pmatrix} c_2(\theta) & 0 \\ 0 & a_2(\theta) \end{pmatrix} \qquad t_{12}(\theta) = \begin{pmatrix} 0 & b_2(\theta) \\ 0 & 0 \end{pmatrix} \end{aligned} \tag{B.1.18}$$

[3]In order to simplify the notation we took $a, b = -\frac{1}{2} \to 1$ and $a, b = \frac{1}{2} \to 2$

The transfer matrix is the trace of the monodromy matrix (B.1.15) over the horizontal space

$$\tau^{[N]}(\theta)\,|^{\{\beta\}}_{\{\alpha\}} = Tr_{\mathcal{H}}\left[T^{[N]}(\theta)\right] = \sum_a T^{[N]}_{aa}(\theta)\,\Big|^{\beta_1,\beta_2,\cdots,\beta_N}_{\alpha_1,\alpha_2,\cdots,\alpha_N} \tag{B.1.19}$$

$$= \sum_{\{a\}=-s}^{s} t^{(1)}_{a,a_1}(\theta)\otimes t^{(2)}_{a_1,a_2}(\theta)\otimes\cdots\otimes t^{(N-1)}_{a_{N-2},a_{N-1}}(\theta)\otimes t^{(N)}_{a_{N-1},a}(\theta) \tag{B.1.20}$$

One may easily check with the help of definition (B.1.16) that the transfer matrix as expressed in (B.1.12) can be recovered from the expression above.

Before proceeding further we note that the asymmetric six–vertex model has a property which allows a significant simplification in the transfer matrix: the number of up arrows is the same in all rows (Lieb 1967a). By inspection of fig. 4 it is clear that the first four vertices do not alter the number of up arrows. The last two vertices do, but since the model is defined on a torus, periodicity in the direction transverse to the transfer implies that they must alternate. Hence, one may work in the subspace specified by the number of up arrows, which means that *the vertical field can be set to zero* since its effect on a given fixed number of up–down arrows is trivial. An obvious Legendre transform allows then the evaluation of the free energy in the presence of this field. This means

$$\left[\tau^{[N]}(\theta)\right]^{\{\beta\}}_{\{\alpha\}} = \sum_{\{a\}}\prod_k^{\otimes} S^{a_{k-1},a_k}_{\alpha_k,\beta_k}(\theta) = e^{2(v+h)(2\mathcal{N}_1-N)}\sum_{\{a\}}\prod_k^{\otimes}\widetilde{S}^{a_{k-1},a_k}_{\alpha_k,\beta_k}(\theta)$$

$$= e^{2(v+h)(2\mathcal{N}_1-N)}\left[\widetilde{\tau}^{[N]}(\theta)\right]^{\{\beta\}}_{\{\alpha\}} \tag{B.1.21}$$

where $\widetilde{S}^{ik}_{jl}$ differs from S^{ik}_{jl} only by having $v=0$. $\mathcal{N}_{1,2}$ are the number operators of up and down arrows respectively. Both transfer matrices are trivially related, the eigenvalues being shifted by a contribution proportional to the number of arrow deviates.

B.1.4 The Factorization and the Yang–Baxter Equation

We can now answer the question stated in the last section, namely what kind of property of the transfer matrix ensues from the factorization of the S–matrix. We assume there exists a nonsingular matrix $\check{R}(\theta-\theta')$ satisfying

$$\check{R}(\theta-\theta')\left[t(\theta)\otimes t(\theta')\right] = \left[t(\theta')\otimes t(\theta)\right]\check{R}(\theta-\theta') \tag{B.1.22}$$

Here $\otimes$ means the tensor product w.r.t. the auxiliary space and $\check{R}$ is a (4×4) matrix acting on the horizontal vector product space $\mathcal{H}\otimes\mathcal{H}$. More explicitly, this equation reads

$$\check{R}^{ef}_{ab}(\theta-\theta')\left[t_{ec}(\theta)\right]_{\alpha\gamma}\left[t_{fd}(\theta')\right]_{\gamma\beta} = \left[t_{ae}(\theta')\right]_{\alpha\gamma}\left[t_{bf}(\theta)\right]_{\gamma\beta}\check{R}^{ef}_{cd}(\theta-\theta') \tag{B.1.23}$$

From fig. 14 the interpretation of (B.1.22) follows: one may shift one line belonging to the quantum space through a vertex of horizontal lines provided that the angles θ, θ' and $(\theta-\theta')$ are kept constant. Using (B.1.22) recursively, multiplying both sides of this equation by a vertical line $t(\theta)\otimes t(\theta')$ and using this 'going-through-a-vertex' property as many times as there are vertical bonds in the lattice leads to

$$\check{R}(\theta-\theta')\left[T^{[N]}(\theta)\otimes T^{[N]}(\theta')\right] = \left[T^{[N]}(\theta')\otimes T^{[N]}(\theta)\right]\check{R}(\theta-\theta') \tag{B.1.24}$$

where $T^{[N]}(\theta)$ is the monodromy matrix. After multiplying the above equation by $\check{R}^{-1}(\theta-\theta')$ and using the cyclic property of the trace one gets

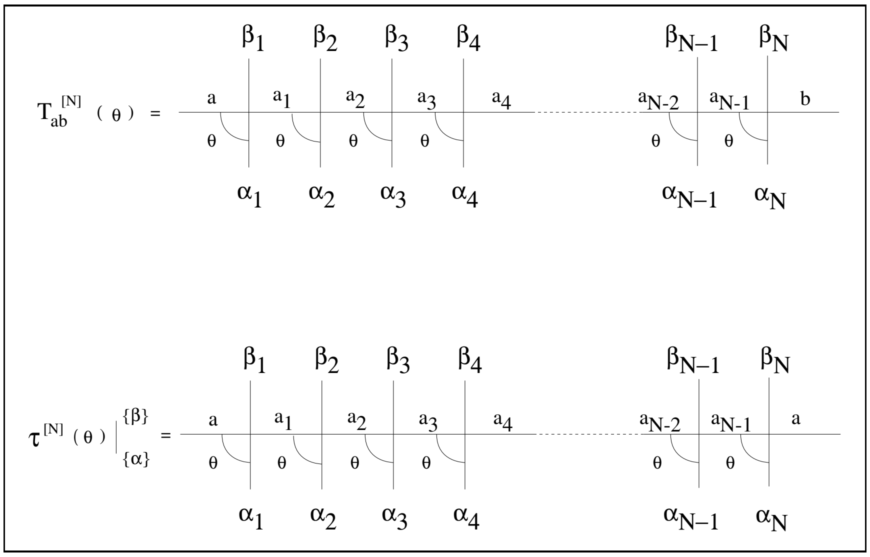

Figure 13. Diagrammatic Representation of the Monodromy and Tranfer Matrices.

$$
\begin{aligned}
Tr\left[T^{[N]}(\theta)\right] Tr\left[T^{[N]}(\theta')\right] &= Tr\left[T^{[N]}(\theta')\right] Tr\left[T^{[N]}(\theta)\right] \\
\tau^{[N]}(\theta)\,\tau^{[N]}(\theta') &= \tau^{[N]}(\theta')\,\tau^{[N]}(\theta) \\
\left[\tau^{[N]}(\theta),\tau^{[N]}(\theta')\right] &= 0
\end{aligned}
\tag{B.1.25}
$$

where in going from the first to the second line we used the property $Tr(A \otimes B) = Tr(A)Tr(B)$. The fundamental result of the theory of 2–dimensional integrable models is thus the existence of a one–parameter family of commuting transfer matrices.

It is not at all clear that such a non–trivial matrix $\check{R}$ should exist. It must be determined for each model by solving (B.1.24), a highly overdetermined set of algebraic equations: There are 2^6 equations for *a priori* 2^4 unknowns (the elements of $\check{R}$). In the general case one has $(2s+1)^6$ equations for $(2s+1)^4$ unknowns. Nevertheless a rich set of solutions is known (De Vega, 1989). In our case, setting the vertical field to zero, it is not difficult to show that $\check{R}$ is given by (Jayaprakash and Sinha, 1982)

$$
\check{R} = \begin{pmatrix} 1 & 0 & 0 & 0 \\ 0 & p & q & 0 \\ 0 & q & p & 0 \\ 0 & 0 & 0 & 1 \end{pmatrix}
\tag{B.1.26}
$$

where

$$
\begin{aligned}
p(\theta) &= \frac{\sinh\gamma}{\sinh(\gamma+\kappa\theta)} \\
q(\theta) &= \frac{\sinh\theta}{\sinh(\gamma+\kappa\theta)}
\end{aligned}
\tag{B.1.27}
$$

This is the same as the $\check{R}$–matrix for the symmetric six–vertex. It plays a crucial role in the study of integrable models, for it defines the underlying algebraic structure of the theory through (B.1.24).

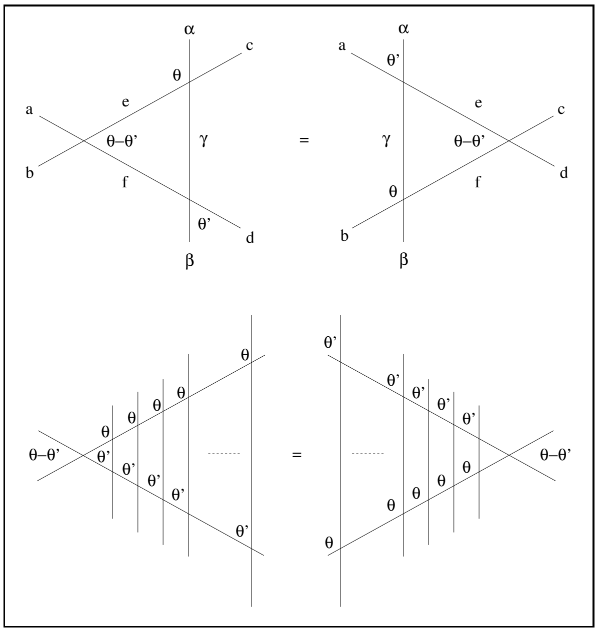

Figure 14. Schematic representation of equations (B.1.23) and (B.1.24).

B.2 The Algebraic Method

One may rewrite the Monodromy $T^{[N]}(\theta)$ in a more compact notation, namely

$$T^{[N]}(\theta) = \begin{pmatrix} A(\theta) & B(\theta) \\ C(\theta) & D(\theta) \end{pmatrix} \tag{B.2.1}$$

with

$$\begin{aligned}
A(\theta) &= \sum_{a_1,\cdots,a_{N-1}=1}^{2} t^{(1)}_{1,a_1}(\theta) \otimes t^{(2)}_{a_1,a_2}(\theta) \otimes \cdots \otimes t^{(N-1)}_{a_{N-2},a_{N-1}}(\theta) \otimes t^{(N)}_{a_{N-1},1}(\theta) \\
B(\theta) &= \sum_{a_1,\cdots,a_{N-1}=1}^{2} t^{(1)}_{2,a_1}(\theta) \otimes t^{(2)}_{a_1,a_2}(\theta) \otimes \cdots \otimes t^{(N-1)}_{a_{N-2},a_{N-1}}(\theta) \otimes t^{(N)}_{a_{N-1},1}(\theta) \\
C(\theta) &= \sum_{a_1,\cdots,a_{N-1}=1}^{2} t^{(1)}_{1,a_1}(\theta) \otimes t^{(2)}_{a_1,a_2}(\theta) \otimes \cdots \otimes t^{(N-1)}_{a_{N-2},a_{N-1}}(\theta) \otimes t^{(N)}_{a_{N-1},2}(\theta) \\
D(\theta) &= \sum_{a_1,\cdots,a_{N-1}=1}^{2} t^{(1)}_{2,a_1}(\theta) \otimes t^{(2)}_{a_1,a_2}(\theta) \otimes \cdots \otimes t^{(N-1)}_{a_{N-2},a_{N-1}}(\theta) \otimes t^{(N)}_{a_{N-1},2}(\theta)
\end{aligned} \tag{B.2.2}$$

where the t–matrices are defined in (B.1.18). Since the vertical field has been set to zero we have

$$\begin{aligned}
a_{2,1}(\theta) &= \frac{\sinh(\gamma + \kappa\theta)}{\sinh\gamma} e^{\pm h} \\
c_{2,1}(\theta) &= \frac{\sinh\theta}{\sinh\gamma} e^{\pm h}
\end{aligned} \tag{B.2.3}$$

As an example we consider the 2–site case. In this situation

$$T^{[2]}(\theta) = \begin{pmatrix} T_{11} & T_{21} \\ T_{12} & T_{22} \end{pmatrix}_\theta = \begin{pmatrix} t_{11}^{(1)} \otimes t_{11}^{(2)} + t_{12}^{(1)} \otimes t_{21}^{(2)} & t_{21}^{(1)} \otimes t_{11}^{(2)} + t_{22}^{(1)} \otimes t_{21}^{(2)} \\ t_{11}^{(1)} \otimes t_{12}^{(2)} + t_{12}^{(1)} \otimes t_{22}^{(2)} & t_{21}^{(1)} \otimes t_{12}^{(2)} + t_{22}^{(1)} \otimes t_{22}^{(2)} \end{pmatrix}_\theta \tag{B.2.4}$$

then

$$\begin{aligned} A(\theta) &= t_{11}^{(1)} \otimes t_{11}^{(2)} + t_{12}^{(1)} \otimes t_{21}^{(2)} & \qquad B(\theta) &= t_{21}^{(1)} \otimes t_{11}^{(2)} + t_{22}^{(1)} \otimes t_{21}^{(2)} \\ C(\theta) &= t_{11}^{(1)} \otimes t_{12}^{(2)} + t_{12}^{(1)} \otimes t_{22}^{(2)} & \qquad D(\theta) &= t_{21}^{(1)} \otimes t_{12}^{(2)} + t_{22}^{(1)} \otimes t_{22}^{(2)} \end{aligned} \tag{B.2.5}$$

To solve for the eigenvalues of the transfer matrix means to solve for the eigenvalues of the monodromy matrix. We look therefore for a reference state Ω which should be an eigenstate of $A(\theta)$ and $D(\theta)$ but should be annihilated by $C(\theta)$. In the $N = 2$ case it is simple to see that such a state is given by

$$\Omega^{[2]} = |\uparrow\rangle \otimes |\uparrow\rangle = \begin{pmatrix} 1 \\ 0 \end{pmatrix} \otimes \begin{pmatrix} 1 \\ 0 \end{pmatrix} \tag{B.2.6}$$

since one may easily check that

$$A(\theta)\Omega^{[2]} = a_1^2(\theta)\Omega^{[2]} \tag{B.2.7}$$

Also we have

$$D(\theta)\Omega^{[2]} = c_2^2(\theta)\Omega^{[2]} \tag{B.2.8}$$

$$C(\theta)\Omega^{[2]} = 0 \tag{B.2.9}$$

In the general case with N sites one has

$$\begin{aligned} \Omega^{[N]} &= \prod^{\otimes} \begin{pmatrix} 1 \\ 0 \end{pmatrix} \\ T^{[N]}(\theta)\Omega^{[N]} &= \begin{pmatrix} a_1^N(\theta) & B(\theta) \\ 0 & c_2^N(\theta) \end{pmatrix} \Omega^{[N]} \end{aligned} \tag{B.2.10}$$

since $T^{[1]}$ acting on $|0\rangle = |\uparrow\uparrow \cdots \uparrow\rangle$ is triangular and the product of triangular matrices is also triangular. The Monodromy Matrix obeys the Yang–Baxter Equation (B.1.22) which, in terms of the operators defined above, can be written as

$$\begin{pmatrix} 1 & 0 & 0 & 0 \\ 0 & p & q & 0 \\ 0 & q & p & 0 \\ 0 & 0 & 0 & 1 \end{pmatrix}'' \begin{pmatrix} AA' & AB' & BA' & BB' \\ AC' & AD' & BC' & BD' \\ CA' & CB' & DA' & DB' \\ CC' & CD' & DC' & DD' \end{pmatrix} = \begin{pmatrix} A'A & A'B & B'A & B'B \\ A'C & A'D & B'C & B'D \\ C'A & C'B & D'A & D'B \\ C'C & C'D & D'C & D'D \end{pmatrix} \begin{pmatrix} 1 & 0 & 0 & 0 \\ 0 & p & q & 0 \\ 0 & q & p & 0 \\ 0 & 0 & 0 & 1 \end{pmatrix}'' \tag{B.2.11}$$

Hereafter we use the shorthand notation $A = A(\theta)$, $A' = A(\theta')$, $p'' = p(\theta - \theta')$, and so on. This equality yields sixteen important relations among the operators, four of which are

$$[A, A'] = [B, B'] = [C, C'] = [D, D'] = 0 \tag{B.2.12}$$

The elements $(1,3)$ and $(2,4)$ of the matricial YBE yield

$$\begin{aligned} A'B &= \frac{1}{q''}BA' - \frac{p''}{q''}B'A \\ DB' &= \frac{1}{q''}B'D - \frac{p''}{q''}BD' \end{aligned} \tag{B.2.13}$$

The main idea is to look for an eigenstate of the transfer matrix $\tau^{[N]}(\theta) = trT^{[N]}(\theta) = A(\theta) + D(\theta)$ of the form

$$\Psi(\theta_1, \theta_2, \cdots, \theta_n) = B(\theta_1)B(\theta_2)\cdots B(\theta_n)\Omega^{[N]} \tag{B.2.14}$$

because $B(\theta)\Omega^{[N]} \neq 0$ and $B(\theta)\Omega^{[N]} \neq \Omega^{[N]}$.

We first consider the 1–particle state $\Psi(\theta_1) = B(\theta_1)\Omega^{[N]}$. In this case we have

$$\tau^{[N]}(\theta)\Psi(\theta_1) = (A(\theta) + D(\theta))\, B(\theta_1)\Omega^{[N]} \tag{B.2.15}$$

Since $\Omega^{[N]}$ is an eigenstate of both $A(\theta)$ and $D(\theta)$, we interchange the order of these operators in the above expression using the algebraic relations among them. After some trivial manipulation it gives

$$\begin{aligned} \tau^{[N]}(\theta)\Psi(\theta_1) &= \left(\frac{1}{q(\theta_1-\theta)}a_1^N(\theta) + \frac{1}{q(\theta-\theta_1)}c_2^N(\theta)\right)B(\theta_1)\Omega^{[N]} \\ &- \underbrace{\left(\frac{p(\theta_1-\theta)}{q(\theta_1-\theta)}a_1^N(\theta_1) + \frac{p(\theta-\theta_1)}{q(\theta-\theta_1)}c_2^N(\theta_1)\right)B(\theta)\Omega^{[N]}}_{\text{unwanted}} \end{aligned} \tag{B.2.16}$$

where the 'unwanted' term should be zero because it is not proportional to $\Psi(\theta_1)$. This means

$$c_2^N(\theta_1) = -\frac{p(\theta_1-\theta)}{q(\theta_1-\theta)}\frac{q(\theta-\theta_1)}{p(\theta-\theta_1)}a_1^N(\theta_1) = a_1^N(\theta_1) \tag{B.2.17}$$

and consequently $\Psi(\theta_1) = B(\theta_1)\Omega^{[N]}$ is and eigenstate of $\tau^{[N]}(\theta)$ with eigenvalue

$$\Lambda(\theta_1, \theta) = \frac{1}{q(\theta_1-\theta)}a_1^N(\theta) + \frac{1}{q(\theta-\theta_1)}c_2^N(\theta) \tag{B.2.18}$$

where θ_1 is fixed by the relation $c_2^N(\theta_1) = a_1^N(\theta_1)$, which is the original one–particle Bethe Ansatz equation $e^{ikN-\psi N} = 1$ of appendix A parametrized in terms of the rapidity θ and with $2h = \psi$.

We next consider the 2–particle case, where we look for an eigenstate of the tranfer matrix in the form $\Psi(\theta_1, \theta_2) = B(\theta_1)B(\theta_2)\Omega^{[N]}$, that is

$$\tau^{[N]}(\theta)\Psi(\theta_1, \theta_2) = (A(\theta) + D(\theta))\, B(\theta_1)B(\theta_2)\Omega^{[N]} \tag{B.2.19}$$

One must again use the algebraic relations between the operators $A(\theta)$, $D(\theta)$ and $B(\theta)$ so as to bring both $A(\theta)$ and $D(\theta)$ close to $\Omega^{[N]}$. In this situation, after some algebraic manipulation we obtain

$$\begin{aligned} A(\theta)\Psi(\theta_1, \theta_2) &= \frac{1}{q(\theta_1-\theta)q(\theta_2-\theta)}a_1^N(\theta)\Psi(\theta_1, \theta_2) \\ &- \left[\frac{1}{q(\theta_1-\theta)q(\theta_2-\theta)} - \frac{p(\theta_1-\theta)p(\theta_2-\theta_1)}{q(\theta_1-\theta)q(\theta_2-\theta_1)}\right]a_1^N(\theta_2)B(\theta)B(\theta_1)\Omega^{[N]} \\ &- \frac{p(\theta_1-\theta)}{q(\theta_1-\theta)q(\theta_2-\theta_1)}a_1^N(\theta_1)B(\theta)B(\theta_2)\Omega^{[N]} \end{aligned} \tag{B.2.20}$$

However, since $[B,B']=0$ one should have $A(\theta)\Psi(\theta_1,\theta_2)=A(\theta)\Psi(\theta_2,\theta_1)$. Applying the same procedure on $A(\theta)\Psi(\theta_2,\theta_1)$, we conclude that

$$\frac{1}{q(\theta_1-\theta)q(\theta_2-\theta)}-\frac{p(\theta_1-\theta)p(\theta_2-\theta_1)}{q(\theta_1-\theta)q(\theta_2-\theta_1)}=\frac{p(\theta_2-\theta)}{q(\theta_2-\theta)q(\theta_1-\theta_2)} \tag{B.2.21}$$

In other words

$$\begin{aligned} A(\theta)\Psi(\theta_1,\theta_2) &= \frac{1}{q(\theta_1-\theta)q(\theta_2-\theta)}a_1^N(\theta)\Psi(\theta_1,\theta_2) \\ &- \frac{p(\theta_2-\theta)}{q(\theta_2-\theta)q(\theta_1-\theta_2)}a_1^N(\theta_2)B(\theta)B(\theta_1)\Omega^{[N]} \\ &- \frac{p(\theta_1-\theta)}{q(\theta_1-\theta)q(\theta_2-\theta_1)}a_1^N(\theta_1)B(\theta)B(\theta_2)\Omega^{[N]} \end{aligned} \tag{B.2.22}$$

For $D(\theta)$ a similar calculation leads to the following expression

$$\begin{aligned} D(\theta)\Psi(\theta_1,\theta_2) &= \frac{1}{q(\theta-\theta_1)q(\theta-\theta_2)}c_2^N(\theta)\Psi(\theta_1,\theta_2) \\ &- \frac{p(\theta-\theta_2)}{q(\theta-\theta_2)q(\theta_2-\theta_1)}c_2^N(\theta_2)B(\theta)B(\theta_1)\Omega^{[N]} \\ &- \frac{p(\theta-\theta_1)}{q(\theta-\theta_1)q(\theta_1-\theta_2)}c_2^N(\theta_1)B(\theta)B(\theta_2)\Omega^{[N]} \end{aligned} \tag{B.2.23}$$

If we know write

$$\tau^{[N]}(\theta)\Psi(\theta_1,\theta_2)=\Lambda(\theta,\theta_1,\theta_2)\Psi(\theta_1,\theta_2)+\text{unwanted terms} \tag{B.2.24}$$

then from (B.2.19), (B.2.22) and (B.2.23) we have

$$\Lambda(\theta,\theta_1,\theta_2)=a_1^N(\theta)\prod_{j=1}^{2}\frac{1}{q(\theta_j-\theta)}+c_2^N(\theta)\prod_{j=1}^{2}\frac{1}{q(\theta-\theta_j)} \tag{B.2.25}$$

For $\Lambda(\theta,\theta_1,\theta_2)$ to be an eigenvector of the transfer matrix the unwanted terms must cancel, namely

$$\begin{aligned} &\frac{p(\theta_1-\theta)}{q(\theta_1-\theta)q(\theta_2-\theta_1)}a_1^N(\theta_1)+\frac{p(\theta-\theta_1)}{q(\theta-\theta_1)q(\theta_1-\theta_2)}c_2^N(\theta_1)=0 \\ &\frac{p(\theta_2-\theta)}{q(\theta_2-\theta)q(\theta_1-\theta_2)}a_1^N(\theta_2)+\frac{p(\theta-\theta_2)}{q(\theta-\theta_2)q(\theta_2-\theta_1)}c_2^N(\theta_2)=0 \end{aligned} \tag{B.2.26}$$

After a straightforward manipulation these expressions reduce to

$$\frac{c_2^N(\theta_j)}{a_1^N(\theta_j)}=\frac{q(\theta_j-\theta_k)}{q(\theta_k-\theta_j)} \qquad k\neq j \qquad j,k=1,2 \tag{B.2.27}$$

which are the 2–particle Bethe Ansatz Equations.

If we now iterate this procedure for the general n–particle case we have

$$\begin{aligned} A(\theta)\Psi(\theta_1,\cdots,\theta_n) &= \Lambda(\theta,\theta_1,\cdots,\theta_n)\Psi(\theta_1,\cdots,\theta_n) \\ &- \sum_{j=1}^{n}\Lambda_j(\theta,\theta_1,\cdots,\theta_n)\Psi_j(\theta,\theta_1,\cdots,\theta_{j-1},\theta_{j+1},\cdots,\theta_n) \\ D(\theta)\Psi(\theta_1,\cdots,\theta_n) &= \Lambda'(\theta,\theta_1,\cdots,\theta_n)\Psi(\theta_1,\cdots,\theta_n) \\ &- \sum_{j=1}^{n}\Lambda'_j(\theta,\theta_1,\cdots,\theta_n)\Psi_j(\theta,\theta_1,\cdots,\theta_{j-1},\theta_{j+1},\cdots,\theta_n) \end{aligned} \tag{B.2.28}$$

where

$$\Psi_j(\theta,\theta_1,\cdots,\theta_{j-1},\theta_{j+1},\cdots,\theta_n) = B(\theta)\prod_{k\neq j}^{n} B(\theta_k)\Omega^{[N]} \tag{B.2.29}$$

$$\begin{aligned}
\Lambda(\theta,\theta_1,\cdots,\theta_n) &= a_1^N(\theta)\prod_{j=1}^{n}\frac{1}{q(\theta_j-\theta)}\\
\Lambda'(\theta,\theta_1,\cdots,\theta_n) &= c_2^N(\theta)\prod_{j=1}^{n}\frac{1}{q(\theta-\theta_j)}\\
\Lambda_j(\theta,\theta_1,\cdots,\theta_n) &= a_1^N(\theta_j)\frac{p(\theta_j-\theta)}{q(\theta_j-\theta)}\prod_{k\neq j}^{n}\frac{1}{q(\theta_k-\theta_j)}\\
\Lambda'_j(\theta,\theta_1,\cdots,\theta_n) &= c_2^N(\theta_j)\frac{p(\theta-\theta_j)}{q(\theta-\theta_j)}\prod_{k\neq j}^{n}\frac{1}{q(\theta_j-\theta_k)}
\end{aligned} \tag{B.2.30}$$

The vector $\Psi(\theta_1,\cdots,\theta_n)$ is an eigenvector of the transfer matrix $\tau^{[N]}(\theta)$ if

$$\Lambda_j(\theta,\theta_1,\cdots,\theta_n)+\Lambda'_j(\theta,\theta_1,\cdots,\theta_n)=0 \qquad j=1,2,\cdots,n \tag{B.2.31}$$

These conditions yield a total of n Bethe Ansatz Equations for the variables $\theta_1,\theta_2,\cdots,\theta_n$

$$\frac{c_2^N(\theta_j)}{a_1^N(\theta_j)}=\prod_{k\neq j}^{n}\frac{q(\theta_j-\theta_k)}{q(\theta_k-\theta_j)} \qquad j,k=1,2,\cdots,n \tag{B.2.32}$$

where the eigenvalue of the transfer matrix corresponding to the set of rapidities $\theta_1,\theta_2,\cdots,\theta_n$ is given by

$$\begin{aligned}
\Lambda(\theta,\theta_1,\cdots,\theta_n)+\Lambda'(\theta,\theta_1,\cdots,\theta_n) &=\\
e^{-Nh}\left[\frac{\sinh(\gamma+\kappa\theta)}{\sinh\gamma}\right]^N &\prod_{j=1}^{n}\frac{\sinh(\gamma+\kappa(\theta_j-\theta))}{\sinh(\theta_j-\theta)}\\
+e^{Nh}\left[\frac{\sinh\theta}{\sinh\gamma}\right]^N &\prod_{j=1}^{n}\frac{\sinh(\gamma+\kappa(\theta-\theta_j))}{\sinh(\theta-\theta_j)}
\end{aligned} \tag{B.2.33}$$

The Bethe Ansatz Equations of chapter 3 are reproduced through the substitution $\theta_j=\frac{\gamma}{2}-i\frac{\alpha_j}{2}$. It is easy also easy to check that the BAE (B.2.32) reduce to those in Orbach's parametrization (A.3.43) under an appropriate change of variables, that is the asymmetric 6–vertex and the associated asymmetric XXZ model are diagonalized by the same set of equations. The reason for this is shown in what follows.

B.2.1 From two–dimensional vertex–models to quantum chains

It is known that to each two-dimensional classical model there corresponds a one–dimensional quantum version. Following Baxter (1972) one defines

$$\begin{aligned}
H_0 &= -\sinh\gamma\frac{d}{d\theta}\ln\tau^{[N]}(\theta)\Big|_{\theta=0}\\
&= -\sinh\gamma\left[\tau^{[N]}(\theta)\right]^{-1}\frac{d}{d\theta}\tau^{[N]}(\theta)\Big|_{\theta=0}
\end{aligned} \tag{B.2.34}$$

In the particular case of the asymmetric model, the property that one may take $v = 0$ in the Boltzmann weights considerably simplifies the derivation in (B.2.34). Since the transfer matrices of both cases (with and without v) are trivially related by a shift in the energy spectrum of each charge sector, one may expect that the associated Hamiltonians differ from one another only through an amount proportional to the number of up spins, namely through a contribution H_1 given by (*cf.* eq. (B.1.21))

$$H_1 = -\ln e^{2(h+v)} \tag{B.2.35}$$

Since

$$\mathcal{N}_1 = \sum_{j=1}^{N} \frac{\sigma_j^z + 1}{2} \quad \mathcal{N}_2 = -\sum_{j=1}^{N} \frac{\sigma_j^z - 1}{2} \tag{B.2.36}$$

one has

$$H_1\left(h, v, N\right) = -2(h+v) \sum_{j=1}^{N} \sigma_j^z \tag{B.2.37}$$

To find the H_0 contribution to the Hamiltonian according to (B.2.34), we first evaluate the transfer matrix $\left[\widetilde{\tau}^{[N]}\left(\theta\right)\right]$ at $\theta = 0$. It reads

$$\begin{aligned}\left[\widetilde{\tau}^{[N]}\left(\theta = 0\right)\right]_{\{\alpha\}}^{\{\beta\}} &= \sum_{\{a\}=1}^{2} \delta_{a,\beta_1}\delta_{\alpha_1,a_1}\delta_{a_1,\beta_2}\delta_{\alpha_2,a_1}\cdots\delta_{\alpha_{N-1},a_{N-1}}\delta_{a_{N-1},\beta_N}\delta_{\alpha_N,a} \\ &= \delta_{\alpha_1,\beta_2}\delta_{\alpha_2,\beta_3}\delta_{\alpha_3,\beta_4}\cdots\delta_{\alpha_{N-1},\beta_N}\delta_{a_{N-1},\beta_N}\delta_{\alpha_N,\beta_1}\end{aligned} \tag{B.2.38}$$

From fig. 18a one sees that $\widetilde{\tau}^{[N]}\left(\theta = 0\right)$ is a translation operator since

$$\widetilde{\tau}^{[N]}(0)\left|\alpha_1, \alpha_2, \cdots, \alpha_N\right\rangle = \left|\alpha_2, \alpha_3, \cdots, \alpha_N, \alpha_1\right\rangle \tag{B.2.39}$$

The inverse of this operator reads (fig. 18b)

$$\left[\left[\widetilde{\tau}^{[N]}\left(\theta = 0\right)\right]^{-1}\right]_{\{\alpha\}}^{\{\beta\}} = \delta_{\alpha_1,\beta_N}\delta_{\alpha_2,\beta_1}\delta_{\alpha_3,\beta_2}\cdots\delta_{\alpha_{N-1},\beta_{N-2}}\delta_{a_N,\beta_{N-1}} \tag{B.2.40}$$

Considering now the derivative of $\tau^{[N]}\left(\theta\right)$ we have

$$\begin{aligned}\frac{d}{d\theta}\left[\widetilde{\tau}^{[N]}(\theta)\right]_{\{\alpha\}}^{\{\beta\}}\Bigg|_{\theta=0} &= \sum_{\{a\}=1}^{2}\sum_{l=0}^{N-1} \delta_{a,\beta_1}\delta_{\alpha_1,a_1}\delta_{a_1,\beta_2}\cdots\delta_{a_{l-1},\beta_l}\delta_{\alpha_l,a_l} \\ &\times \left[\frac{d}{d\theta}\widetilde{S}_{\alpha_{l+1}\beta_{l+1}}^{a_l a_{l+1}}\right]_{\theta=0}\delta_{a_{l+1},\beta_{l+2}}\delta_{\alpha_{l+2},a_{l+2}}\cdots\delta_{a_{N-1},\beta_N}\delta_{\alpha_N,a}\end{aligned} \tag{B.2.41}$$

where $a_N = a_0 = a$, $a_{N+1} = a_1$. This gives (fig. 18c)

$$\begin{aligned}\frac{d}{d\theta}\left[\widetilde{\tau}^{[N]}(\theta)\right]_{\{\alpha\}}^{\{\beta\}}\Bigg|_{\theta=0} &= \sum_{l=0}^{N-1} \delta_{\alpha_1,\beta_2}\delta_{\alpha_2,\beta_3}\cdots\delta_{\alpha_{l-1},\beta_l}\left[\frac{d}{d\theta}\widetilde{S}_{\alpha_{l+1}\beta_{l+1}}^{\alpha_l\beta_{l+2}}\right]_{\theta=0} \\ &\times \delta_{\alpha_{l+2},\beta_{l+3}}\delta_{\alpha_{l+2},\beta_{l+2}}\cdots\delta_{\alpha_{N-1},\beta_N}\delta_{\alpha_N,\beta_1}\end{aligned} \tag{B.2.42}$$

Multiplying now this expression with eq. (B.2.40), we finally obtain (fig. $8d$)

$$\left[\left[\widetilde{\tau}^{[N]}(\theta)\right]^{-1}\right]^{\{\beta\}}_{\{\beta'\}}\left[\frac{d}{d\theta}\widetilde{\tau}^{[N]}(\theta)\right]^{\{\beta'\}}_{\{\alpha\}}\Bigg|_{\theta=0} = \sum_{\{\beta'\}}\delta_{\beta'_1,\beta_N}\delta_{\beta'_2,\beta_1}\cdots\delta_{\beta'_l,\beta_{l-1}}\cdots\delta_{\beta'_N,\beta_{N-1}}$$

$$\times\sum_{l=0}^{N-1}\delta_{\alpha_1,\beta'_2}\delta_{\alpha_2,\beta'_3}\cdots\delta_{\alpha_{l-1},\beta'_l}\left[\frac{d}{d\theta}\widetilde{S}^{\alpha_{l+1}\beta'_{l+1}}_{\alpha_l\beta'_{l+2}}(\theta)\right]_{\theta=0}\delta_{\alpha_{l+2},\beta'_{l+3}}\cdots\delta_{\alpha_{N-1},\beta'_N}\delta_{\alpha_N,\beta'_1}$$

$$=\sum_{l=0}^{N-1}\delta_{\alpha_1,\beta_1}\delta_{\alpha_2,\beta_2}\cdots\delta_{\alpha_{l-2},\beta_{l-2}}\left[\frac{d}{d\theta}\widetilde{S}^{\alpha_{l+1}\beta_{l+2}}_{\alpha_{l+2}\beta_{l+1}}(\theta)\right]_{\theta=0}\delta_{\alpha_{l+3},\beta_{l+3}}\cdots\delta_{\alpha_N,\beta_N} \qquad \text{(B.2.43)}$$

Before rewritting this expression in matricial form, we have to notice that

$$\underbrace{\overbrace{\widetilde{S}^{\beta_{l+1},\,\beta_{l+2}}_{\alpha_{l+1},\,\alpha_{l+2}}}^{\text{column}}}_{\text{row}} = E^{\alpha_{l+1}\beta_{l+1}}\otimes E^{\alpha_{l+2}\beta_{l+2}}\widetilde{S}^{\alpha_{l+1}\beta_{l+2}}_{\alpha_{l+2}\beta_{l+1}} = \begin{bmatrix}\widetilde{a}_1(\theta) & & & \\ & \widetilde{b}_2(\theta) & \widetilde{c}_2(\theta) & \\ & \widetilde{c}_1(\theta) & \widetilde{b}_1(\theta) & \\ & & & \widetilde{a}_2(\theta)\end{bmatrix} \qquad \text{(B.2.44)}$$

Therefore

$$H_0 = -\sinh\gamma\sum_{j=1}^{N}\mathbf{1}^{(1)}\otimes\cdots\otimes\mathbf{1}^{(j-1)}\otimes H_0^{(j,j+1)}\otimes\mathbf{1}^{(j+2)}\otimes\cdots\otimes\mathbf{1}^{(N)}$$

$$H_0^{(j,j+1)} = \begin{bmatrix}\frac{d}{d\theta}\widetilde{a}_1(\theta) & & & \\ & \frac{d}{d\theta}\widetilde{b}_2(\theta) & \frac{d}{d\theta}\widetilde{c}_2(\theta) & \\ & \frac{d}{d\theta}\widetilde{c}_1(\theta) & \frac{d}{d\theta}\widetilde{b}_1(\theta) & \\ & & & \frac{d}{d\theta}\widetilde{a}_2(\theta)\end{bmatrix}^{(j,j+1)}_{\theta=0} \qquad \text{(B.2.45)}$$

Calculating the derivatives with respect to θ explicitly and rewriting the 2–body operator in terms of the Pauli matrices one finally has

$$H_0(\Delta,h,N) = -\sum_{k=1}^{N}\left[e^{2h}\sigma_k^+\sigma_{k+1}^- + e^{-2h}\sigma_k^-\sigma_{k+1}^+ + \frac{\Delta}{2}\left(\sigma_k^z\sigma_{k+1}^z+1\right)\right] \qquad \text{(B.2.46)}$$

where Δ is defined in (B.1.7). The total Hamiltonian is given by the sum of H_0 with H_1 of eq. (B.2.37).

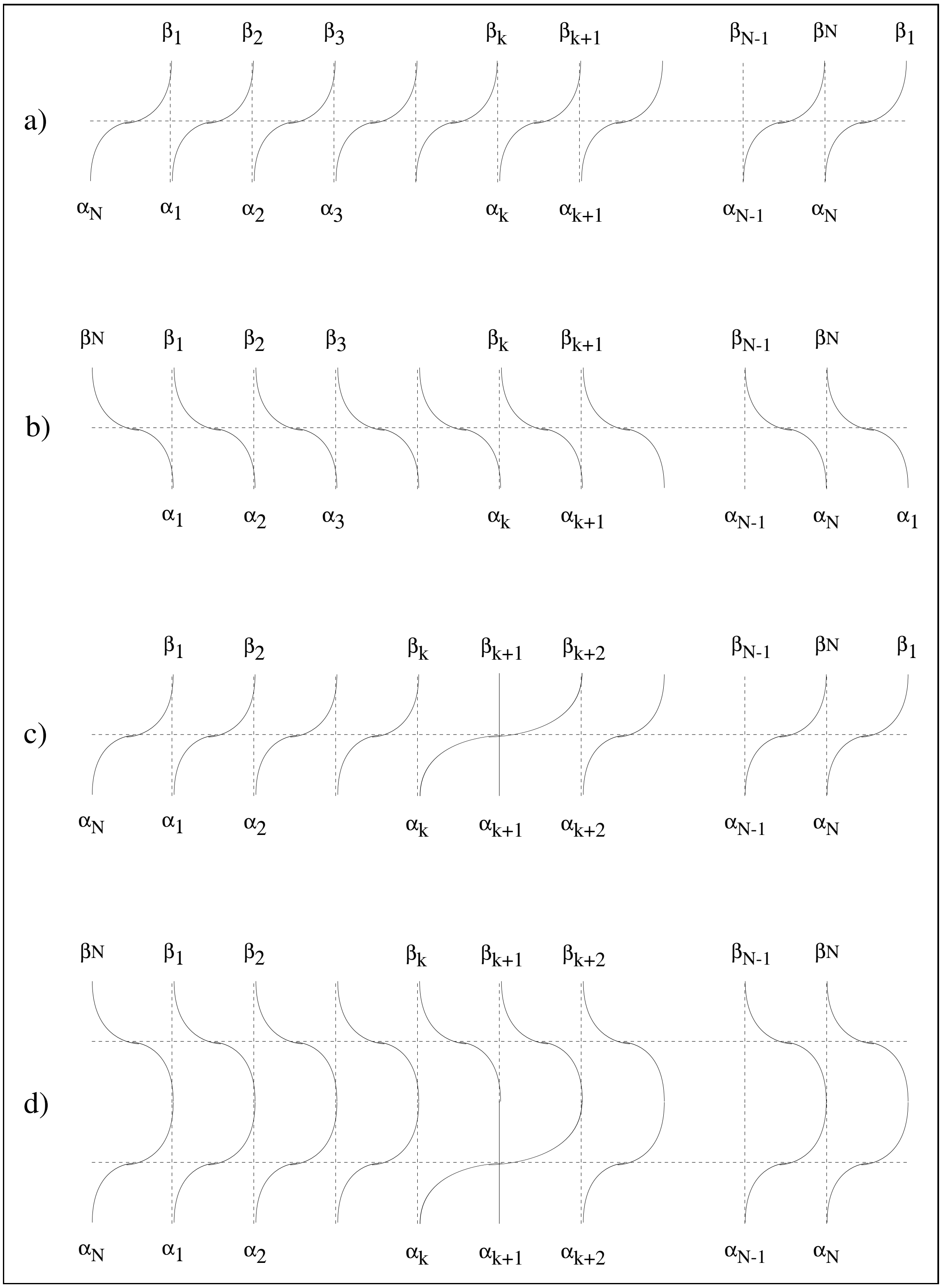

Figure 19. Schematic representation of a) equation (B.2.38); b) equation (B.2.40); c) equation (B.2.42) and d) equation (B.2.43).

Appendix C

Solutions of the Bethe Ansatz Equations

The derivation of the BAE ca be seen as a rather technical method whose execution, at least in the six–vertex or XXZ case, poses no great or challenging obstacles. On the other hand, the ultimate goal of this technique is to give us means of calculating physical quantities, like correlation functions, from the spectrum and wave–functions, which in principle are defined throught the method – and this can be only accomplished by solving the equations, a highly non trivial task. The BAE form a set of coupled and nonlinear equations, having therefore infinitely many solutions, many of which are not physically relevant.

Solving the equations can be understood in two different ways: analytically or numerically, on the computer. In the first case there are a rather few situations where this is possible. As to what regards numerics however, the only limitation is the alloted CPU time and memory, there being in principle no restrictions to the numerical analysis of solutions (even though they are sometimes difficult to obtain). We discuss some of these numerical problems in what follows. The standard analytical analysis (thermodynamic limit) has already been discussed in chapter 3 of this thesis.

C.1 Numerical solutions

It is desirable sometimes to solve the Bethe Ansatz Equations for a finite system. One reason would be to use the spectrum obtained through the Bethe Ansatz as a double–check on the reliability of some other numerical routine, as for example exact diagonalization techniques for the Hamiltonian (brute force or more 'refined' methods, as Lanczos). However, one more important situation arises in the study of finite–size corrections to the thermodynamic limit. Finite Size Scaling (FSS) has gained an important status in the theory of phase transitions after the advent of Renormalization Group and more powerful computers. One typical situation is the determination of critical exponents, or the determination of the spectrum (gaps, for instance), through an extrapolation of the finite lattice data. To find these quantities making use of this asymptotic behavior of the spectrum, one proceeds by determining the spectrum of the model for increasing lattice lengths and then applying some acceleration technique for finite–size data to obtain a convergence towards asymptotic values (two commonly used acceleration routines are those due to Burlisch and Stoer, 1964 and van den Broeck and Schwarz, 1979). However, brute–force diagonalization methods are limited, in the sense that one cannot usually go beyond 20 sites (after implementation of symmetries), leading to poor convergences when the above mentioned techniques are applied. The Bethe Ansatz consists, roughly speaking, in 'trading' the problem of diagonalizing the Hamiltonian by that of solving a system of algebraic coupled equations on the quasi–momenta p_j, in terms of which the energy is given. One can in most cases solve these equations without much hindrance, the only limitation being the lack of a direct proof that the level found really corresponds to the level sought. Apart from the 'uncertainty' of the equations, one may easily find the lowest–lying states of chains of the order of 10^3 sites. This allows an extremely good accuracy in the determination of the relevant physical quantities.

The steps taken are the following: one starts solving the BAE for small chains, say $N = 4$. The results are checked against some reliable diagonalization method to keep track of the position of the level in the whole spectrum of the chain. Once one sought level is found, e.g. the ground state, one proceeds further to higher lattices, always comparing with exact diagonalization results up to the point where this is still feasible. One looks then for some regularity in the pattern of the roots and follows it to obtain the corresponding ground states of larger chains. There is no guarantee that, up to a certain point, the levels found through this procedure really correspond to the right ones, thus the 'uncertainty' we referred to in the last paragraph. However a sudden break in the pattern usually helps identify spurious solutions. Moreover, since the expected corrections to the energy due to the finiteness of the lattice are of order N^{-2} (in the massless case; in the massive these corrections are exponentially decaying), one tracks the sequence of energies which, up to 10 sites, should differ from the previous one by a factor of 1%. A large shift in the energy from one site length to the next usually indicates that one missed the sought–after level.

In the figure below we show some distribution of roots for the first excited state of the asymmetric and antiferromagnetic XXZ chain for different lattice lengths (or equivalently, asymmetric six–vertex model). These rapidities are among the ones used in the numerical study of the asymmetric six–vertex model of chapter 3, since the Bethe Ansatz is the same for both systems. Notice that in contrast to the symmetric case, the rapidities' distribution for the lowest lying state is already complex.

For the solution of the Bethe Ansatz, one may use a Newton–type iteration routine usually available in any good subroutine library. The starting points for this iteration can be provided either by the trivial $\Delta = 0$ solution (free–fermion case) or from a generalization of the method used in Grieger (1984). The distribution of zeros of an infinite chain in the regime $-1 < \Delta < 1$ is given by

$$\alpha_\infty = \frac{2\gamma}{\pi} \ln \tan \pi (x + \frac{1}{4}) \tag{C.1}$$

To obtain starting points one samples this continuous distribution at the discrete points $x = \frac{I_j}{N}$. The deviations of the roots for even relatively small N in comparison to the ones given in the expression above is very small, as one may see in the following table where the roots for the ground state for 16 sites and $\Delta = \frac{1}{2}$ are given (where $-\alpha$ is also a root)

Sampling	Numerical	Difference
0.772595336	0.781831548	1.18%
0.397626319	0.399144352	0.03%
0.208800904	0.209308876	0.02%
0.065874495	0.066007854	0.02%

The asymmetric case is however more complicated, and the distribution of zeroes is not known. One may however use as starting point the roots given by eq. (C.1) and then turn on the asymmetry term $\psi = 2h$ adiabatically. At least for the lowest lying states this procedure works and in this way we were able to study the lowest lying levels of the spectrum. It fails however in some situations, most notably the string–type solutions.

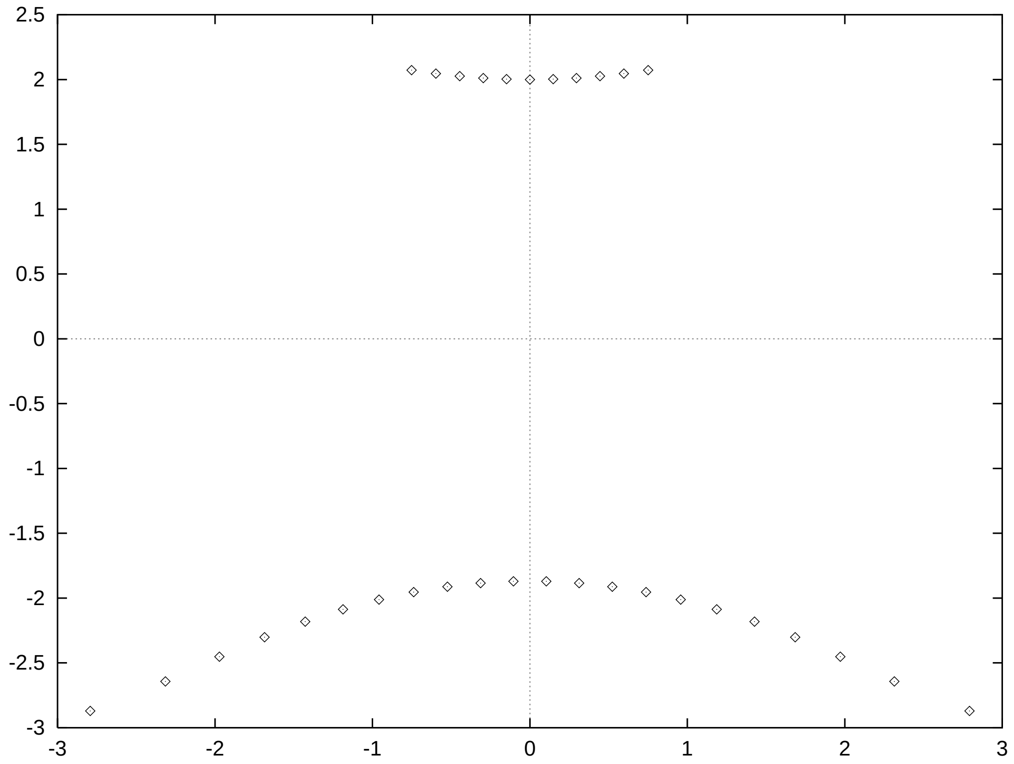

Figure 20: Distribution of the rapidities α_k for $N = 44$. The lower curve corresponds to the ground state in the sector with $n = \frac{N}{2}$ and $\exp(2h) = 9$, the upper curve to the ground state of the sector with $n = \frac{N}{4}$ and $\exp(2h) = \frac{1}{9}$.

Bibliography

[1] Albertini G, Dahmen S R and Wehefritz B (1996a) J. Phys. A: Math. Gen. **29**, L369; (1996b) *The Free Energy Singularity of the Asymmetric* 6–*Vertex Model and the Excitations of the Asymmetric* XXZ *chain*, Bonn Preprint TH–96–14; (1996c) *A Novel Exponent for the Equilibrium Shape of Crystals*, in preparation

[2] Alcaraz F C, Arnaudon D, Rittenberg V and Scheunert M (1994a) Int. J. Mod. Phys. A **9**, 3473

[3] Alcaraz F C, Droz M, Henkel M and Rittenberg V (1994b) Ann. Phys. **230**, 250

[4] Alcaraz F C and Wreszinski W F (1990) J. Stat. Phys. **58**, 45

[5] Andreev A F (1981), Sov. Phys. JETP **53**, 1063

[6] Baxter R J (1982). *Exactly Solved Models in Statistical Mechanics*, Academic Press, New York

[7] Baxter R J (1972) Ann. Phys. **70**, 193

[8] van Beijeren H (1977), Phys. Rev. Lett **18**, 993

[9] Bethe H (1931) Zeit. Phys. **71**, 205

[10] van den Broeck J M and Schwarz L W (1979), SIAM J. Math. Anal. **10**, 658

[11] Burlisch R and Stoer J (1964) Num. Math. **6**, 413

[12] Carmi Y, Lipson S G and Polturak E (1987) Phys. Rev. B **36**, 1894

[13] Chopard D, Droz M, Karapiperis T and Rácz Z (1993) Phys. Rev. **E47**, R40

[14] Dahmen S R (1994) Phys. A: Math. Gen. **28**, 905

[15] De Vega H (1989) Intl. J. Mod. Phys A **4**, 2371

[16] Erdélyi A *et al* eds. (1953). *Higher Transcendental Functions*, McGraw Hill, New York

[17] Gantmacher F R (1959). *Matrix Theory*, Chelsea, New York

[18] Gaudin M (1983). *La fonction d'onde de Bethe*, Masson, Paris

[19] von Gehlen G, Rittenberg V and Ruegg H (1986) J. Phys. A **19**, 107

[20] Grassberger P and Scheunert M (1980) Fortsch. Phys. **28**, 547

[21] Grieger W (1984) Phys. Rev. B **30**, 344

[22] Halperin B I, Hohenberg P C and Ma S–K (1974 Phys. Rev. B **10**, 139

[23] Henkel M and Schütz G (1994) Physica A **206**, 187

[24] Herring C (1951) Phys. Rev. **82**, 87

[25] Iagolnitzer D (1978) Phys. Rev. **D18**, 1275

[26] Jayaprakash C and Saam W F (1984) Phys. Rev. **B7**, 3916

[27] Jayaprakash C and Sinha A (1982) Nucl. Phys. **B210**, 93

[28] Johnson J D, Krinsky S and McCoy B M (1973) Phys. Rev. A **8**, 2526

[29] Johnson J D and McCoy B M (1972) Phys. Rev. A **6**, 1613

[30] Kadanoff L P, Swift J (1968) Phys. Rev. **165**, 310

[31] Kandel D, Domany E and Nienhuis E (1990) J. Phys. A: Math Gen. **23**, L755 and references therein.

[32] Kang K and Redner S (1984) Phys. Rev. Letters **52**, 955; Phys. Rev. **A30**, 2833

[33] Kim D, private communication.

[34] Kramers H A and Wannier G H (1941) Phys. Rev. **60**, 252

[35] Landau L D (1965) in *The Collected Papers of L.D. Landau*, Teer Har D ed., Pergamon, Oxford

[36] Lieb E H (1967a) Phys. Rev. Lett. **18**, 692; (1967b) Phys. Rev. Lett. **19**, 108

[37] Lieb E H and Wu F Y (1972) in *Phase Transitions and Critical Phenomena vol. 1*, Domb C and Green M eds., Academic Press, New York

[38] Lopes E (1992) Nucl. Phys. **B370**, 636

[39] Martin P P and Rittenberg V (1992) Int. J. Mod. Phys. **A7** Suppl.1B, 707 and references therein.

[40] McKenzie J K, Moore A J W and Nicholas J F (1962) J. Phys. Chem. Solids **23**, 185

[41] Noh J D and Kim D (1995) Phys. Rev. E **53**, 3225

[42] Nolden I M (1992) J. Stat. Phys. **67**, 155

[43] Ohachi T and Taniguchi T (1985) Proc. of the OJI Seminar on Morphology and Crystal Growth Units of Crystals, Zao, Japan

[44] Orbach R (1958) Phys. Rev. **112**, 309

[45] Perk J and Schultz C L (1983) in *Non–linear integrable systems – Classical theory and quantum theory*, Jimbo M and Miwa T eds., World Scientific, Singapore

[46] Pokrovskii V L and Talapov A L (1980) Sov. Phys. JETP **51**, 124

[47] Reshetikhin N (1990) Lett. Math. Phys **20**, 331

[48] Rodriguez M A, Abramson G, Wio H and Bru A (1993) Phys. Rev. **E48**, 829

[49] Rottman C and Wortis M (1984) Phys. Rep. **103**, 59

[50] Rottman C, Wortis M, Heyraud J C and Métois J J (1984) Phys. Rev. Lett. **52**, 1009

[51] Schütz G (1993) J. Stat. Phys. **71**, 471 (1993); Phys. Rev. **E47**, 4265

[52] Schultz C L (1983) Physica **A122**, 71

[53] Slater J C (1941) J. Chem. Phys. **9**, 16

[54] Smoluchowski M V (1917) Z. Phys. Chem. **92**, 215

[55] Spouge J L (1988) Phys. Rev. Lett. **60**, 871

[56] Sutherland B (1975) Phys Rev B **12**, 3795

[57] Sutherland B, Yang C N and Yang C P (1967) Phys Rev. Lett. **19**, 588

[58] Toussaint D and Wilczek F (1983) J. Chem. Phys. **78**, 2642

[59] Yang C N (1967) Phys. Rev. Lett. **19**, 1312; (1968) Phys. Rev. **168**, 1920

[60] Yang C N and Yang C P (1966) Phys. Rev **150**, 321

[61] Zamolodchikov A B and Zamolodchikov Al B (1979) Ann. Phys. **120**, 253